NOTICE

The quality of this microform is heavily dependent upon the quality of the original thesis submitted for microfilming. Every effort has been made to ensure the highest quality of reproduction possible.

If pages are missing, contact the university which granted the degree.

Some pages may have indistinct print especially if the original pages were typed with a poor typewriter ribbon or if the university sent us an inferior photocopy.

Reproduction in full or in part of this microform is governed by the Canadian Copyright Act, R.S.C. 1970, c. C-30, and subsequent amendments.

AVIS

La qualité de cette microforme dépend grandement de la qualité de la thèse soumise au microfilmage. Nous avons tout fait pour assurer une qualité supérieure de reproduction.

S'il manque des pages, veuillez communiquer avec l'université qui a conféré le grade.

La qualité d'impression de certaines pages peut laisser à désirer, surtout si les pages originales ont été dactylographiées à l'aide d'un ruban usé ou si l'université nous a fait parvenir une photocopie de qualité inférieure.

La reproduction, même partielle, de cette microforme est soumise à la Loi canadienne sur le droit d'auteur, SRC 1970, c. C-30, et ses amendements subséquents.

Noncoherently Combined Modulation-Coding for Frequency Hopping Acquisitionless Systems

Md. Anisur Rahman

A Thesis

In

The Department

of

Electrical and Computer Engineering

Presented in Partial Fulfillment of the Requirements
for the Degree of Doctor of Philosophy at
Concordia University
Montréal, Québec, Canada

November, 1990

ISBN 0-315-64719-1

ABSTRACT

Noncoherently Combined Modulation-Coding for Frequency Hopping Acquisitionless Systems

Md. Anisur Rahman, Ph. D.,

Concordia University

Spread spectrum systems require code acquisition for their operation. Problems of code acquisition and some code acquisition techniques for Frequency Hopping (FH) are discussed. The acquisition operating characteristics are evaluated under multi access jamming and single user tone jamming cases.

Coding is critical for Frequency Hopping spread spectrum multiple access systems. Concatenated coding can provide the desired performance. Bounds on concatenated convolutional coding performance of Frequency Hopping multiple access systems has been evaluated.

The performance of Frequency Hopping multiple access systems using combined modulation and coding technique (Trellis) concatenated with Reed-Solomon (RS) codes in partial band jamming is introduced and the performance compared to the one using RS outer/RS inner concatenated codes. Noncoherent soft detection of MFSK in association with trellis coding is introduced and the performance compared to RS outer/ RS inner concatenated codes.

A new spread spectrum system that does not have a separate acquisition state for initial code acquisition is presented. A uniform random variate selects

one of the few Gold codes for transmission thus taking out completely the notion of pseudo-random codes in spread spectrum systems and making the effective code length infinite, and leading to acquisitionless systems. The algorithmic detection which combines the code detection, with forward error correction coding (FEC) is another added benefit.

Throughput performance of the new acquisitionless spread spectrum system has been evaluated and compared against the classic SS systems that require code acquisition for their operation.

ACKNOWLEDGEMENTS

I would like to express my deepest gratitude to my advisor Dr. A. K. Elhakeem for his guidance, encouragement and friendship throughout the research period at Concordia University. Dr. Elhakeem's suggestions and encouragement and particularly his continuous availability to discuss scientific issues was valuable in maturing new concepts and ideas.

I also express my deep gratitude to the supervisory committee for their interest in the work and to Dr. Bhattacharya for suggesting a criterion for throughput comparison in our system.

Mr. Nouri Daoud deserves a special word of thanks for his help in preparation of figures on a very tight schedule. Sincere thanks are extended to several colleagues, particularly to Hamid Jamali for useful discussions and assistance.

To my wife I owe so much for her patience, sacrifice and understanding and also to our parents and to my brothers and sisters for their motivation and support.

To my childrens Muntasir and Rifaquat I offer my deepest regret for all this period.

Table of Contents

List of figures

List of Symbols

α	probability of one matched filter output exceeding it threshold
α_i	coefficient multipliers
δf	composite frequency error less than the hop spacing
Δ	ratio of acquisition time to total transmission time
Δ_i	distaces beween signal points
ϵ_s	probability of symbol erasure
γ_b	signal to noise ratio per bit
$\Lambda(\eta)$	coded symbol SNR
ρ	duty facor
σ^2	noise variance
σ_j^2	jammer variance
μ_N	mean of noise
μ_{S+N}	mean of signal plus noise
τ	timing offset between received sequence and transmitted hop sequence
τ_d	dwell time
B_i	i-th bank
C_i	threshold setting in the matched filter peaking
d_{free}	free distance
$E_c(R)$	exponential bound parameter
J	jamming power
J/P	jamming to signal power
K	constraint length of convolutional code
L	number of subcode
M	$M-ary$ size
N_{free}	number of paths with free distance
N_h	normalized dwell time / number of hops per sub code
N_s	number of symbols per hop
$n(t)$	AWGN noise of n single sided density
P	power of each user
P_{ACQ}	probability of acquisition
p_s	probability of symbol error
P_b	probability of bit error
P_D	probability of detection
P_{FA}	probability of false alarm
P_h	probability of hit

PG	processing gain
$Q(x)$	Gaussian probability integral
$q(x)$	input symbol distribution
q_j	number of jamming tones
R_b	bit rate
R_s	symbol rate
$R_0(q)$	computational cutoff rate
SNR	signal to noise ratio
t	error correction capability of code
T_h	hop time
T_s	symbol time
U	number of users
W	spread spectrum bandwidth
W_d	data bandwidth

CHAPTER I

INTRODUCTION

1.1 Introduction

Spread spectrum (SS) signals used for the transmission of digital information are distinguished by the characteristic that their bandwidth is much greater than the information rate. The use of spread spectrum signals is considered because they have some very good properties. Some of these are (1) combating or suppressing the detrimental effects of interference due to jamming, (2) hiding a signal by transmitting it at a low power and thus making it difficult for an unintended listener to detect in the presence of noise, (3) achieving message privacy in the presence of other listener and (4) multi access resulting from Frequency Hopping or code division. All of these properties came about as a result of the coded signal format and the wide signal bandwidth that results [1.1].

In a radio communications network where many radios communicate among themselves there must be some means of sharing the available channel capacity. This means dividing up the overall channel into sub-channels and then assigning these to radios. A single receiver or a group of receivers can be addressed by assigning a given reference code to them, whereas others are given different codes. When codes are properly chosen for low cross correlation, minimum interference occurs between users [1.2].

Spread spectrum communications, long a favorite technology of the mil-

tary, is now on the verge of potentially explosive commercial development. The noninterference capability of the spread spectrum opens up crowded frequency spectra to vastly expanded use.

Demonstration projects have already been authorized by Federal Communications Commission (FCC) where a new spread spectrum personal communication network will share the 1.85-1.99 GHz band with local utilities [1.3]. Spread spectrum subscribers carrying small battery operated handsets will be able to dial any other subscriber in the area as well as conventional telephone subscribers around the world through a link to the wired telephone network [1.3].

Many regard this and similar projects as the first step towards a wireless office, wireless cities and a wireless world in which the non interfering qualities of spread spectrum technology could vastly expand the voice and data services accommodated [1.3].

For example, mobile cellular telephone systems, already feeling a capacity squeeze, in major metropolitan areas will be able to accept many more new customers. Also, likely to benefit are digital stereo radio and police radar and radio. Many manufacturers are already manufacturing spread spectrum equipment for commercial use.

There are many types of SS systems such as Direct Sequence (DS) system, Frequency Hopping (FH) system, time hopping (TH) system, hybrids, etc. Where many users share a common bandwidth in a multi user system, FH spread spectrum signals are primarily used. Because, for a lightly loaded system, FH spread spread spectrum signals are less affected by near far problem. In a FH spread spectrum communications system the available channel

bandwidth is sub-divided into a large number of contiguous frequency slots. In any time interval, the transmitted signal occupies one or more of the available frequency slots as determined by a pseudo-random code generator.

For a Frequency Hop system binary FSK (Frequency Shift Keying) or $M-ary$ FSK may be used for transmission but $M-ary$ transmission has the advantage that more data per chip can be transmitted and a simple receiver format is possible.

Spread spectrum systems have certain immunity to jamming but smart jammers and multi user interference can severely degrade system performance. Moreover, $M-ary$ Frequency Hop transmission is vulnerable to interference. If any one of the M channels other than intended is hit by an interfering signal an error is possible. To overcome these errors, error correction coding should be used. A concatenated coded scheme is the preferred one since decoding is performed on two or more simpler codes and the overall complexity is reduced.

In conventional communications the two primary communication resources are the transmitted power and channel bandwidth. A general system design objective would be to use these resources as efficiently as possible. In power limited channels, coding schemes are generally used to save power at the expense of bandwidth. Whereas in bandlimited channels 'spectrally efficient modulation' would be used to save bandwidth.

In spread spectrum communication the channel bandwidth employed is much larger than that used in conventional communications system. Although the bandwidth of spread spectrum systems is large, it is not unlimited and they are limited by allocations [1.4]. In such systems it is most often possible

to achieve the desired throughput with either modulation techniques or coding techniques. But instead the integration of a bandwidth efficient modulation scheme with some form of coding will exploit the best possible attributes of both.

One problem with all spread spectrum systems is that they require acquisition. Acquisition is the process by which a SS communications receiver synchronizes its locally generated code (which is a replica of the code transmitted by the transmitter) to the received code. It would be productive to have a system that does not go from acquisition to verification and back and so on and for that objective an acquisitionless spread spectrum, namely, the 'SUGARW' system, is proposed.

1.2 Scope of the thesis

The aim of the thesis is to investigate the effects of concatenated coding on the performance of spread spectrum Frequency Hopping MFSK system, particularly concatenated combined modulation and coding technique in a multiple access environment. Acquisition is inherent with any spread spectrum system. An acquisitionless system concept is introduced and the throughput performance of the acquisitionless system is compared with the conventional spread spectrum system.

In chapter-II, some preliminaries of the spread spectrum system, acquisition methods and problems associated with the acquisition are described. The acquisition operating characteristics are evaluated under multi access jamming and single user tone jamming cases in the two cases of parallel and serial

search schemes.

In chapter-III, coding counter measures against different jamming scenarios and multi user interference are discussed.

Previous work of some authors and literature survey of frequency hopping MFSK under different jamming scenarios are presented.

In chapter-IV, the performance of spread spectrum multiple access system using concatenated convolutional coding is evaluated. Because coding is critical to the spread spectrum multiple access Frequency Hopping (FH) systems (both acquisition and acquisitionless types) we search for more powerful codes.

In chapter-V, the Frequency Hop (FH) multiple access performance of noncoherent soft detection of MFSK (*M-ary* frequency shift keying) in association with the combined modulation and coding technique (trellis coding) is introduced and the performance compared to the one using Reed-Solomon (RS) outer/RS inner concatenated codes.

For bandlimited channels the combined modulation and coding technique (trellis coding) has been the subject of intensive research. However, its applicability has been restricted to coherent PSK, PAM, and QAM systems. The extension of this technique to noncoherent FH/MFSK in a multiple access environment is the subject of this chapter.

In chapter- VI, an acquisitionless system concept is introduced. Modifications necessary for application of this technique to FH/MFSK is described. We analyze and evaluate the throughput performance of the new acquisitionless spread spectrum (SS) "SUGARW' system and compare it against the SS systems that require code acquisitions for their operations. Acquisitionless SS system realization is one of the major objective of this

research.

In chapter-VII, we make the conclusion of our research findings, moreover, we identify further research problems and extension of this work.

1.3 Research Contributions

* Spread spectrum acquisition operating characteristics have been evaluated under multi access jamming and multi tone jamming cases in the two cases of parallel and serial search schemes

* Concatenated convolutional code application in multiple access Frequency Hopping MFSK and evaluation of its error performance have been done. Relation between the exponential bound parameter $E_c(R)$ and rate R for different levels of concatenation has been found.

* Combined modulation and coding application in noncoherent FH/MFSK systems has been tried and performance of inner combined modulation and coding and outer RS code has been compared with RS inner/ RS outer code.

* The architecture and basic concepts of a new acquisitionless system namely 'SUGARW' (an entirely new concept in spread spectrum systems) have been presented.

* The throughput performance of the new acquisitionless system has been analyzed and evaluated and its performance compared to that of conventional spread spectrum systems that require code acquisition for their operation.

REFERENCES

[1.1] R.C. Dixon, ' Spread Spectrum Systems', Wiley- Inter Science

[1.2] M.K. Simon, J.K. Omura, R.A. Scholtz, B.K. Levitt, 'Spread Spectrum Communications', Computer Science Press.

[1.3] D.L. Schilling, R.L. Pickholtz, L.B. Milstein, 'Spread Spectrum Goes Commercial', IEEE, Spectrum, pp. 40-45, August 1990.

[1.4] A.J. Viterbi, 'Spread Spectrum Communications Myths and Realities', IEEE, Communications Magazine, pp. 11-18, May 1979.

CHAPTER II

SPREAD SPECTRUM ACQUISITION PROBLEMS, METHODS OF ACQUISITION AND ACQUISITION OPERATING CHARACTERISTICS

2.1 Introduction

Spread spectrum systems have been found to provide the user with security, selective calling, interference, interception and jamming rejection and multi access capability [2.1, 2.2, 2.4]. The use of spread spectrum systems are considered because they have these good properties.

The two main modulation techniques employed in spread-spectrum systems are

1. Direct Sequence (DS) and
2. Frequency Hopping (FH)

Combining these two we get a spread-spectrum technique called the hybrid FH/DS system. One reason for using hybrid techniques is that some of the advantages of the two types of system are combined in a single system.

In this chapter, we describe briefly both the Direct Sequence (DS) and the Frequency- Hopping (FH) spread spectrum techniques. FH spread spectrum technique has some advantages over DS system and we will consider the FH system primarily in this thesis.

One problem with all SS systems is that they require acquisition. Acquisition is the process by which a SS communications receiver synchronizes its locally generated code (which is a replica of the code transmitted by the

transmitter) to the received code [2.1, 2.2]. There are problems inherent with the acquisition which we review in this chapter; we will also review some of the acquisition techniques commonly used. The acquisition operating characteristics (i.e., the relation between the probability of false alarm vs. the number of post detection integration) is evaluated under multi-access and tone jamming cases.

2.2.1 Direct Sequence Systems

Direct sequence also called pseudo-noise or direct spread, is a system in which a carrier is modulated by a digital code sequence having a bit rate much higher than the information signal bandwidth. If the bandwidth of the spreading signal is large relative to the data bandwidth, spread spectrum transmission is dominated by the spreading signal and is nearly independent of the data signal.

Direct sequence spread spectrum systems are so called because they employ high speed code sequences, which is used to modulate the data modulated carrier. Fig. 2.1.a and Fig. 2.1.b shows the block diagram of a simplified Direct Sequence PN (Pseudo-Noise) system; the message to be transmitted can be considered to be first modulated on a carrier resulting in a signal with a spectral width that is proportional to the message bandwidth. The signal is then phase modulated by a code generator which has a specific code pattern. The code generator is a binary *M−sequence* generator which has the desirable properties that it can be constructed from binary shift registers stages and it produces a stream of binary digits that are uncorrelated (pseudo-random noise).

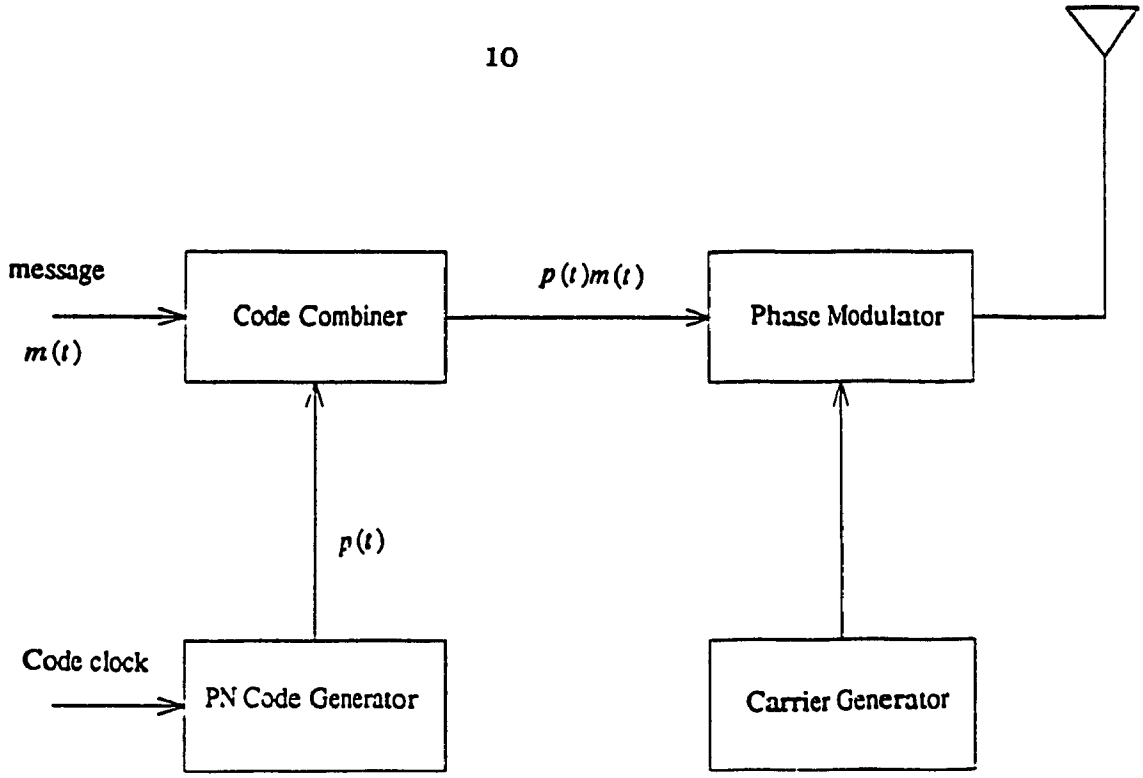

Fig. 2.1.a. Block diagram of a direct sequence transmitter

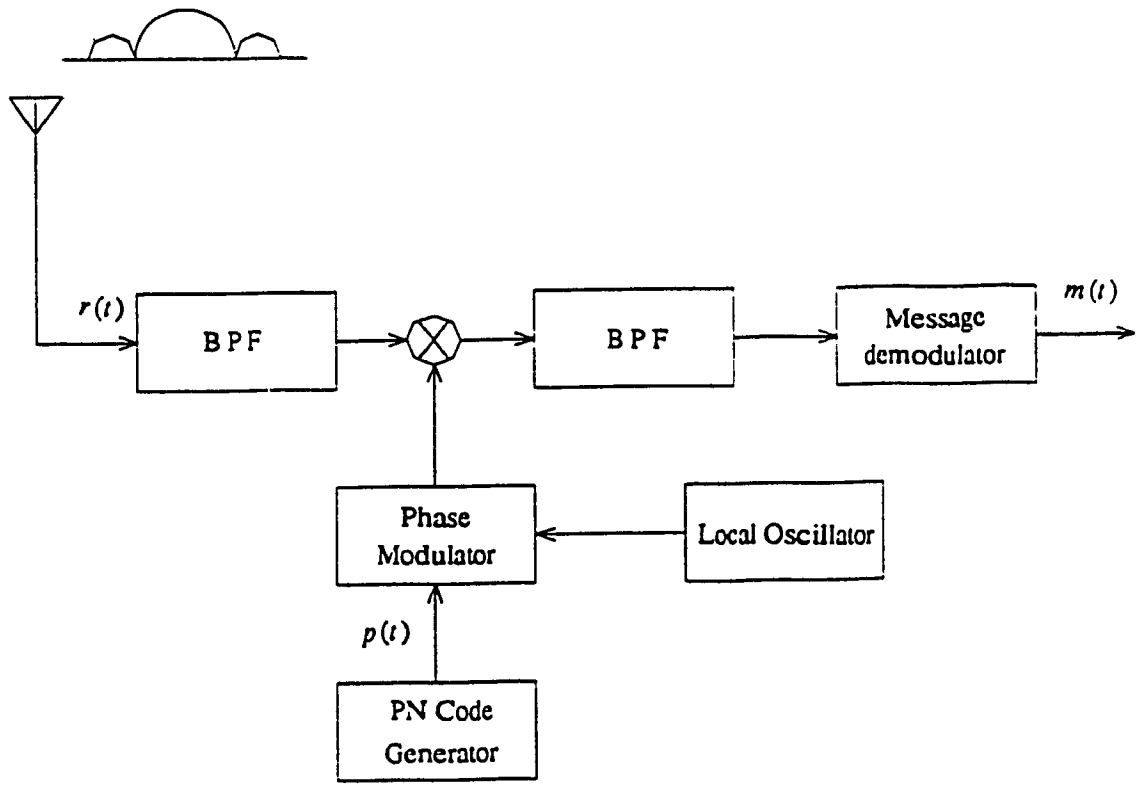

Fig. 2.1.b. Receiver of a direct sequence system

2.2.2 Frequency Hopping (FH)

Frequency hopping (FH) is a spread spectrum technique where the carrier frequency changes under the control of a pseudo-random user code. The specific order in which the frequencies are occupied is a function of code sequence, and the rate of hopping from one frequency to another is a function of the rate at which information is to be sent. The code sequence types are the same as those used by the Direct Sequence system, with the exception that the code rate is usually low (where Direct Sequence code rates are in the 1 mbits/s to 100 mbits/s range, frequency hopping codes do not normally exceed a few hundred kilobits/s)

The rate of hopping from frequency to frequency and the number of frequency choices in any Frequency Hopping system is governed by the requirements placed on it for a particular use [2.4].

Fig. 2.2.a shows the block diagram of a transmitter of a FH system. The working principle of this system is very simple; spreading of the spectrum is obtained by changing the carrier frequency f_i over the whole available band, according to a pseudo-noise sequence (PN channels).

The receiver of a conventional FH/SS system is as shown in Fig. 2.2.b At the receiver the frequency synthesizer is driven by a PN (pseudo-random) code generator. The output of this frequency synthesizer is mixed with the incoming received signal and the received signal is despread.

Frequency hopped (FH) systems are classified into two types called Slow Frequency Hop (SFH) and Fast Frequency Hop (FFH) system. In the SFH the hop time (time of one clock period) is greater than the symbol time. In contrast to the SFH system, where the hop frequency band changes more slowly

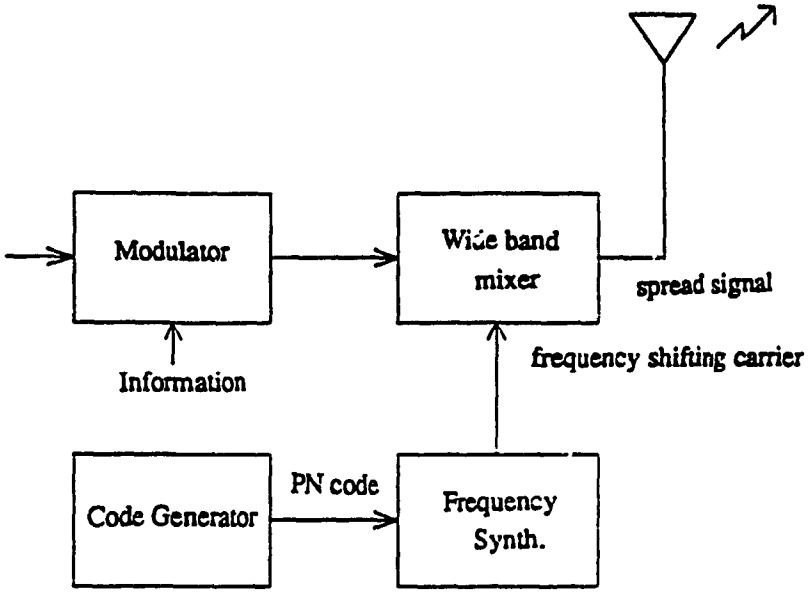

Fig. 2.2.a. Block diagram of the transmitter of a frequency hopping system

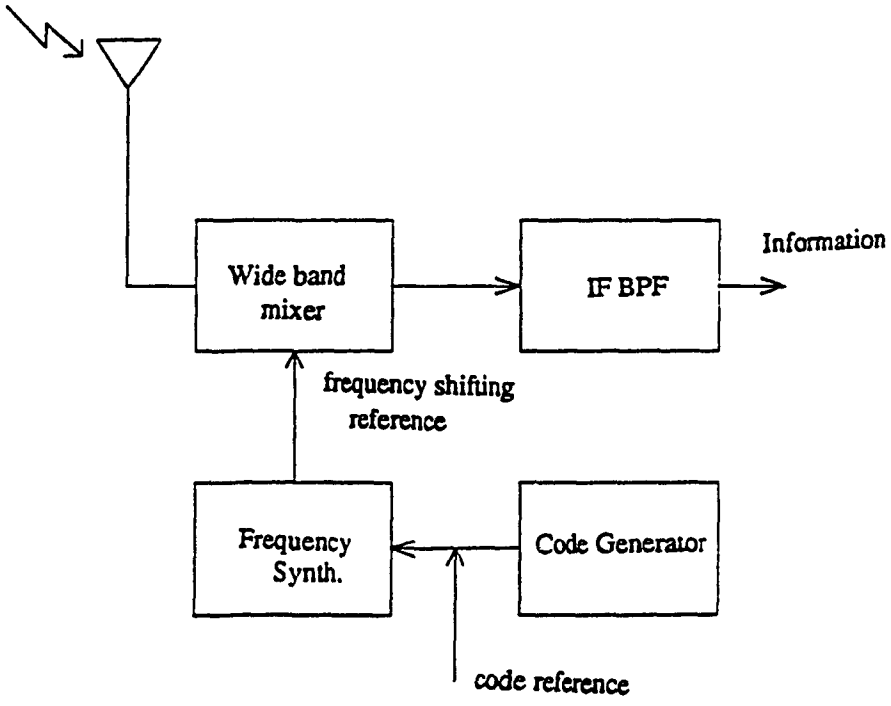

Fig. 2.2.b. Block diagram of the receiver of a frequency hopping system

than symbols come out of the data modulator, the hop frequency band can change many times per symbol in a FFH system.

For a Frequency Hop (FH) system binary FSK or *M-ary* FSK may be used for transmission but *M-ary* transmission has the advantage that more data per chip (spreading code symbol duration is referred to as a spreading code chip) can be transmitted and a simple receiver format is possible. Moreover, *M-ary* transmission in frequency hopping has the advantage that they are well adapted to the use of powerful error correction code [2.4].

The FH system has certain advantages over the Direct Sequence system. One of the main advantages is the greater bandwidth spreading achievable with the Frequency Hopping (FH) technology. Current technology permits FH bandwidths of the order of several GHz, which is an order of magnitude larger than implementable DS bandwidths.

There are situations in which it is desirable to avoid certain regions of the radio frequency band (e.g., fading or narrow band jamming), and here the FH enjoys a distinct advantage over the DS systems. The synthesizer algorithms which maps the k chip PN segments into specific carrier frequencies can be modified to eliminate these bands, resulting in a discontinuous spectrum.

The advantages and disadvantages of the FH/SS systems are summarized below.

advantages

Greater amount of spreading

Can be programmed to avoid portions of the spectrum

Relatively short acquisition time

Less affected by near far problem for lightly loaded system

disadvantages

Complex frequency synthesizer

Not useful for range and range rate measurements

Error correction required

The desirable properties of the Frequency Hopping outweigh its disadvantages, and this is the reason for us for mainly considering the Frequency Hopping system in this thesis.

2.3.1 Problems of Acquisition and different methods of acquisition

The problem of synchronization in the spread spectrum context is that of aligning the receiver's locally generated waveform, which is used to demodulate the incoming signal with the spreading modulation superimposed on the incoming signal. Synchronization problems in spread spectrum communications systems have much more effect on the system performance than in a classic digital communications.

Pseudo-random codes have typically been used for DS, FH and time hopping spread spectrum (SS) systems. It was not possible for a SS receiver to synchronize to a completely random spreading code and the acquisition stage emerged as the most important component in the system [2.5]. Acquisition time ranges from milliseconds to few seconds in both military and civilian systems [2.6]. Moreover, the inconvenience of plugging in the (time of the day) in some secure systems make such systems inappropriate for real time or short mission time applications. Even if these waveforms were synchronized at some previous time and the clocks were independently maintained, normal

tolerances in equipment parameters would allow them to become misaligned after some time.

Additional discrepencies can be introduced by propagation effects such as in multipath transmission, Doppler shift when there is relative motion between the transmitter and the receiver is another source of error. Successful jamming of the receiver during code acquisition mode is a major threat for any spread spectrum system, and subsequent data modulation will not be possible in many jamming scenarios. FH systems are particularly vulnerable in this sense, and this is true of applications where communication between spread spectrum users (such as mobile radio units) is bursty and includes large period of silence. The combined effects of these factors produce uncertainty at the receiver about the timing and frequency of the incoming signal, i.e., acquisition[2.4].

The synchronization process is often considered to be composed of two parts; acquisition and tracking. Acquisition involves a search through the time frequency uncertainty and a determination that the locally generated code and the incoming code are closely enough aligned.

Tracking is the process of maintaining the alignment of the two signals. This is usually accomplished using some type of feed back loop which also serves to reduce alignment error remaining after the acquisition process.

Specific synchronization requirements depend largely on the intended application, i.e., where the transmitter continuously emits the spread spectrum signal. For example, acquisition of a ranging signal or of a continuously operating link are different from situations where the communications are bursty or intermittent and characterized by frequent periods of radio silence.

Many acquisition techniques have been developed up to now. The recent

development in device technology, i.e., Surface Acoustic Wave Devices (SAWD), Charge Coupled Devices and large scale integrated circuits together with the advances in the acquisition techniques has resulted in the reduction of the mean acquisition time, but the notion of acquisition mode still remains there.

Though in the systems we propose in this thesis (chapter-vi) we do not have an acquisition mode, we still use some matched filters to indicate how the local code is offset from the received code epoch, in which case we use this information efficiently while data bits are demodulated parallel in time. For the purpose of analysis the results of few acquisition techniques will be needed and it will be instructive to review some of these FH acquisition techniques.

2.3.2. Acquisition Techniques for DS and FH Receivers

Acquisition is the process by which a spread spectrum communication receiver synchronizes its locally generated code (which is a replica of the code transmitted by the transmitter) to the received code [2.1, 2.2]. This synchronization is usually accomplished in two stages. Initially a coarse alignment of the two PN signals is produced to within a small (typically less than a fraction of chip) residual relative timing offset. This synchronization is accomplished by generating a local replica of the PN code. In almost all the PN acquisition techniques the received and local PN signals are first multiplied to produce a measure of correlation between the two. This correlation measure is then processed by a suitable detector and search strategy to decide whether the two codes are in synchronism and what to do if they are not. The difference between the various schemes depend on (1) the type of detector used which in turn is dependent on the form of the received signal and (2) the nature of the

search algorithm which acts on the detector outputs to reach the final verdict.

All of the detector structures of interest make decisions based on a threshold comparison test of one form or another. A classification of detectors for PN acquisition depends on whether they are of fixed or variable integration time type. Fixed integration time type detectors can be further subdivided into single dwell [2.7, 2.8] and multiple dwell types [2.9].

Following a threshold exceedance of the first dwell output, the additional dwells in combination with threshold testing are used in accordance with a verification algorithm to produce a final decision on whether the code phase position under test corresponds to true synchronization [2.2].

Several techniques have been proposed for minimizing the mean acquisition time in spread-spectrum communications. Among those currently attracting interest are the multiple dwell and parallel acquisition methods [2.9]. A parallel bank of filters each searching in one segment of the uncertainty region, yields a smaller acquisition time but requires an expensive design of filters.

In the following we will briefly review some of the techniques commonly used for coarse acquisition of Frequency Hopped SS signal.

2.3.3 Acquisition of Frequency Hopped receivers

Coarse frequency synchronization is the process by which the local generated hop sequence is aligned with the received hop sequence to within a fraction of a hop interval. This acquisition process is normally thought of as being accomplished in two steps. First, the degree of alignment is determined. Second, the correlation measure is processed by a suitable detector and decision/search algorithm to decide whether or not to continue the search. If at any point the search terminates the coarse frequency acquisition is assumed

to have occurred.

2.3.3.1 Serial Search Techniques with Active Correlation [2.2]

The serial search acquisition system is illustrated in Fig. 2.3. In this system the received signal is mixed with the output (hop sequences) of the FH synthesizer. The frequency synthesizer is driven by a PN generator and the epoch of the PN generator is controlled to continue the search for getting acquisition. The result of the multiplier (correlator) is passed through an IF filter followed by an energy detector. Integration of the energy detector output after detection produces a signal whose mean value is zero when they are partially or fully aligned. Now, whether to continue the process or not depends on the results of comparison of the results of integration with a threshold (preset).

Fig. 2.4 shows the sequence of frequencies indicating the difference signal from the mixer when the received and local hop signals are not aligned by less than a single hop interval. Where δf indicates the composite frequency error less than the hop spacing and τ indicates the timing offset between the received sequence and the synthesizer sequence with magnitude less than a hop interval T_h. The signal component of the IF filter output will consist of $m = T_h / T_s$ bursts of sinusoid $T_h - \tau$ in each symbol interval T_s. These m bursts are all at the same frequency but have random phases which are independent of one another.

A measure of the lack of coarse time synchronization can be obtained by separately combining the energies detected in each hop interval at each of the M possible MFSK frequencies and then choosing the largest of these $m - f\,old$ diversity combinations. Since this selection is made only once per symbol interval, post detection accumulation (over say N_{FFH} symbols) is required, the

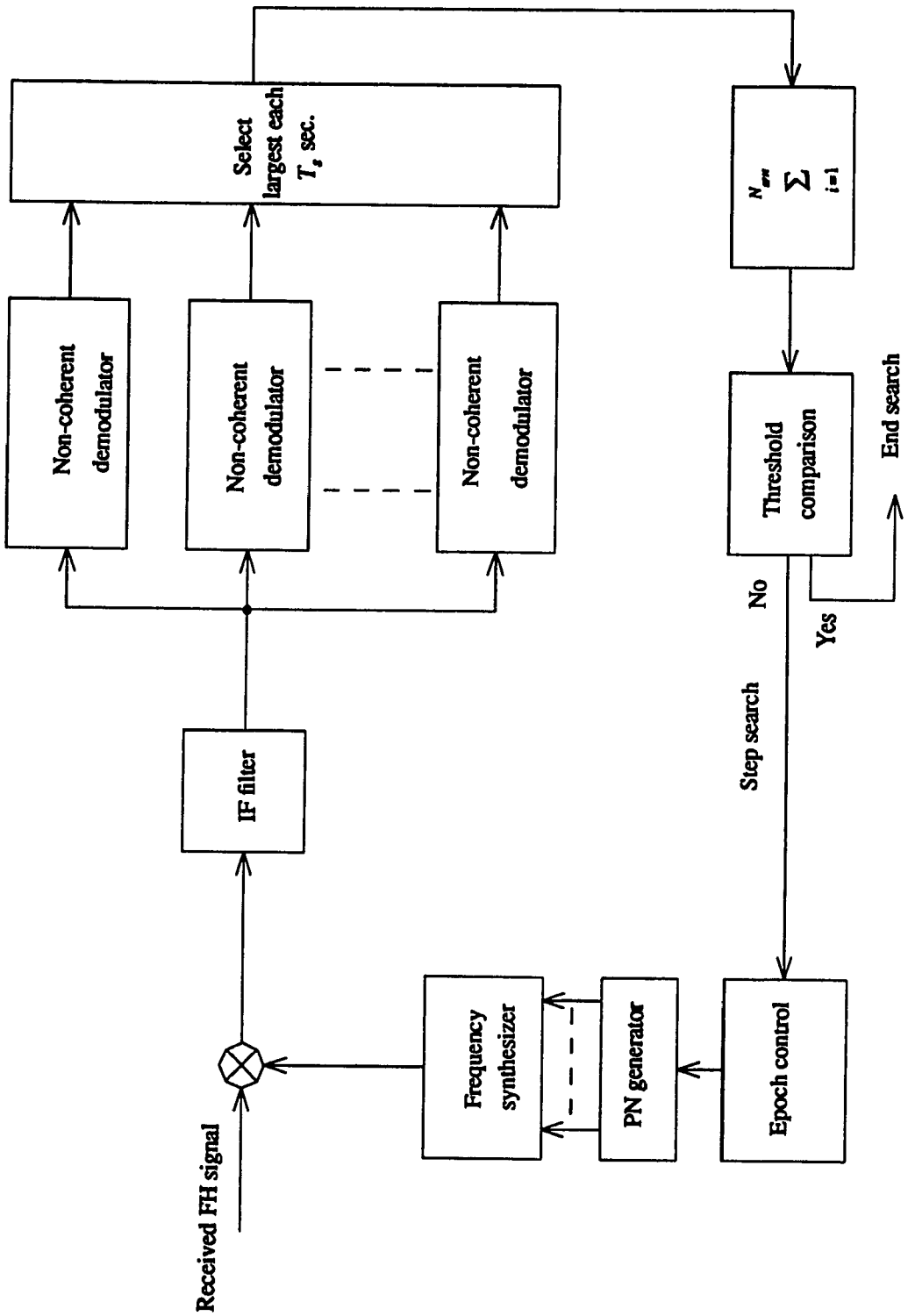

Fig. 2.3. A basic serial search acquisition configuration for SFH/MFSK

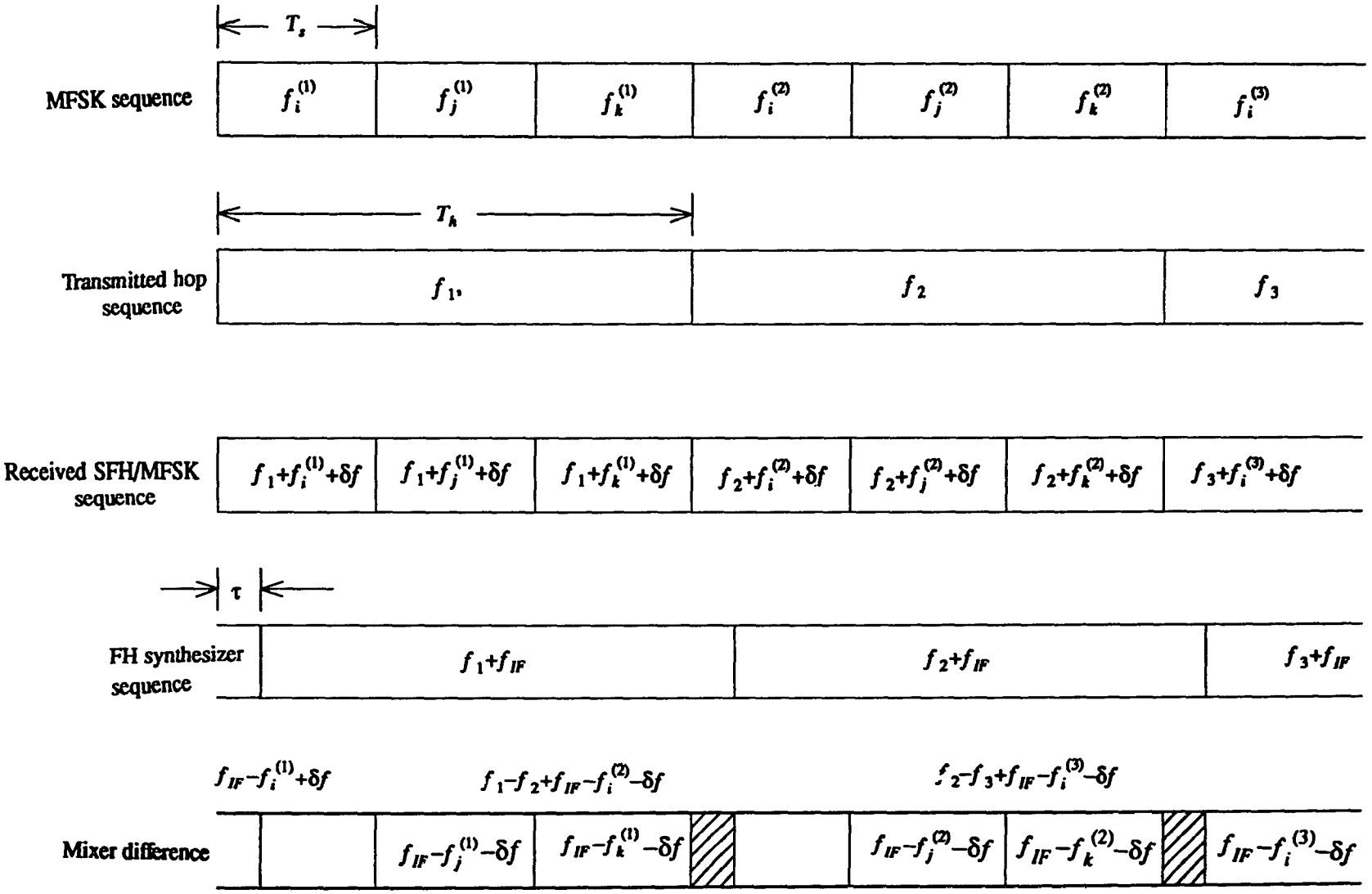

Fig. 2.4. Serial search acquisition and corresponding time frequency diagram [2.2]

result of which is compared with a preset threshold to determine whether or not to continue the search.

2.3.3.2 Serial Technique with Passive Correlation (matched filters)

An approach for demodulation of a spread spectrum signal is to employ a filter matched to the incoming sequence. The rapid search capability of serial search scheme with passive correlation can be realized in FH receivers. A block diagram of optimum matched filter for detection of Frequency Hopped signals is shown in Fig. 2.5. A sequence of m consecutive frequencies $f_1, f_2, \ldots, f_m$ within the overall hop sequence is chosen as the sync. pattern to which the receiver tries to match itself [2.2, 2.11].

The *ith* arm of the device contains a mixer (which has its one input a CW tone at frequency $F_i = f_i + f_o$), a bandpass limiter centered at f_0, a square law envelope detector integrator and delay. The received FH signal is simultaneously mixed with these m frequencies (shifted to IF) and the result of each mixture is passed through a noncoherent demodulator (band-pass filter and square law envelope detector). The outputs corresponding to the energy in successive hop interval correlations can be formed and tested against a threshold. When the input sequence $f_1, f_2, \ldots, f_m$ has just passed through the receiver matched filter, the above sum will have its maximum value.

It can be seen that the complexity of the implementation grows proportionately with the length of the sequence to be detected. It is because of this that active correlation is often used.

Comparison of active correlators with matched filtering shows that there is some initial increase in complexity in going to the structure (a Frequency

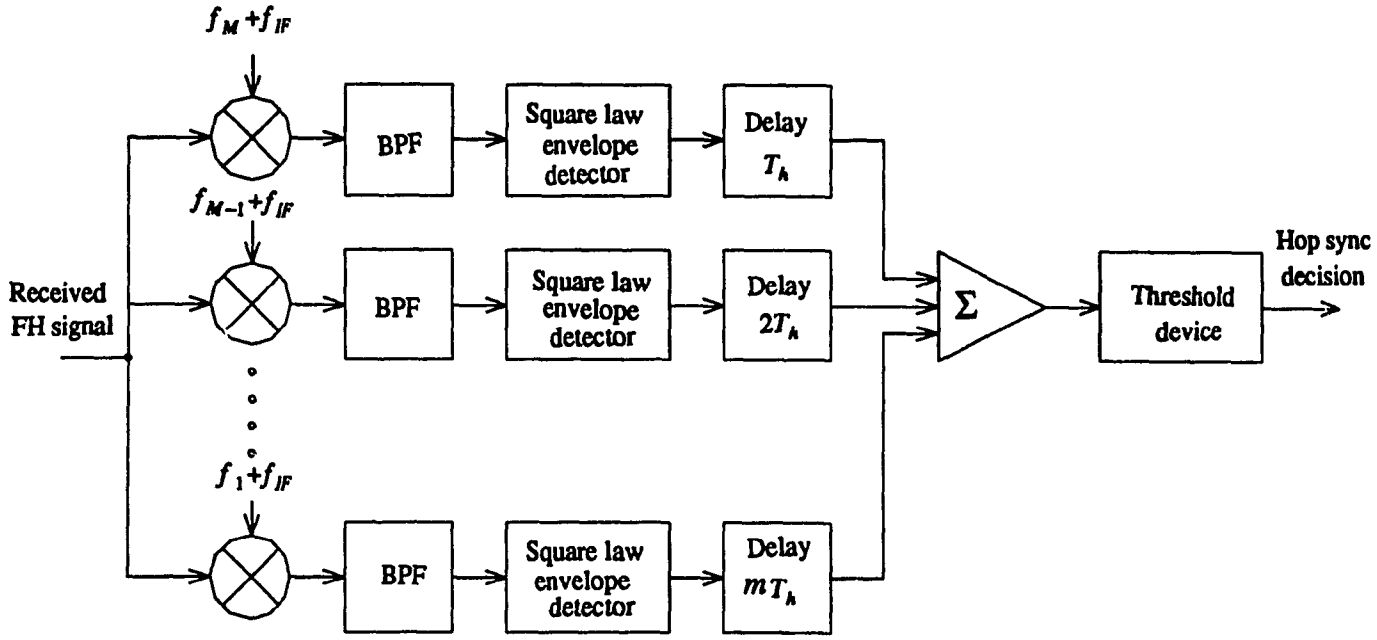

Fig. 2.5 A matched filter detection of the frequency hopped signal sequence $f_1, f_2, \ldots, f_m$.

Hopper and PN code generator) compared to an active correlator but once this investment is made the complexity of the implementation will not grow in proportion to sequence length.

2.3.3.3 Other FH Acquisition Techniques

A scheme combining the rapid search capability of passive correlation and the decision reliability of active correlation was proposed by S. S. Rappaport and D. L. Schilling and later compared with the more conventional FH acquisition techniques in [2.12]. Such a scheme was used in the ground mobile radio environment.

In such a system at the on set of a transmission prior to message transmission, the user sends a leader consisting of several repititions of the hopped carrier patterns. Each of the hop patterns begins with a specific short segment (say m hop long) referred to as the sync. prefix. A passive correlator ($m-stage$) matched filter is used to detect these short m hop prefix and generate a code start sequence for those intervals in which its decision threshold exceeded. Noncoherent detection and post detection integration over these $k-hop$ intervals produces an output which is compared against a second threshold. If this threshold is exceeded the test terminates and sync. acquisition is declared. Otherwise the active correlator is again made available to the common bank. If all active correlators are engaged (none are idle) when a code start signal occurs, then this signal is ignored.

Estimation from the received signal the state of the linear feed-back shift register that generates the local PN code can also be applied in FH/SS systems. Estimation of the received frequency over say n_1 successive hop intervals requires a form of sequential spectral estimation. In FH/SS an estimate of

the frequency in a single hop interval provides information about the entire state of the LFSR [2.13].

In autoregressive spectral estimation acquisition technique [2.14] the sampled received signal plus noise is modeled as an autoregressive process, thus allowing identification of the instantaneous frequency of the signal by algorithm developed by Elhakeem and Gupta [2.14]. This technique is highly vulnerable to narrow band interference.

2.4.1 Operating Characteristics Under Multi Access Jamming (under both serial and parallel searches)

In this section we evaluate the acquisition † operating characteristics P_D and P_{FA} of a spread spectrum SS system in terms of systems parameters under multi access and single user multitone jamming situations. We assume that there is no Doppler present and we treat the two cases of classic serial code acquisition [2.7] and matched filtering technique [2.15]. This evaluation is necessary for data throughput comparison purposes with the conventional systems (in chapter- VII).

The serial search acquisition system is described in section 2.3.3.1 and illustrated in Fig. 2.3. In this scheme the received FH signal is multiplied in a mixer with the FH synthesizer output (hop sequence) determined by a PN generator. The epoch of the PN generator is serially stepped for determining acquisition. The result of the multiplier is passed through an IF filter followed by an energy detector. Integration of the energy detector output after detection produces a signal whose mean is zero when the received and local codes are not aligned and non zero when they are partially and fully aligned. Comparing this signal with a preset threshold allows a decision to be made as to whether or not acquisition has been achieved.

In the single user case, the input to the square law envelope detector (Fig. 2.6) for the case when there is a signal present can be expressed as

$$x(t) = s(t)+n(t)=\sqrt{2}A\cos(\omega_0 t+\phi)+\sqrt{2}n_c(t)\cos(\omega_0 t+\phi)$$

† Our system does not have a separate acquisition state, we introduce this analysis only for comparison purposes. Even in the parallel matched filtering technique that we use in our system all code epoch evaluations are done in parallel with data demodulations.

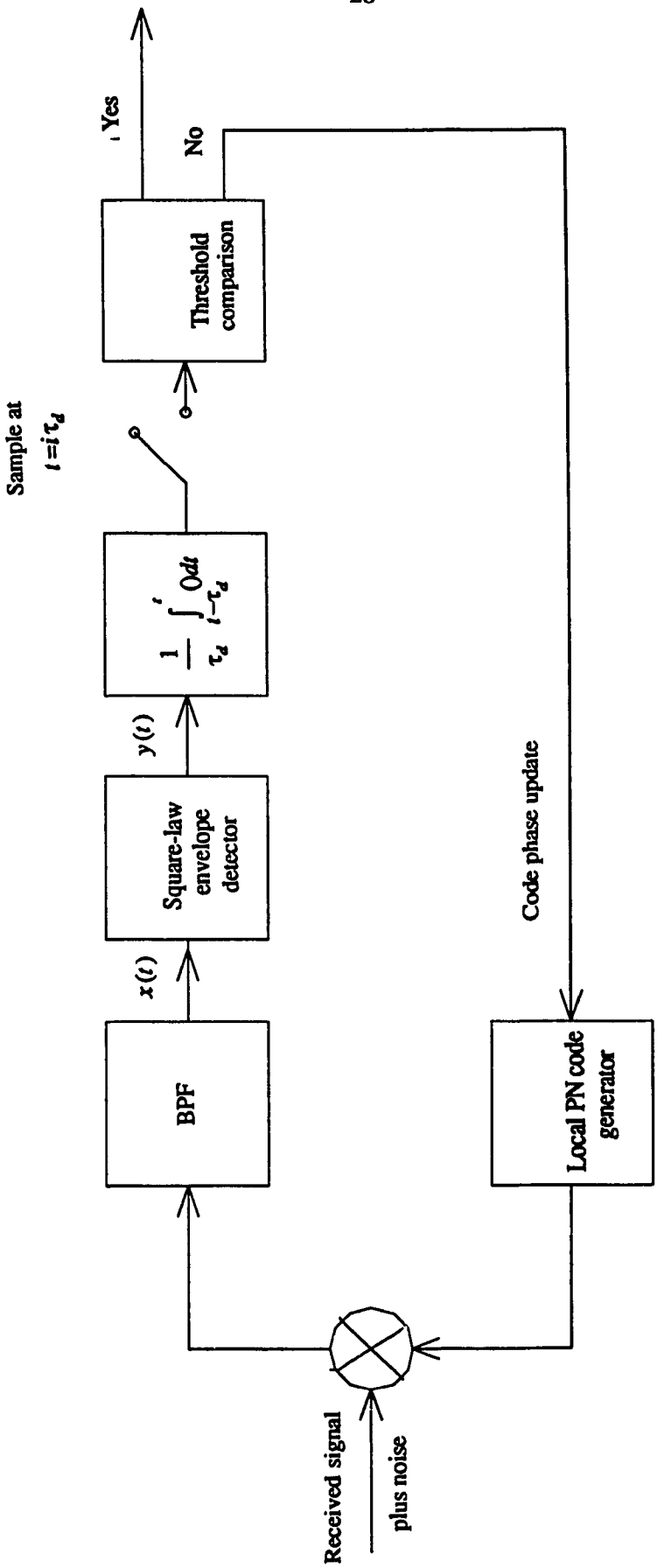

Fig. 2.6. Square law envelope detector schematic diagram

$$-\sqrt{2}n_s(t)\sin(\omega_0 t+\phi) \tag{2.1}$$

$$= \sqrt{2}R(t)\cos(\omega_0 t+\phi+\theta(t)),$$

$$R(t)=\sqrt{(A+n_c(t))^2+n_s^2(t)}\,;\quad \theta(t)=\tan^{-1}\left(\frac{n_s(t)}{A+n_c(t)}\right) \tag{2.2}$$

In eq. (2.1) A is the rms signal amplitude and $n_c(t)$ and $n_s(t)$ are band limited, independent, low-pass zero mean Gaussian noise process with variance σ^2 equals $N_0B/2$, where N_0 is the single sided noise spectral density and B is the noise bandwidth of the bandpass filter.

The output of the square law envelope detector in response to the input $x(t)$ is given by

$$Y(t)\equiv x^2(t)=R^2(t)=(A+n_c(t))^2+n_s^2(t)$$

If we consider the multiple access interference effects in addition to the Gaussian noise in the envelope detector (assuming that the like user interferers have the same power as the desired signal). In that case the pdf's are given by the following equations,

For the case when there is a signal present [2.2],

$$p(y)=\begin{cases}\dfrac{1}{2(\sigma^2+\sigma_j^2(i))}\exp\left[-\left(\dfrac{y}{2(\sigma^2+\sigma_j^2(i))}+\lambda\right)\right]I_0\left(2\left(\dfrac{\lambda y}{2(\sigma^2+\sigma_j^2(i))}\right)\right); & y\geq 0,\\ 0; & \textit{otherwise}\end{cases} \tag{2.3}$$

and for the banks not containing the signal

$$p(y)=\begin{cases}\dfrac{1}{2(\sigma^2+\sigma_j^2(i))}\exp\left(-\dfrac{y}{2(\sigma^2+\sigma_j^2(i))}\right); & y\geq 0,\\ 0; & \textit{otherwise}\end{cases} \tag{2.4}$$

where $\sigma_j^2(i)$ represents the equivalent total variance of j users hitting the i-thy bank

For an $M-ary$ system we analyze the pdf situations in each bank separately and then group those densities according to the (maximum of) decision rule followed at the $M-ary$ demodulation again for the purpose of code acquisition. And assuming first the out of sync condition ($\tau \geq T_h$) then the mixer output is noise only plus multi access interference and the M noncoherent demodulator outputs have the probability density function as given in eq. (2.4) (i.e., found for square law envelope detector under no signal presence).

For the ideal in sync condition, i.e., when the timing error is equal to zero ($\tau = df = 0$) the demodulator outputs containing the desired signal is given by eq. (2.3) and the $(m-1)$ demodulator outputs will be represented by eq. (2.4).

If Y_i^* denote the random variable corresponding to the largest of the M-noncoherent demodulator outputs at the $i-th$ sampling instant then the probability density function of Y_i^* under noise only situations in all banks is given by

$$q_N(Y_i^*) = \frac{d}{dY_i^*}[\prod_{i=1}^{M} P_N(Y_i^*)]$$

$$= p_1(Y_i^*) \prod_{j=2}^{M} P_{Nj}(Y_i^*) + P_{N1}(Y_i^*) \sum_{j=2}^{M} p_{Nj}(Y_i^*) \prod_{\substack{k=1 \\ k \neq j}}^{M} P_{Nk}(Y_i^*) \qquad (2.5)$$

Where the CDF of Y^* is

$$P_N(Y^*)=\int_{-\infty}^{Y^*} p_N(y^*)dy^*$$

$$= 1 - \exp\left[-\frac{Y^*}{2(\sigma^2+\sigma_j^2(i))}\right] \tag{2.6}$$

$$q_N(Y_i^*) = \sum_{i=1}^{M} \alpha_i e^{-\alpha_i Y_i^*} \prod_{\substack{k=1 \\ k\neq i}}^{M} (1-e^{\alpha_i Y_i^*}) \tag{2.7}$$

Where

$$\alpha_i = \frac{1}{2(\sigma^2+\sigma_j^2(i))} \tag{2.8}$$

Under the signal presence condition (i.e., received and local codes are aligned) the CDF of one of the M demodulator banks is given by

$$P_{S+N}(Y^*)=\int_{0}^{Y^*} p_{S+N}(y^*)dy^*$$

$$\int_0^{Y^*} \frac{1}{2(\sigma^2+\sigma_j^2(i))} \exp\left[-\frac{y}{2(\sigma^2+\sigma_j^2(i))}+\lambda\right] \times I_0\left(2\sqrt{\lambda \frac{y}{2(\sigma^2+\sigma_j^2(i))}}\right)dy^* \tag{2.9}$$

and pdf of the maximum of the M banks is given by

$$q_{S+N}(Y_i^*)= p_{S+N}(Y_1^*)\left[\prod_{i=2}^{M}(1-e^{-\alpha_i Y_i^*})\right] + P_{S+N}(Y_1^*)\left[\sum_{i=2}^{M} \alpha_i e^{-\alpha_i Y_i^*} \prod_{\substack{j=1 \\ j\neq i}}^{M} (1-e^{\alpha_i Y_i^*})\right] \tag{2.10}$$

Evaluations of these integrals in closed form were not feasible so we had to take recourse to numerical integration. In order to evaluate the operating

characteristics of the serial acquisition system, we need to determine the first two central moments of Y_i. For the in sync. condition as

$$\mu_{S+N} \equiv \int_{-\infty}^{\infty} Y_i^* q_{S+N}(Y_i^*)\, dY_i^* \tag{2.11}$$

And for the out of sync condition

$$\mu_N \equiv \int_{-\infty}^{\infty} Y_i^*\, q_N\ (Y_i^*)\, dY_i^* \tag{2.12}$$

The in-sync and out of sync variances of Y_i are given by

$$\sigma_{S+N}^2 = \overline{(Y_i^*)_{S+N}^2} - \mu_{S+N}^2 \tag{2.13}$$

$$\sigma_N^2 = \overline{(Y_i^*)_N^2} - \mu_N^2 \tag{2.14}$$

Post detection accumulation of Y_i^* produces approximately Gaussian (N_h *large*) random variable

$$Z^* = \sum_{i=1}^{N_h} Y_i^* \tag{2.15}$$

which when compared with the threshold η^* gives the false alarm probability,

$$P_{FA} = \int_{\eta^*}^{\infty} \frac{1}{\sqrt{2\pi N_h \sigma_N^2}} \exp\left[-\frac{(Z^* - N_h \mu_N)^2}{2N_h \sigma_N^2}\right] dZ^*$$

$$= Q\left(\frac{\eta^* - N_h \mu_N}{\sqrt{N_h \sigma_N^2}}\right) \equiv Q(\beta) \tag{2.16}$$

The system operating characteristics can be written as

$$P_{FA} = Q\left(\frac{Q^{-1}(P_D) - (\mu_N - \mu_{S+N})\sqrt{\dfrac{N_h}{\sigma_{S+N}^2}}}{\dfrac{\sigma_N}{\sigma_{S+N}}}\right) \tag{2.17}$$

The next step is to evaluate in each bank the mean and variance of the acquisition detection variable under each jamming scenarios (certain number of interferers B_1, B_2, B_3, B_4 in each bank, i.e., certain $\sigma_j^2(i)$ and the mean and the variances are conditional, i.e., $(\mu_N \mid B_1,B_2,B_3,B_4)$, $(\mu_{S+N} \mid B_1,B_2,B_3,B_4)$, $(\sigma_N^2 \mid B_1,B_2,B_3,B_4)$, and $(\sigma_{S+N}^2 \mid B_1,B_2,B_3,B_4)$)

Now, to average over all these scenarios the multinomial probability of having B_1 interferers in bank 1, B_2 in bank 2,....., etc., is given by (assuming independence of the condition of interference in all filters)

$$P(B_1,B_2,B_3,B_4) = \prod_{i=1}^{4} \binom{U}{B_i} \left(\frac{1}{N_h}\right)^{B_i} \left(1-\frac{1}{N_h}\right)^{U-B_i} \tag{2.18}$$

where B_1, B_2, B_3 and B_4 denote the numbers of the interferers in the four banks in the system (assuming an $M-ary$ system of $M=4$), U represents the maximum number of interferers per bank.

We average the conditional means and variances over all jamming scenarios (given by the above multinomial probability) to find the average mean and variances of the detection variable, i.e.,

$$\mu_N = \sum_{B_4=0}^{U} \sum_{B_3=0}^{U} \sum_{B_2=0}^{U} \sum_{B_1=0}^{U} (P(B_1,B_2,B_3,B_4,))(\mu_N \mid B_1,B_2,B_3,B_4)$$

$$\mu_{S+N} = \sum_{B_4=0}^{U} \sum_{B_3=0}^{U} \sum_{B_2=0}^{U} \sum_{B_1=0}^{U} (P(B_1,B_2,B_3,B_4,))(\mu_{S+N} \mid B_1,B_2,B_3,B_4)$$

$$\sigma_N^2 = \sum_{B_4=0}^{U} \sum_{B_3=0}^{U} \sum_{B_2=0}^{U} \sum_{B_1=0}^{U} (P(B_1,B_2,B_3,B_4,))(\sigma_N^2 \mid B_1,B_2,B_3,B_4)$$

$$\sigma_{S+N}^2 = \sum_{B_4=0}^{U} \sum_{B_3=0}^{U} \sum_{B_2=0}^{U} \sum_{B_1=0}^{U} (P(B_1,B_2,B_3,B_4,))(\sigma_{S+N}^2 \mid B_1,B_2,B_3,B_4) \tag{2.19}$$

we replace the average values of means and variances in eq. (2.17) by these given by eq. (2.18) to get the average P_D and P_{FA} over all statistics. That is because the false alarm probability P_{FA} of eq. (2.17) are based on specific multi access interference scenarios in the M filter banks (but could also represent single user case in an evident way). N_h represent the number of available Frequency Hop tones and $1/N_h$ is the probability of hitting any bank by like user interference. Probabilities of false alarm P_{FA} vs. N_h (P_D being a parameter) has been plotted in Fig. 2.7 assuming that all the multi access users have the same power.

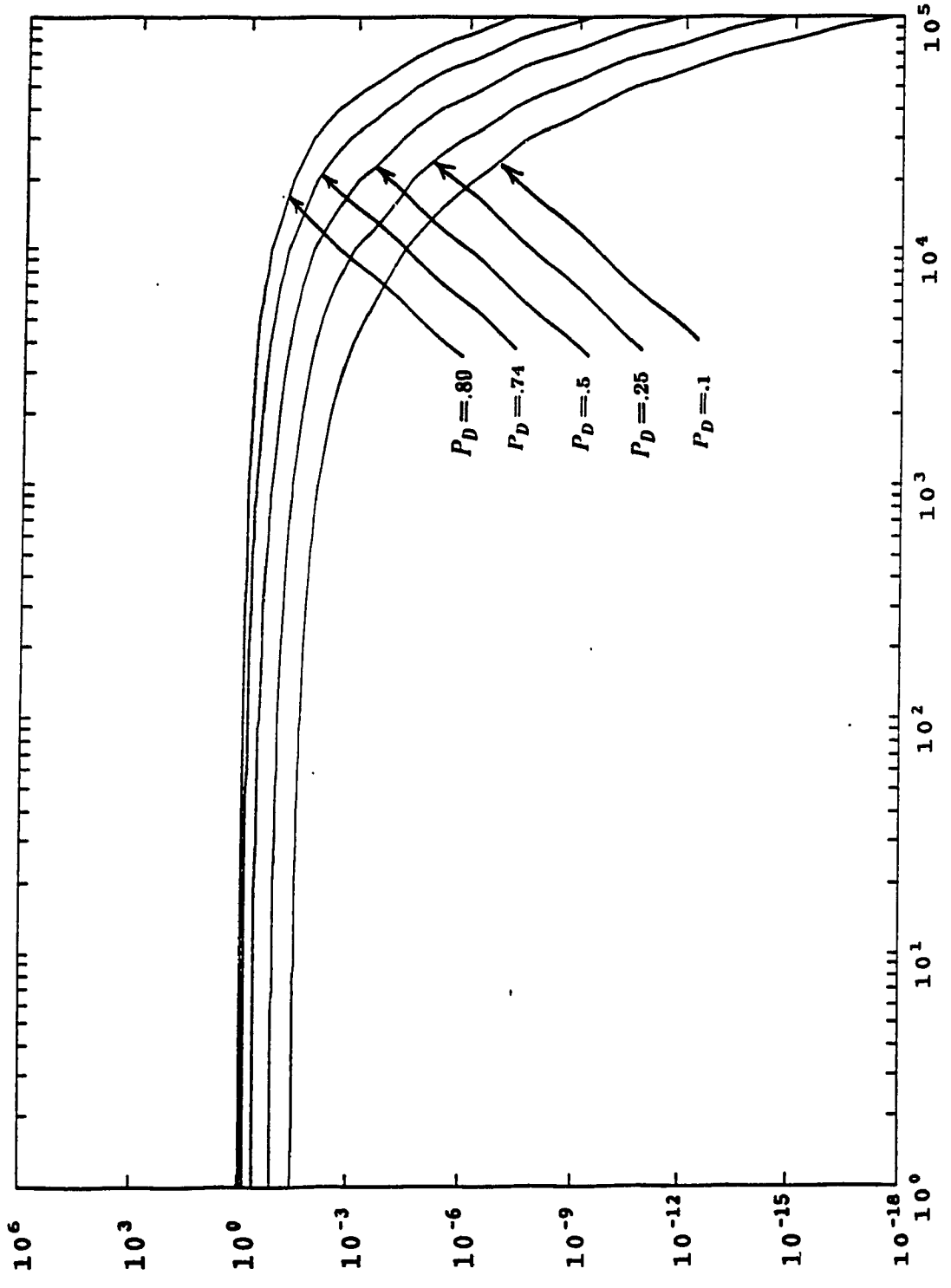

Fig. 2.8. Probabilities of false alarm P_{FA} vs. N_h (dwell time/hop time) for single user tone jamming. The parameters of the system are for an M-*ary* system of $M = 4$, the signal to noise ratio $SNR = .1$, the jamming power $J = 200$, the normalized signal power is equal = .5.

2.4.2 Operating Characteristics Under Single User and Multitone Jamming or Equivalently † Partial Band Jamming (both serial and parallel search cases)

The multiple tone jammer is the tone equivalent of the partial band noise jammer and is most effective against FH systems. We assume an intelligent jammer that has knowledge of the form of data and spread spectrum modulation, including such items as data rate, spreading bandwidth and hop rate, but no knowledge of the code for determining the spectrum spreading hop frequencies. The total jamming power is divided into q tones. The task of the jammer is to choose q and the tone spacing such that the received bit error is maximized [2.1]. The number of tones hitting the system is given by

$$q_j = \frac{J}{P} \tag{2.20}$$

where J is the jamming power and P is the signal power. The total spread spectrum transmission band W contains W/W_d FH bands so that the probability that any one of the M transmission bank is hit is given by

$$p = \frac{q_j}{\frac{W}{W_d}M} \tag{2.21}$$

The final value for P_{FA}, P_D in this case are determined still by eq. (2.17) where μ_N, μ_{S+N}, σ_N^2 and σ_{S+N}^2 are the average means and variances of the detection variable averaged over the multinomial probability of eq.(2.18) except for replacing $1/N_h$ by p of eq. (2.21) and U by q of eq. (2.20) and B_1, B_2, B_3 and B_4 denote the number of tones hitting the four banks of the

† Partial band jamming is translated into and and approximately equal in effect to a set of multi tone jamming.

system.

Probabilities of false alarm P_{FA} vs. N_h (P_D being a parameter) has been plotted in Fig. 2.8. The dwell time τ_d (affecting eq. (2.17)) in this case is given by

$$N_h = \frac{\tau_d}{T_h} \tag{2.22}$$

where τ_d is the integration time per sub code, T_h is the hop time. $LN_h T_h$ equals the total code length (one code length contains several sub code).

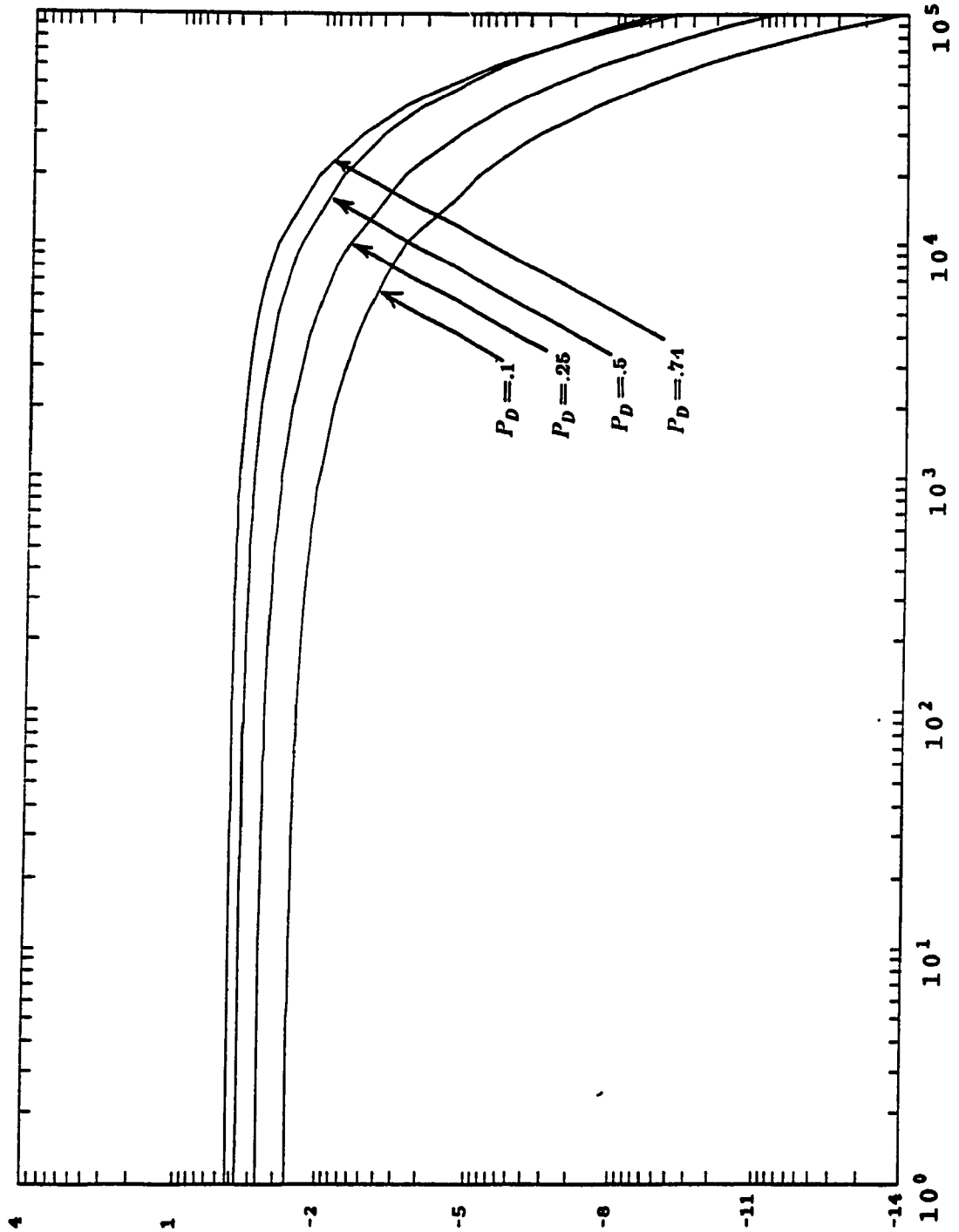

Fig. 2.7. Probabilities of false alarm P_{FA} vs. N_h (dwell time/hop time) for multi access jamming. The parameters of the system are for an *M–ary* system of $M = 4$, $SNR = .1$ and number of users in the system $U = 16$.

REFERENCES

[2.1] L. Zeimer, R.L. Peterson, 'Digital Communications and Spread-spectrum Systems', Mc-Millan Book Company, 1985, Ch-8.

[2.2] M.K. Simon, J.K. Omura, R.A. Scholtz, B. K. Levitt 'Spread Spectrum Communications', Computer Science Press.

[2.3] R. C. Dixon, 'Why Spread Spectrum ?', IEEE Communications Magazine, pp. 21-25, July 1975.

[2.4] R. C. Dixon, 'Spread-Spectrum Systems', Wiley & Sons, New York, 1985.

[2.6] W.K. Alem, G.K. Huth, J.K. Holmes, 'Spread Spectrum Acquisition and Tracking Performance for Shuttle Communication Link', IEEE, Trans. on Communication, Vol. Com. 26, pp.1689-1702, Nov. 1978

[2.7] D. M. Dicarlo, and C.L. Weber, 'Statistical Performance of Single Dwell Serial Synchronization System', IEEE, Trans. on Comm., Com-25, pp. 778-783, August 1977

[2.8] J.K. Holmes and C.C. Chen, 'Acquisition Time Performance of PN Spread Spectrum System', IEEE, Trans. on Comm., Com-25, pp. 778-783, August 1977

[2.9] D.M. Dicarlo, C.L. Weber, 'Multiple Dwell Serial Search: Performance and Application to Direct Sequence Code Acquisition', IEEE, Trans.

on Communications., Vol. Com-31., No. 5, pp. 650-659, May 1983.

[2.11] S.S. Rappaport, D.M. Greleco, 'Spread Spectrum Signal Acquisition: Methods and Technology', IEEE, Communications Magazine, Vol. 22, No. 6, pp. 6-21, June 1984.

[2.12] S.S. Rappaport and D.L. Schilling, 'A Two Level Coarse Code Acquisition Scheme for Spread Spectrum Radios', NTC' 79, Conference Record, Nov. 1979, pp. 54.6.1-54.6.6, Birmingham, AL.

[2.13] G.K. Huth, A. Polydoros, and M.K. Simon, 'Frequency Synchronization of a Frequency Hopped MFSK Communication System', ICC' 81, Conference Record June 1981, pp. 34.1.1-34.1.5, Denver, Co.

[2.14] A.K. Elhakeem, G.S. Takhar, S.C. Gupta, 'New Code Acquisition Techniques in Spread Spectrum Communications', IEEE, Trans. on Comm., Vol. COM-28, pp. 246-259, February 1980.

[2.15] L.B. Milstein and P.K. Das, 'Spread Spectrum Receiver Using Surface Acoustic Wave Technology', IEEE, Trans. on Communications, Com. 25, No. 8, pp. 841-847, August 1977

CHAPTER III

CODING COUNTER MEASURES FOR FH/M-ARY FSK MULTI ACCESS SPREAD SPECTRUM COMMUNICATIONS

3.1 Introduction

Spectrum spreading produces large system performance improvement by spreading the jammer power over the full spread communication bandwidth. But smart sophisticated jammers can severely degrade the system performance of the spread spectrum system [3.1], [3.2]. In the most effective jamming strategies all jamming resources are concentrated on some fraction of the transmitted symbols, although a small fraction of the data may be hit, those data may suffer a high conditional error rate and the demodulator output error occurs in burst. Moreover, to any spread spectrum transmitter/receiver pair that is communicating in a network of radios, other spread spectrum signals can be collectively regarded as a jamming signal each such link should be able to achieve reliable communications with this unintentional mutual interference [3.2]. An effective counter measure against these forms of jamming is to use the error control redundancy [3.2]. Evaluation of the coded error probabilities [3.3], [3.4], [3.5] for antijam communications systems show that gains of the order of 30-40 db can be obtained over uncoded systems.

In a FH/MFSK system when the jammers optimize their system parameters based on their assumed knowledge of the FH/MFSK target, the resulting performance degradation can be severe, particularly at low error probabilities. To counteract this threat, the FH system must incorporate some coding redun-

dancy.

There are several issues that arise when considering coding for spread-spectrum communications [3.6]. One issue is that whether or not the decoder knows if the received signal has been jammed or not. In analyzing these coded systems the use of a detection metric that assumes that the receiver can determine with certainty whether a given hop is jammed is called the perfect jamming state knowledge or *side information*. The decoder knowing and using these *side information* can improve the performance compared to coding without *side information*.

For a high performance system in benign and hostile environment it is desirable to provide reliable communications with a choice of coded transmissions. A concatenated coded scheme is the preferred one (for a given code length) since decoding is performed on two or more simpler codes. Reliable communication is achieved with a decoder whose complexity grows algebraically rather than exponentially with block length [3.7].

In this chapter, we review some of the previous work on the performance of codes under different jamming scenarios, multi-access interference, fading, etc. We caution the reader that our intentions are to evaluate coding performance bounds rather than generation of new code types or discussion of their algebraic properties.

3.2 The performance of some coded systems

The performance of a coded system in most text books and papers has not been derived in a closed form error rate expressions. In most of these cases Chernoff bounding techniques has been used [3.5, 3.6, 3.9, 3.10, 3.11]. The accuracy of these bounds remains a source of concern and raises concern

about their credibility [3.12, 3.13]. In the literature the effectiveness of various block, convolutional and concatenated codes for FH/MFSK system in partial band noise [3.5, 3.10, 3.11, 3.13, 3.14] has been determined. It has been determined in the literature that RS codes alone do not provide sufficient redundancy to produce acceptable FH/MFSK performance in worst case jamming [3.10, 3.14]. The next recourse is to concatenate RS outer code with a suitable inner code usually RS or convolutional code. Selected combinations of (n, k) and the concatenated scheme show significant performance improvements over the dual k or RS codes alone.

Milstein, Davidovici and Schilling [3.14] compared the performance of various forward error correction techniques to binary FSK and $M-ary$ FSK over a Rayleigh fading channel in the prescence of pulse burst jammer [3.14]. They used both binary and non-binary codes as well as concatenated codes consisting of either block or a convolutional inner code and RS outer code. They found that, when RS codes alone are used with binary FSK modulation it was not powerful enough to achieve the desired performance (10^{-5}). Multiaccess interference was not taken into consideration.

Torrieri evaluated the performance analysis of FH/MFSK against partial band jamming [3.14]. The effects of RS, binary block and convolutional codes were analyzed. He found that the non binary modulation and RS coding does not appear to be advantageous. Binary FSK with convolutional or concatenated coding offers a simpler implementation and superior performance [3.14].

Stark investigated the performance of codes in a FH/SS system with partial band interference [3.5]. He also found the gain achievable when the use of *side information* in decoding is used. He tabulated the values of E_b/N_j

necessary for bit error probability of (10^{-5}) for soft decision with *side information* and for hard decisions both with and without *side information*. When *side information* is available, the difference between hard and soft decision is 1 db. He found that the difference between hard decision with and without *side information* varies considerably [3.5].

Pursley and Stark studied the performance of a FH binary and $M-ary$ system under diversity transmission, RS coding and parallel error correction and erasure correction decoding in partial band interference [3.14]. They found the SNR (E_b/N_j) that is required to achieve a specified bit error rate as a function of ρ (partial band jamming factor) for two different codes and various diversity levels.

A common characteristics of the work described above is that although the effects of combined jamming and fading or combined other-user interference and fading on FH/SS systems have been studied, the effects of combined hostile and other user interferences have not been investigated. A comprehensive analysis of a FH/SS systems with binary or $M-ary$ FSK modulation which employ forward error control (FEC) coding and operate in a combined partial band noise jamming, other-user interference, Rician nonselective fading and additive white Gaussian noise (AWGN) environment was conducted by Geraniotis and Gluck [3.8] which we describe in the next section.

3.3 Performance in the Prescence of Partial Band Noise Jamming, Rician Nonselective Fading, and Multi Access Interference

Geraniotis and Gluck [3.8] made a detailed analysis of combating combined interference in SSMA (spread spectrum multiple access) FH/MFSK systems [3.8]. The interference environment consisted of partial band noise jamming, non selective Rician fading, other user interference and thermal noise. The authors evaluated the maximum number of users that can be supported by the system as a function of ρ keeping E_b/N_j fixed.

In the following we describe some of the coding schemes considered i Geraniotis and Gluck in their work. In particular, 3.3.1) Reed-Solomon (RS) codes, 3.3.2) repetition code

The FH/SSMA system considered was that of [3.11] in a partial-band jamming and Rician nonselective fading environment. MFSK data modulation with noncoherent demodulation with slow Frequency Hopping (SFH) was considered. The partial-band noise interference is the one commonly used in the literature.

The nonselective Rician fading channel model is that of [3.15] and [3.16]. The received signal consists of a nonfaded component and an attenuated faded component. The probability of error of an $M-ary$ FSK with noncoherent demodulation is given by

$$P_{e,M}=\sum_{m=1}^{M-1}\binom{M-1}{m}\frac{(-1)^{m+1}}{m+1+m\,\beta(\eta)}\exp\left\{\frac{-m\,\delta(\eta)}{m+1+m\,\beta(\eta)}\right\} \qquad (3.1)$$

where $\beta(\eta)=\Lambda(\eta)/(1+\gamma^{-2})$, $\delta(\eta)=\Lambda(\eta)/(1+\gamma^2)$. $\Lambda(\eta)=\overline{E}_b \log_2 M/\eta$ is the received signal to noise ratio. γ^2 is the ratio of the expected relative strength of the scatter component to the strength of the nonfaded component. $\gamma^2=0$

implies that $\beta(\eta)=0$ and $\delta(\eta)=\Lambda(\eta)$, so that the Rician fading channel becomes an AWGN channel. Similarly, $\gamma^2=\infty$ implies that $\beta(\eta)=\Lambda(\eta)$ and $\delta(\eta)=0$, so that the channel becomes a Rayleigh fading channel.

3.3.1 Reed Solomon Codes [3.8]

RS code has a large minimum distance. It can correct burst errors as well as random errors and the implementation is economical for the performance attainable [3.7], and they are relatively straight forward to implement. RS codes are usually taken as the outer code. The following three cases were considered i) error correction, ii) erasure/error correction, and iii) parallel erasure/error correction. In case i) there is no information about the state of the channel, and thus, the RS decoder only attempts to correct the errors. In case ii) it was assumed that channel monitoring provides information about the state of the channel which can be used by the RS decoder to erase the symbols which are subject to heavy interference. In this case the decoder attempts to correct the erasures and the few errors due to thermal noise.

$(n\,,\,k)$ RS codes over $GF(2^{km})$ are employed, there are m $M-ary$ symbols in each RS symbol and each $M-ary$ symbol contain k bit. For case i) the probability of symbol error for uncoded system was upper bounded by

$$p_s \leq 1-(1-P_h)^{(K-1)}[(1-\rho)(1-P_0)^m+\rho(1-P_{j0})^m] \tag{3.2}$$

In (3.1) P_h denotes the probability of hit from another user (i.e., both users use the same frequency for the part of their dwell times. The probability of a hit for any RS symbol and $M-ary$ FH/SS asynchronous system has been shown [3.9] to be upper bounded by

$$P_h=(1+\frac{m}{N_s})\frac{1}{q} \tag{3.3}$$

(the m in the numerator is due to the fact that each RS symbol contains an m $M-ary$ FSK symbols, and thus it is more likely to be hit than a single $M-ary$ FSK symbol); q is the number of available frequencies, N_s is the number of symbol per hop. The probabilities P_0 and $P_{J,0}$ in (3.2) denote the error probabilities of an $M-ary$ FSK system with noncoherent demodulation disturbed by AWGN of one sided spectral densities N_0 and (N_0+N_j/ρ), respectively. Thus $P_0 = P_{e,M}(N_0)$ and $P_{j,0} = P_{e,M}(N_0 + N_j/\rho)$, where $P_{e,M}(\ .\ )$ is defined in (1). In (3.1), $(1-\rho)(1-P_0)^m + \rho(1-P_{J,0})^m$ is the probability of no error due to Gaussian noise in an $M-ary$ symbols (after averaging over partial band jamming); $(1-P_h)^K$ is a lower bound on the probability of no error due to any of the other $K-1$ users.

When decoding of RS codes with hard decision is employed, the symbol error probability of the coded system is given by

$$P_{e,s} = \sum_{j=t+1}^{n} \frac{j}{n} \binom{n}{j} p_s^j (1-p_s)^{n-j} \tag{3.4}$$

where $t = \lfloor (n-k)/2 \rfloor$ is the error correction capability of the RS (n, k) code. Eqn. (3.4) is valid when all the RS symbols in the same hop (dwell time) are subject to independent errors and serves as an upper bound for the $M-ary$ symbol error probability of the coded system.

For case ii) the probability of an erasure is

$$\epsilon_s = \rho + [1 - (1-P_h)^{K-1}] - \rho[1 - (1-P_h)^{K-1}] \tag{3.5}$$

In their work it was assumed that the decoder erases a symbol if the jammer is present and/or if interference from other users is present. The probability of a symbol error is

$$p_s = [1-(1-P_0)^m](1-\epsilon_s) \tag{3.6}$$

since $(1-\epsilon_s)$ is the probability of no interference from the jammer or from other users, and $(1-(1-P_0)^m)$ is the probability of error due to the thermal noise alone. In this case, the probability of a RS symbol error at the decoder is

$$P_{e,s} = \sum_{l=0}^{n} \sum_{\substack{j=e-2l+1 \\ j\geq 0}}^{n-l} \frac{j+l}{n} \binom{n}{j} \binom{n-j}{l} p_s^l \epsilon_s^j (1-p_s-\epsilon_s)^{n-l-j} \tag{3.7}$$

In case iii) parallel erasures/errors decoding algorithm (Appendix 3A) [3.11] is applied. When the number of erasures is less than or equal to $e=n-k$, the erasure correction capability of the code the contribution to the decoder's error probability is

$$P_{e,s;1} = \sum_{\substack{j=0 \\ l+j\leq n}}^{e} \binom{n}{j} \epsilon_s^j (1-\epsilon_s)^{n-j} \sum_{l=0}^{n-j} \frac{j+l}{n} \binom{n-j}{l} P_0^l (1-P_0)^{n-j-l} \tag{3.8}$$

where ϵ_s was defined in (3.5) and P_0 is the error probability of an $M-ary$ symbol due to thermal noise.

In (3.8), j is the number of erased symbols, $n-j$ is the number of symbols that were not erased, and l is the number of symbols out of those last $n-j$ symbols that resulted in a receiver error due to the thermal noise alone.

When the number of erasures is larger than $e=n-k$ the contribution to the decoders error probability becomes

$$P_{e,s;2} = \sum_{j=e+1}^{n} \binom{n}{j} \epsilon_s^j (1-\epsilon_s)^{n-j} \sum_{\substack{l_1=0 \\ t-1\leq l_1+l_2 \\ n}}^{j} \sum_{l_2=n-l_1}^{n-j} \frac{l_1+l_2}{n} \binom{j}{l_1} \overline{p}^{l_1} (1-\overline{p})^{j-l_1} \binom{n-j}{l_2} P_0^{l_2} (1-P_0)^{n-j-l_2} \tag{3.9}$$

In (3.9), $\overline{p}$ denotes the probability error given that there is partial-band or multiple access interference and is given by

$$\overline{p} = \frac{\epsilon_1}{\epsilon_s}[1-(1-P_{j,0})^m] + \frac{\epsilon_2}{\epsilon_s}(1-\frac{1}{M^m}) \tag{3.10}$$

where ϵ_1 denotes the probability of being noise jammed but not hit by other users, and ϵ_2 denotes the probability of being hit by other users and are given by

$$\epsilon_1 = \rho(1-P_h)^{K-1} \tag{3.11a}$$

$$\epsilon_2 = 1-(1-P_h)^{K-1} \tag{3.11b}$$

In (3.9), j is the number of symbols in an RS codeword which are subject to either partial-band interference or multiple-access interference, whereas $n-j$ is the number of symbols subject only to AWGN. Then l_1 out of j symbols which are subject to interference are received in error, whereas $j-l_1$ are not: and l_2 out of the $n-j$ symbols subject to only AWGN are received in error, whereas $n-j-l_2$ are received correctly. The decoder commits an error when the total number of errors l_1+l_2 exceeds t the error correction capability of the RS code. Finally, the total error probability at the output of the RS decoder is given by $P_{e,s} = P_{e,s;1} + P_{e,s,2}$.

In Fig. 3.1 E_b/N_j is plotted versus ρ for a Reed-Solomon RS(64, 32) code (rate 1/2) with either error-only or parallel erasure/errors decoding. The values of the system and channel parameters are $P_e = 10^{-3}$, $K = 5$ $E_b/N_0 = 12$ db, and the relative power of the component of the Rician channel γ^2 is varying [$\gamma^2 = 0$ (AWGN), 0.01, 0.1, 1 and 10]. In the same figure it can be noticed the improvement that the parallel erasure/error decoding scheme

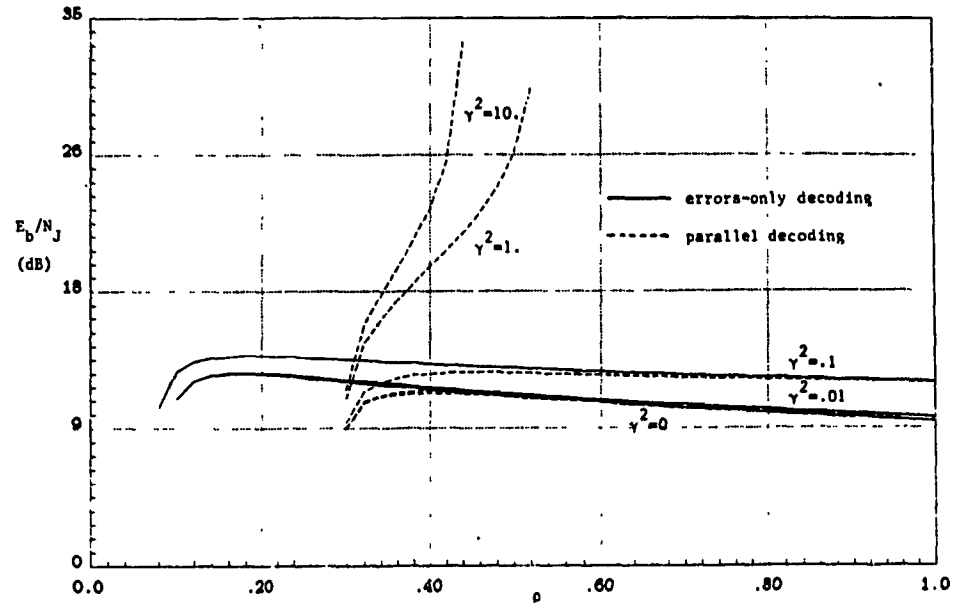

Fig. 3.1. Minimum E_b/N_j required for $P_e = 10^{-3}$ versus ρ for asynchronous FH/SSMA communications employing RS (64, 32) codes with error-only and parallel erasure/error decoding ($q = 100, N_b = 12, M = 8, m = 2, E_b/N_o = 12$ db , $K = 5$); Rician fading channel with varying γ^2 [3.8].

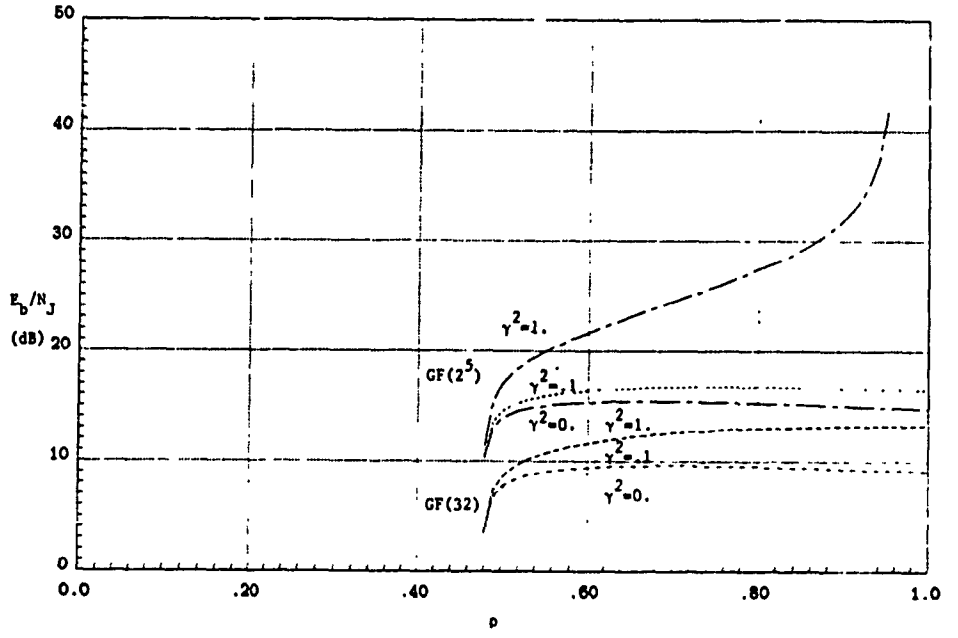

Fig. 3.2. Minimum E_b/N_j required for $P_e = 10^{-3}$ versus ρ for asynchronous FH/SSMA communications employing RS(32, 8) codes with parallel erasure/error decoding over various $GF(M^m)$, with corresponding *M–ary* FSK modulation ($q = 100, N_b = 10, E_b/N_0 = 20$ db, $K = 5$); Rician fading channel with varying γ^2 [3.8].

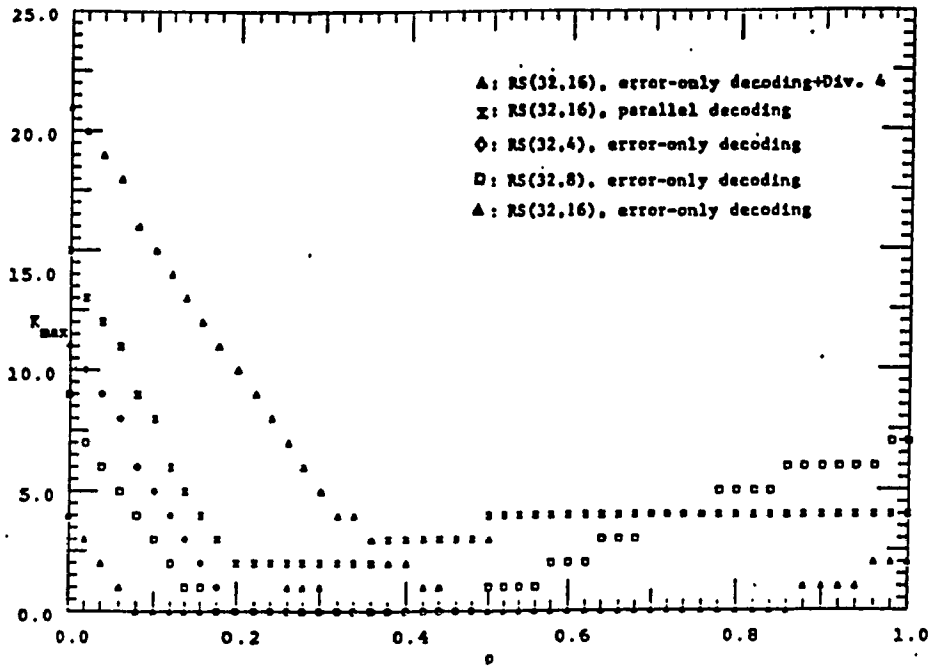

Fig. 3.3 k_{max} versus ρ for asynchronous FH/SSMA communications employing 32-*ary* FSK and Reed-Solomon coding with various rates and decoding methods with and without diversity ($q = 100, N_b = 10, E_b/N_0 = 20$ db. AWGN, $E_b/N_j = 10$ db, AWGN, $P_e = 10^{-5}$) [3.8].

offers over the error only decoding scheme for both $(E_b/N_j)_{\max}$, which shows the merits of the parallel erasure/error decoding over the error only decoding scheme and should be preferred for combating severe interference.

In Fig. 3.2 E_b/N_j vs. ρ is plotted for RS(32, 8) code (rate 1/4) parallel error/erasures decoding and the cases ($M = 2$, $m = 5$), ($M = 32$, $m = 1$) for $K = 5$ and a Rician fading channel with varying γ^2. A comparison of the two case indicates that ρ^* does not change considerably but $(E_b/N_j)_{\max}$ does. As the relative power in the fading component increases from $\gamma^2 = 0$ to 0.1 and then to 1, the difference in the required $(E_b/N_j)_{\max}$ increases substantially less signal to jammer power ratio to achieve the same bit error probability. Therefore, it is preferable to employ $M-ary$ instead of binary FSK modulation in this case.

In Fig. 3.3 the multiple access capability versus ρ is presented for several RS coded FH/SS systems. For small values of ρ, RS(32, 16) with diversity 4 outperforms all the other systems; in this range of ρ, the other user interference is dominant. For large values of ρ, the RS(32, 8) code outperforms the other schemes; in this range of ρ, the jamming interference is dominant.

3.3.2 Repetition code [3.8]

When information about the state of the channel is not available, majority vote decoding (in which the decoder decides in favor of the symbol which was received most times) with hard decisions in the maximum likelyhood decoding algorithm is used. For binary repetition code of block length n, the bit error rate is

$$P_{e,b} = P_2(n;p) = \begin{cases} \sum_{l=(n+1)/2}^{n} \binom{n}{l} p^l (1-p)^{n-l} & ; n \text{ odd} \\ \sum_{l=n/2+1}^{n} \binom{n}{l} p^l (1-p)^{n-l} + \frac{1}{2}\binom{n}{n/2}[p(1-p)]^{n/2} & ; n \text{ even} \end{cases} \tag{3.12}$$

where p denotes the error probability for a binary channel with combined multiple-access interference, partial-band jamming, Rician nonselective fading, and thermal noise, which can be obtained from (3.2). For M-*ary* repetition code ($M>2$) the symbol error probability can be obtained from the formula

$$P_{e,s} = P_M(n;p) = 1-\sum_{i=0}^{n-1} a_i\, p^i (1-p)^{n-i} \tag{3.13}$$

where the coefficients a_i are provided in Appendix A of [3.5], and p is as above.

In Fig. 3.4, E_b/N_j is plotted vs. ρ for repetition codes of rates $1/L = 1/4, 1/5, 1/6, 1/7, 1/8$, and $1/9$ without side information and 32-*ary* FSK modulation. For the parameters given it appears that the rate 1/8 repetition code is the optimal such code.

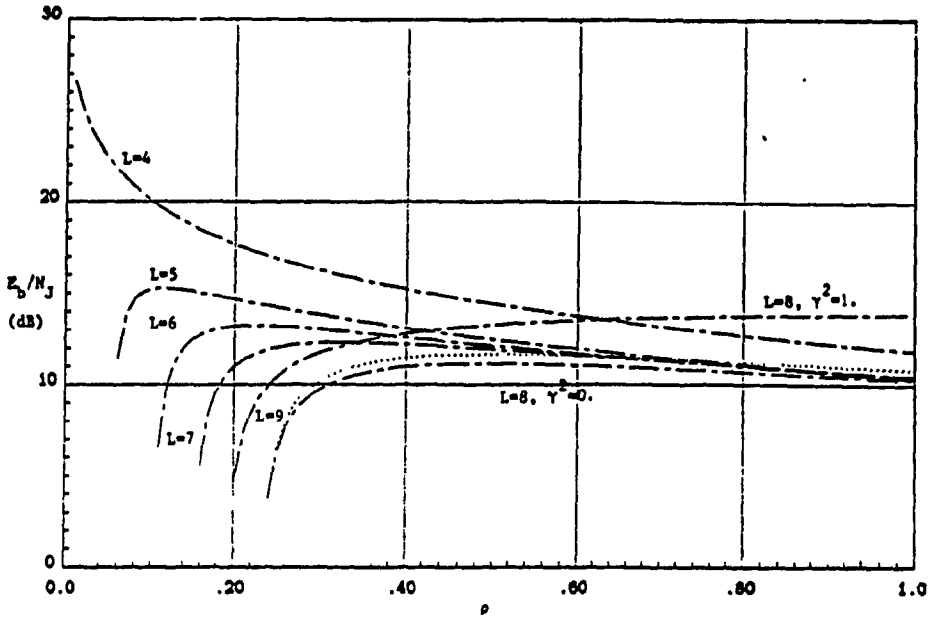

Fig. 3.4. Minimum E_b/N_j required for $P_e = 10^{-3}$ versus ρ for asynchronous FH/SSMA communications employing 32–*ary* FSK and varying diversity without side information ($q = 100, N_b = 10, E_b/N_0 = 20$ db, $K = 5$); AWGN channel; for $L = 8$, AWGN channel and Rician fading channel with $\gamma^2 = 1$ [3.8].

APPENDIX 3A

Parallel Error and Erasure Decoding Algorithm

The block diagram of the parallel error erasure decoding algorithm [3.8], [3.9] is illustrated in Fig. 3.6. In this decoding decoding algorithm the signal is first dehopped and demodulated. The output of the dehopper is a sequence of L diversity receptions for each of the n code symbols ($L = 1$ in eqns (3.1)-(3.11)). Side information regarding the prescence of interference is derived from the dehopper and demodulator. The decision statistic is formed from the information from the L diversity combiner and from the information from the side information. The side information is used to attach flags to unreliable diversity receptions. The diversity combiner forms the square law combination of all unflagged diversity receptions. If at least one of the diversity receptions is not flagged the decision device is presented with a noise-free symbol. A (hard) $M-ary$ decision is made on the symbol, and this decision is fed into the error correction decoder. For any symbol in which all diversity receptions are flagged, the erasure correction decoder sees only an erasure.

An (n, k) Reed-Solomon code will correct up to $e \triangleq n-k$ erasures out of n symbols or up to $t \triangleq \lfloor (n-k)/2 \rfloor$ errors out of n symbols. More generally it will correct any combination ϵ erasures and τ errors provided that $2\tau+\epsilon$ does not exceed $n-k$.

The input to the error correction decoder contains no erasures; it is sequence of $M-ary$ symbols from the output of the decision device. The erasure correction decoder has an erasure in each position where all diversity receptions are flagged, and an $M-ary$ symbol in each position where all

diversity receptions is not flagged. The erasure system counts how many erasure it makes, and if the number does not exceed e, the erasure correction algorithm produces a correct answer. The erasure correction decoder does not attempt to decode if the number of erasures exceed e. If there are too many erasures erasure correction decoder defaults to the error correction decoder.

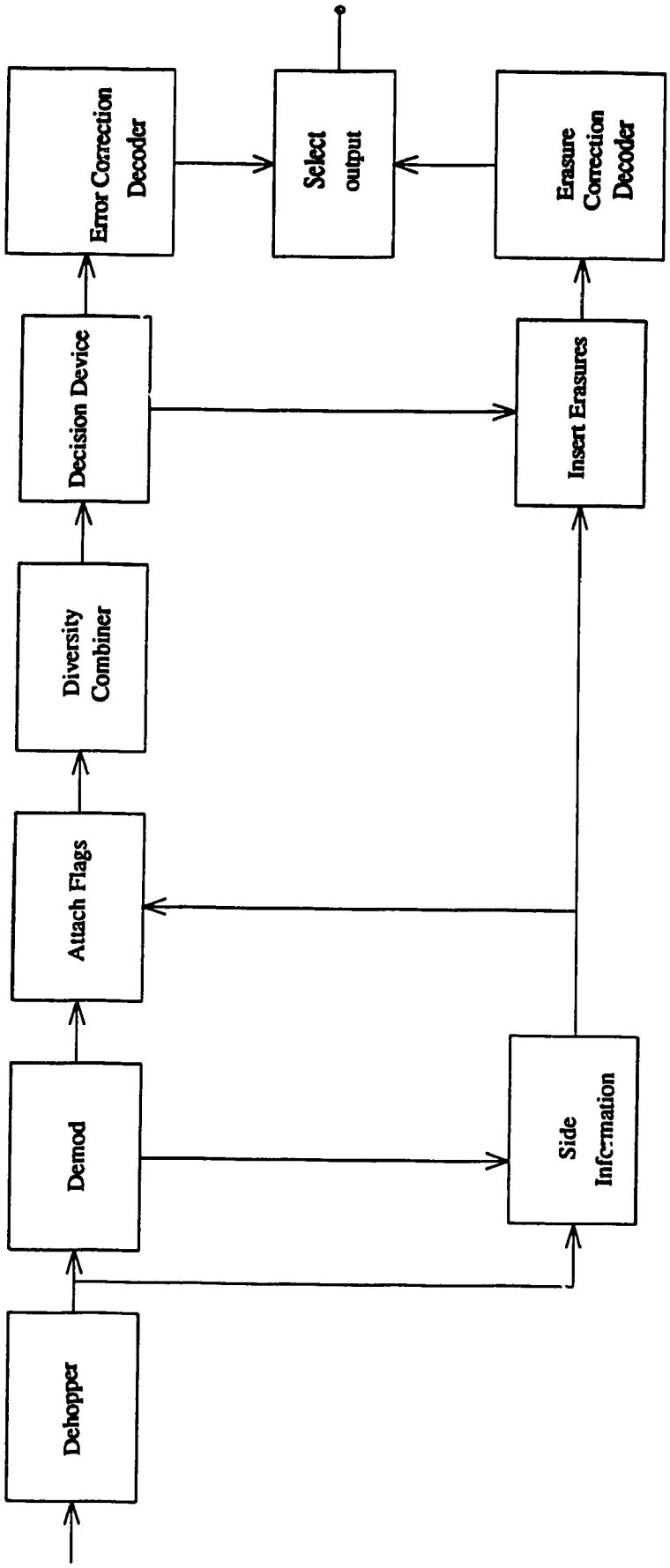

Fig. 3.5. Block diagram of demodulator/decoder for parallel error and erasure correction [3.9]

REFERENCES

[3.1] L. Zeimer, R.L. Peterson, 'Digital Communications and Spread Spectrum Systems', McMillan Publishers, New York.

[3.2] M.K. Simon, J.K. Omura and R.A. Scholtz, B. K. Levitt, 'Spread Spectrum Communications', Computer Science Press.

[3.3] J.K. Omura and B.K. Levitt, 'A General Analysis of Antijam Communication Systems', Nat. Telecommunications Conference Record, Nov. 1981, pp B7.3.1-B 7.3.5

[3.4] G.C. Clark and J. B. Cain, 'Error-Correction Coding for Digital Communications, New York: Plenum, 1981

[3.5] W.E. Stark, 'Coding for Frequency-Hopped Spread-Spectrum Communication with Partial-Band Interference - Part II: Coded Performance', IEEE, Trans. on Comm., Vol. Com. 33, No 10, pp. 1045-1057, Oct. 1985

[3.6] W.E. Stark, 'Coding for Frequency-Hopped Spread-Spectrum Communication with Partial-Band Interference- Part 1 : Capacity and Cutoff Rate', IEEE Trans. on Comm., Vol. Com.33, No.10, pp. 1036-1044, October 1985.

[3.7] A. Hauptschein, 'Practical High Performance Concatenated Coded Spread- Spectrum Channel for JTID's', NTC'77

[3.8] E. Geraniotis, J.W. Gluck, 'Coded FH/SS Communications in the Combined Partial-Band Noise Jamming, Rician Nonselective Fading Multiuser Interference', IEEE Journal on Selected Areas in Communications, Vol. SAC-5, No.-2, pp. 194-213, Feb. 1987.

[3.9] E.A. Geraniotis, M.B. Pursley, 'Error Probabilities for Slow Frequency Hopped Spread-Spectrum Multiple-Access Communications over Fading Channel', IEEE, Trans. on Comm., Vol. Com-30, pp. 996-1009, May, 1982.

[3.10] Don J. Torrieri, 'Frequency Hopping with Multiple Frequency Shift Keying and Hard Decisions', IEEE, Trans. on Comm., Vol. Com 32, No. 5, pp. 574-582, May 1984.

[3.11] M.B. Pursley, W.E. Stark, 'Performance of Reed-Solomon Coded Frequency Hopped Spread-Spectrum Communications in a Partial-Band Interference Fading Channel', IEEE Trans. on Comm., Vol. Com-33, No-8, pp. 767-774, August 1985.

[3.12] J.S. Lee, L.E. Miller, R.H. French, 'The Uncoded Performance for Certain ECCM Receiver Design Strategies for Multihops/Symbols FH/MFSK Waveform', IEEE, Journal on Selected Areas in Communications, Vol. SAC 3, No. 5, September 1985

[3.13] L.E. Miller, J.S. Lee, A.P. Kadrichu, ' Probability of Error Analyses of a BFSK Frequency Hopping System with Diversity Under Partial Band Jamming Interference - Part III : Performance of a Square Law Self Normalizing Soft Decision Receiver', IEEE, Trans. on Comm.,

Vol. Com-34, pp. 669-675, July 1986.

[3.14] L.B. Milstein, S. Davidovici, D.L. Schilling, 'Coding and Modulation Techniques for Frequency Hopped Spread-Spectrum Communications Over a Pulse Burst Jammed Rayleigh Fading Channel', IEEE, Journal of Selected Areas in Communications, Vol. SAC 3, No. 5, pp. 664-651, Sept. 1985

[3.15] M.B. Pursley, 'Coding and Diversity for Channels with Fading and Pulsed Interference', in Proc. 1982 conf. Informn. Sci. Syst., Mar. 1982, pp 413-418.

[3.16] A.M. Michelson and A.H. Levesque, 'Error Control Technique for Digital Communication', Wiley, New York, 1985

CHAPTER IV

BOUNDS ON CONCATENATED CONVOLUTIONAL CODING PERFORMANCE OF FREQUENCY HOPPING MULTI ACCESS SYSTEMS

4.1 Introduction

The complexity of conventional coding systems grows exponentially with the block length for block codes (or with the constraint length for convolutional codes). To overcome the complexity of very long codes, the idea of cascading two or more codes of lesser complexity to achieve highly reliable communications was considered by Elias [4.1] and later by Forney [4.2]. The technique of using two or more block codes over different alphabets to obtain a very low error rate is known as concatenated coding.

Forgetting for the moment synchronization and delay issues, a convolutional code generally performs better than a block code of the same complexity. Maximum likelihood (i.e., Viterbi [4.3]) decoding of convolutional codes with a moderate constraint length can provide an error rate less than 10^{-2} at a rate slightly higher than the R_{comp} of the noisy channel. Forney's work [4.4] suggested that a concatenated coding system with a powerful outer code can perform reasonably well when its inner decoder is operating with a probability of error in the range between 10^{-2} and 10^{-3}.

In this chapter, we use convolutional codes for concatenation with convolutional codes and the purpose is to determine the number of levels of concatenation required to achieve an acceptable error rate.

Moreover, we use the ensemble average error bound of convolutional code [4.5], [4.6] for determining the error probability at different stages of concatenation and to determine the relationship between the exponential bound parameter $E_c(R)$ and the rate R at different stages of concatenation.

4.2 Analysis of the Concatenated Convolutional Coding Systems

We assume that we have a perfect mechanism for obtaining the side information, i.e., the information relating exact number of interferers in a certain Frequency Hop (FH) to all users.

We represent α_1 as the probability of number of interferers in a certain Frequency Hop (FH) equalling one.

α_2 represents the probability of number of interferers in a certain Frequency hop (FH) equalling two or more.

P_0 equals the probability of symbol error under a channel contaminated only by all white Gaussian noise (AWGN). P_1 is the probability of error when there is one interferer and P_2 is the probability of error when there are two or more interferers in the system. It follows that,

$$P_1 = \alpha_1.\beta_1 \tag{4.1}$$

$$P_2 = \alpha_2.\beta_2 \tag{4.2}$$

In (4.1) β_1 equals the probability of error when there is one interferer in all bits and symbols of the hop. α_1 is as described earlier. In (4.2) β_2 equals the probability of error when there are two or more interferer in all bits and symbols of the hop and also α_2 is described earlier.

$$P_0 = (1 - \alpha_1 - \alpha_2)P_0 \tag{4.3}$$

Where P_0 is the probability of bit error under pure AWGN noise.

$$\bar{P}_b = P_0 + P_1 + P_2 \tag{4.4}$$

Now, the average probability of error $\bar{P}_b$ given in eq. (4.4) can be expressed as

$$\bar{P}_b = \alpha_1\beta_1 + \alpha_2\beta_2 + (1 - \alpha_1 - \alpha_2)\beta_0 \tag{4.5}$$

We replace the transmission channel, the side information and the demodulation channel by an equivalent BSC channel (shown in Fig 4.1). Whose transfer rate R_0 and the capacity C can be found from the cross over probability $\bar{P}_b$.

In our system, detection of the cases of no interferer, one interferer or two or more interferer occur per hop. The envelope of the output of the $M-ary$ bank is sampled and the contribution of all the symbols per hop are added and compared with a threshold.

The probabilities α_1 and α_2 are found out as follows: If there are U users in the system and N is the frequency hop (FH) base bands in the W spread spectrum bandwidth. α_1 is given by

$$\alpha_1 = \binom{U}{1}\left(\frac{1}{N}\right)\left(1-\frac{1}{N}\right)^{U-1} \tag{4.6}$$

where N is given by

$$N = \frac{W}{M\dfrac{R_b}{\log_2 M}} \tag{4.7}$$

In (4.7) R_b is the bit rate and M is the alphabet size. α_0 is given by

$$\alpha_0 = \binom{U}{0}\left(\frac{1}{N}\right)\left(1-\frac{1}{N}\right)^{U} = \left(1-\frac{U}{N}\right)^{U} \tag{4.8}$$

and so

$$\alpha_2 = 1-\frac{U}{N} - \left(1-\frac{U}{N}\right)^{U} \tag{4.9}$$

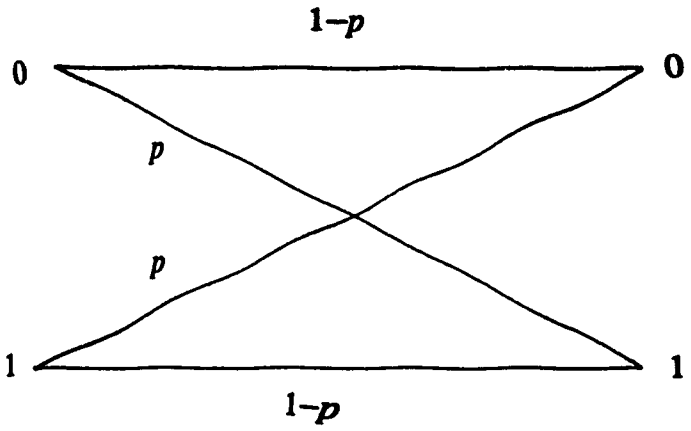

Fig. 4.1 Schematic of the cross over probabilities of binary symmetric channel

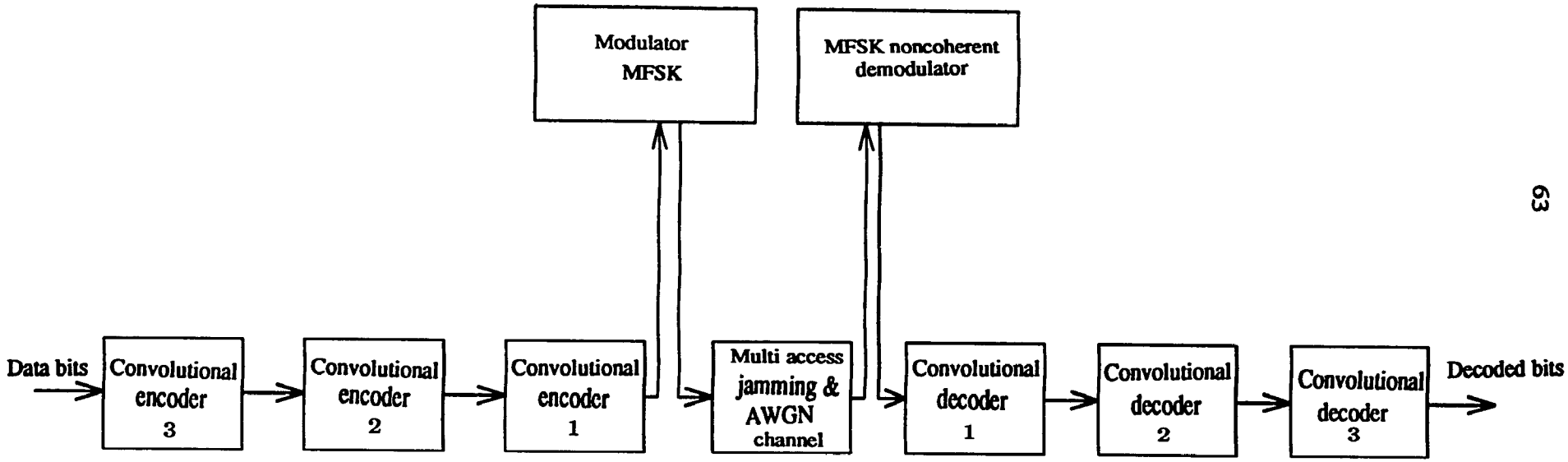

Fig. 4.2 Block diagram of the concatenated convolutional coding system

Here, we make an assumption that when a like user interferer hits a specific hop he hits the same filter banks in all the symbols constituting the hop (a quasi static analysis).

For finding β_0, β_1 and β_2, we assume the modulation format to be non-coherent MFSK with hard decision. The symbol error probability is given by the relationship

$$P_m = \sum_{n=1}^{M-1} (-1)^{n+1} \binom{M-1}{n} \frac{1}{n+1} e^{-nk\gamma_b/(n-1)} \tag{4.10}$$

where M is the $M-ary$ size, k is the number of bits per symbol and γ_b is the signal to noise ratio per bit ($M = 2^k$). β_1 and β_2 are given by the following relationship

$$\beta_1 = \left[\frac{1}{M} P_m + \left(\frac{M-1}{M}\right)\left(\frac{M-1}{M}\right) \right] \frac{M}{2(M-1)} \tag{4.11}$$

$$\begin{aligned} \beta_2 = \frac{1}{U-2} \Bigg[& \left(\frac{1}{M^2} P_M \right) + \left(1-\frac{1}{M^2}\right)\left(\frac{M-1}{M}\right) \\ & + \frac{1}{M^3} P_m + \left(1-\frac{1}{M^3}\right)\left(\frac{M-1}{M}\right) \\ & + \frac{1}{M^4} P_m + \left(1-\frac{1}{M^4}\right)\left(\frac{M-1}{M}\right) \\ & + \cdots\cdots\cdots\cdots\cdots\cdots\cdots\cdots \Bigg] \frac{M}{2(M-1)} \end{aligned} \tag{4.12}$$

For a binary symmetric channel with cross over probability $p < 1/2$, beginning with the ensemble average bound of coding theorem and we have from the Gallager function [4.5], [4.6]

$$E_0(\rho, q) = \ln \sum_y \left[\sum_x q(x)\, p(y \mid x)^{1/1+\rho} \right]^{1+\rho} \tag{4.13}$$

where $q(x)$ is an arbitrary input weighting distribution, $p(y \mid x)$ is the conditional transition probabilities of the channel. The function $E_0(\rho, q)$ is a positive increasing function for positive ρ approaching 0 (zero) as $\rho \to 0$. To minimize the bounds for asymptotically large K, ρ should be as large as possible [4.5], [4.6].

$$E_0(\rho) = \max_q \quad E_0(\rho, q) = \rho \ln 2 - (1+\rho) \ln [p^{1/1+\rho} + (1-p)^{1/1+\rho}] \tag{4.14}$$

Now, the capacity of a binary symmetric channel with cross over probability p is given by

$$C = 1 + p \ln p + (1-p) \ln (1-p) \tag{4.15}$$

Now,

$$R_0(q) = E_0(1, q) \tag{4.16}$$

where R_0 is the cutoff rate of the code. The exponential bound parameter $E_c(R)$ in the ensemble average error probability of convolutional code after decoding becomes (for rates less than R_0)

$$E_c(R) = R_0 \quad 0 \leq R \leq R_0(1-\epsilon) \tag{4.17}$$

for rates greater than the cutoff rate R_0, $E_c(R)$ is given by the following relationship

$$\begin{cases} E_c(R) = \max_q \quad E_0(\rho, q) & 0 \leq \rho < 1 \\ R = (1-\epsilon) \left[\max_q \quad \dfrac{E_0(\rho, q)}{\rho} \right] & R_0(1-\epsilon) \leq R \leq C(1-\epsilon) \end{cases} \tag{4.18}$$

where ϵ is any positive number. For asymptotically large K, ϵ may be chosen asymptotically small [4.5]

$$R_0 = E_0(R) = 1 - 2 \ln [p^{1/2} + (1-p)^{1/2}] \quad 0 \leq R \leq R_0(1-\epsilon) \tag{4.19}$$

If the transition probability p is known $E_c(R)$ can be expressed in terms of capacity

For higher rates

$$R = (1-\epsilon)\left[\max_{q} \frac{E_0(\rho, q)}{\rho}\right] \qquad R_0(1-\epsilon) \leq R \leq C(1-\epsilon) \quad (4.20)$$

$$= (1-\epsilon)[\rho \ln_2 2 - (1+\rho)]$$

$$\ln [\rho^{1/(1+\rho)} + (1-p)^{1/1+\rho}] \quad R_0(1-\epsilon) \leq R \leq C(1-\epsilon) \quad (4.21)$$

If R is known, the transition probability p (in our case $\bar{P}_b$) is also known and ϵ is assumed a very low value then the equation (4.14) can be solved for ρ.

But it is not feasible to solve this equation analytically, so we take recourse to iterative solution.

Once ρ is found its value is replaced in eqn. (4.18) for finding out $E_c(R)$

$$E_c(R) = \max_{q} E_0(\rho, q) \qquad 0 < \rho < 1 \quad (4.22)$$

$E_c(R)$ given by (4.22) is to be used in the bound [4.5], [4.6] for the error probability calculation in the convolutional code decoding as shown below

$$P_{\bar{m}} < (2^b - 1)\frac{2^{-KbE_c(R)/R}}{[1-2^{-\epsilon bE_c(R)/R}]^2} \quad \epsilon > 0 \quad (4.23)$$

This error probability becomes the cross over probability for the next concatenation level (Fig. 2) and we find the $E_c(R)$, R_0, etc., for the next stage and so on and appropriate values that are to be replaced in the ensemble average error probability bound (23).

4.3 Results

Using concatenated convolutional code and using the ensemble average error probability bound, we find the decoded error probability of a multi access system at different stages of concatenation.

For M equals 8, SNR equals 10, overall rate R equals .125 and the number of symbols per hop N_s equals 2 and ϵ equals .01 in the bound (eq. (23)) we plot the error probability vs. the number of users (Fig. 4.3). As can be seen from Fig. 4.3, at the inner most concatenation level we have the constraint length of the convolutional decoder K equals 20, R equals .23. For the next level K =20, and R =.6 and for the outer most level K = 30, R =.905, which makes an overall rate of .125.

Similarly, for M = 8, SNR =10, overall rate R = 27/64, N_s = 2 and ϵ = .01 we plot the error probability vs. number of users (Fig. 4.4).

Keeping all the other parameters as in Fig. 4.4 except N_s = 4 we plot the error probability vs. the number of users in Fig. 4.5. As N_s increases the probability of a hit increases and as such has an influence on the error probability. Which can be seen by comparing Fig. 4.4 and Fig. 4.5, respectively.

For M = 8, R = 27/64 and the number of users in the system U equal to 10 we plot the error probability vs. SNR. in Fig. 4.6.

In Fig. 4.7, we plot the exponential bound parameter $E_c(R)$ vs. the rate R for different concatenation levels keeping the system parameters as M = 8, U = 10, N_s = 5, and SNR =10.

The computational cutoff rate for the inner most decoder is represented by R_{01} and the corresponding exponential bound parameter $E_c(R)$ (as shown in Fig. 4.7) is small compared to the other concatenation levels. As can be seen

from Fig. 4.7, in the inner most decoder the exponential bound parameter $E_c(R)$ falls less rapidly than in the other concatenation level, that means operating at rate greater than the cutoff rate at this stage has less effect than on the other concatenation levels.

For $M = 8$, $U = 20$, $N_s = 5$, $SNR = 10$ we plot $E_c(R)$ vs. R in Fig. 4.8 and we get results similar to that of Fig. 4.7.

Going to four levels of concatenation did not produce much improvement.

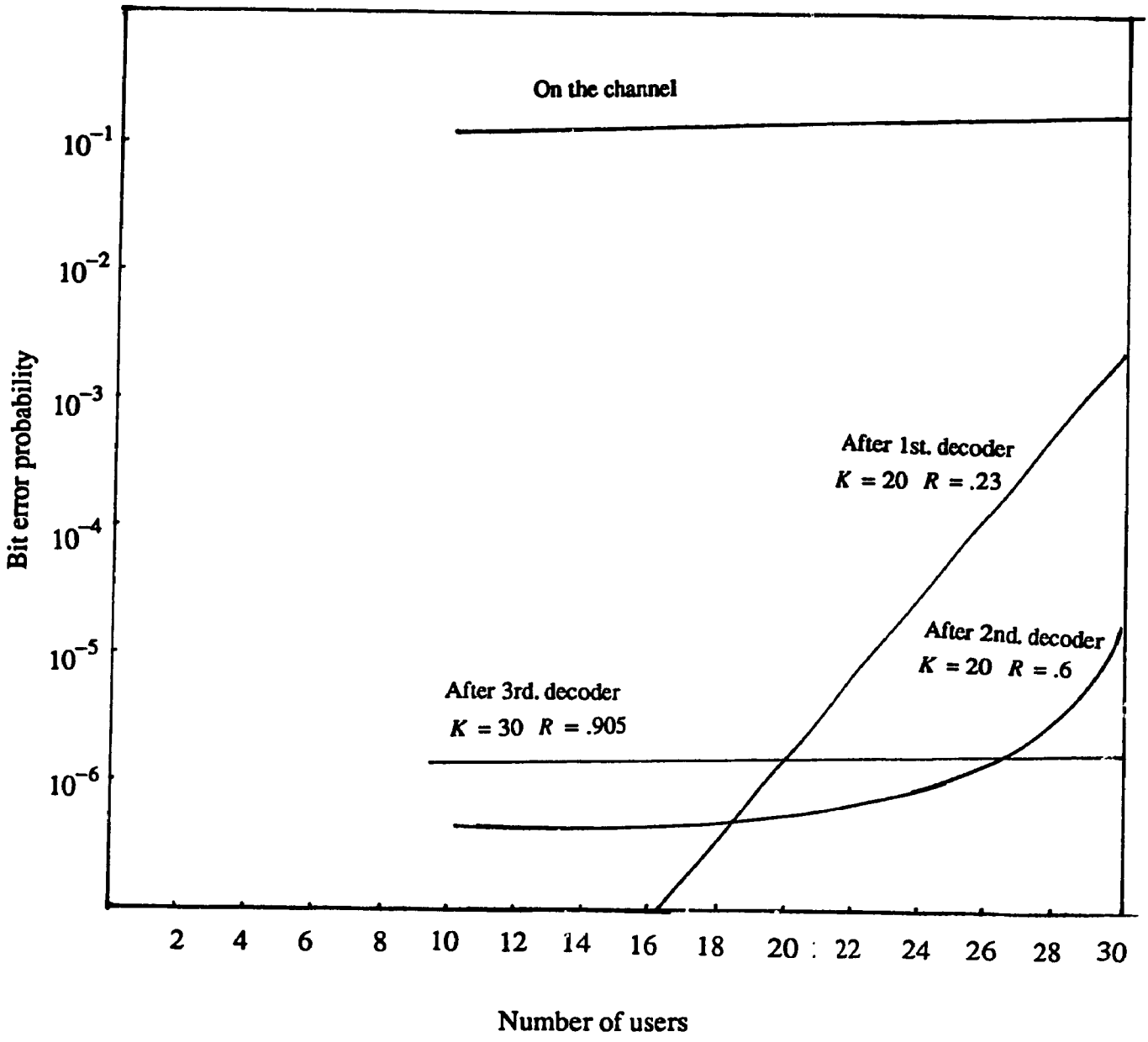

Fig. 4.3 Error probability versus number of users, the parameters are; M–*ary* system of M =8, signal to noise ratio (SNR) = 10.0, total rate R = .125. number of symbols per hop $N_s = 2, \varepsilon = .01$

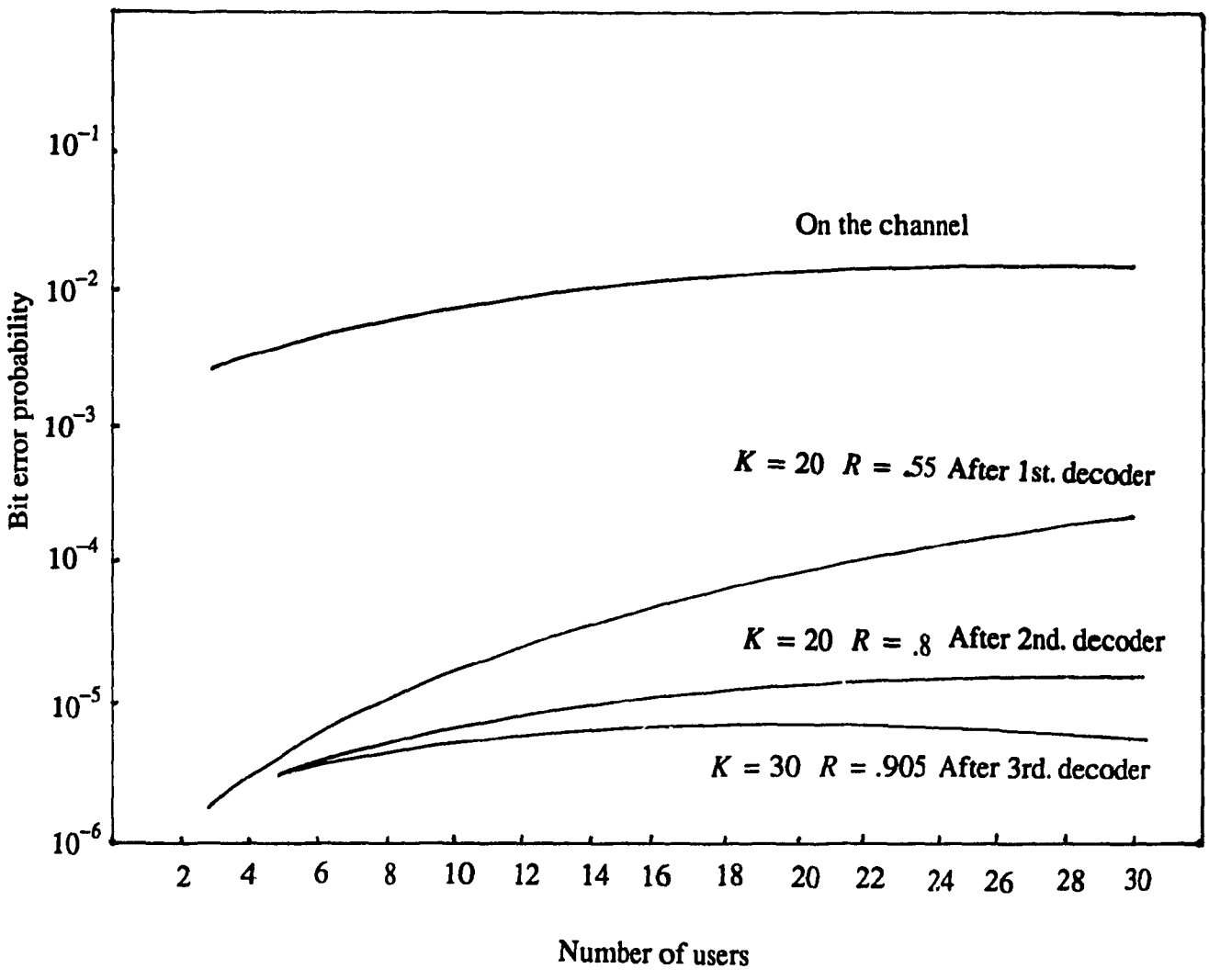

Fig. 4.4 Error probability versus number of users, the parameters are; *M –ary* system of M =8, signal to noise ratio (SNR) = 10.0, total rate R = 27/64, number of symbols per hop $N_s = 2$, $\varepsilon = .01$

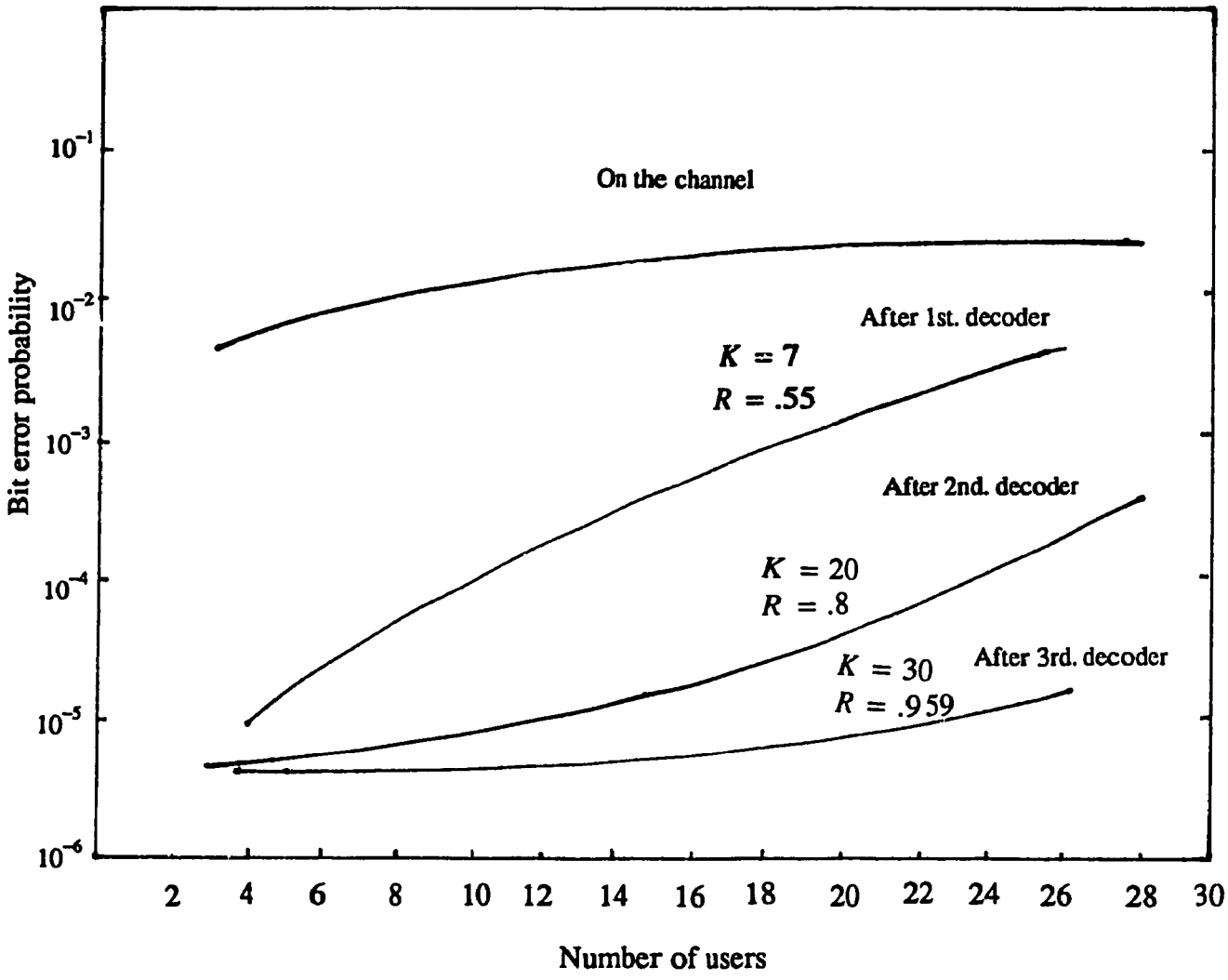

Fig. 4.5 Error probability versus number of users, the parameters are; M–*ary* system of M =8, signal to noise ratio (SNR) = 10.0, total rate R = 27/64, number of symbols per hop $N_s = 4$, $\varepsilon = .01$

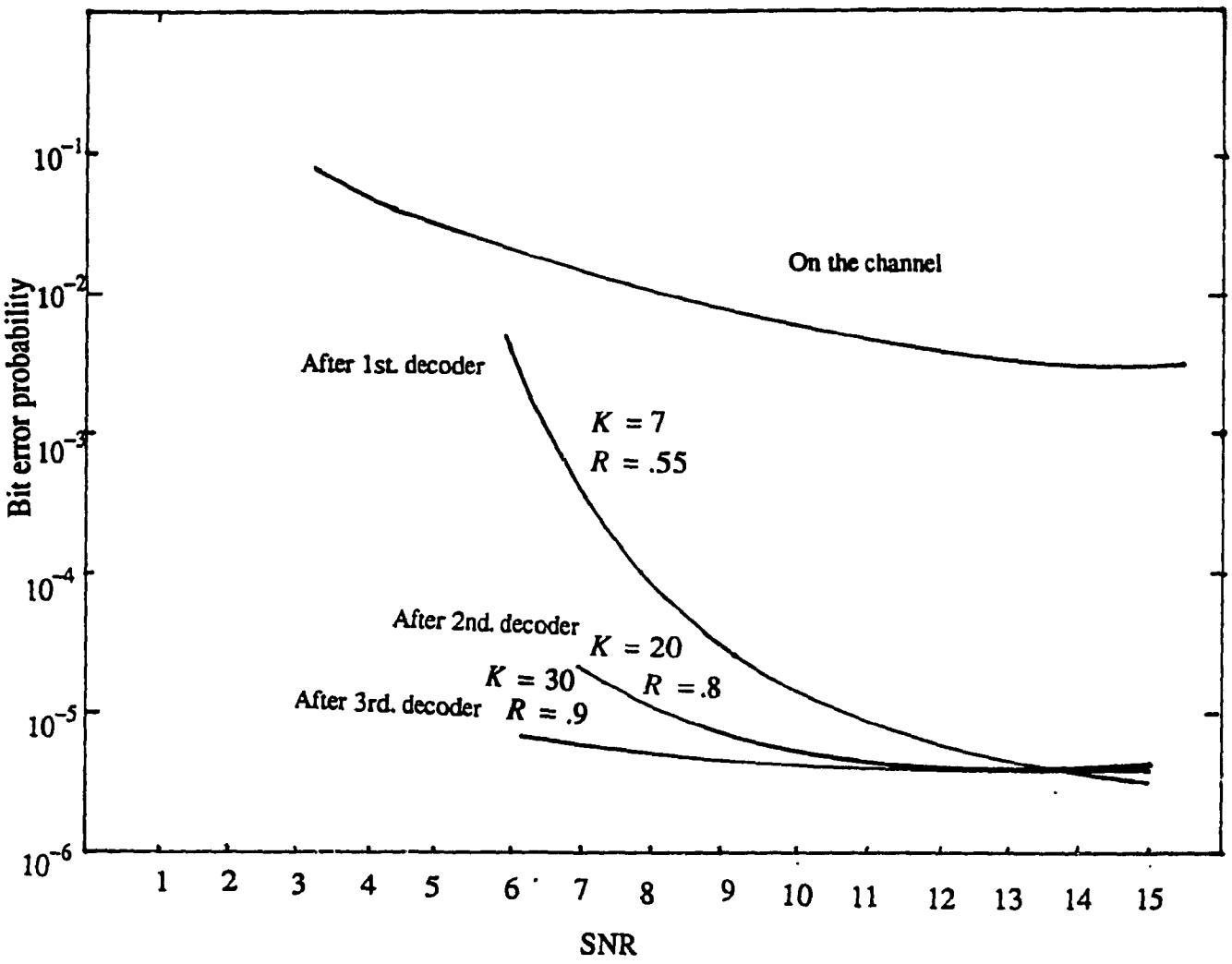

Fig. 4.6 Error probability vs. signal to noise ratio (SNR), the parameters are; M = 8, total rate $R = 27/64$, number of users in the system $U = 10$. number of symbols per hop $N_s = 2$, $\varepsilon = .01$

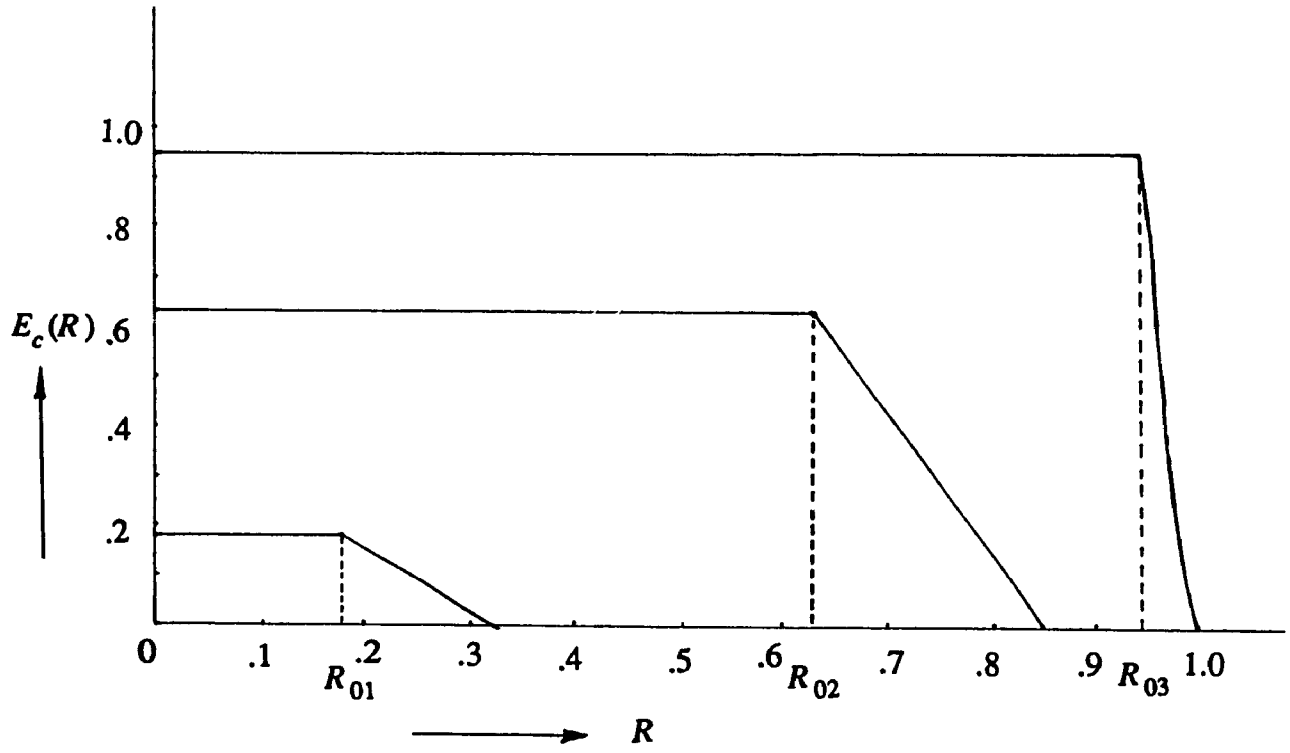

Fig. 4.7 Exponential bound parameter $E_c(R)$ versus rate R, the parameters are; $M = 8$, the number of users $U = 10$, number of symbols per hop $N_s = 5$, signal to noise ratio (SNR) = 10. For detemining the above plot the point of operations are as follows: Probability of bit error on the channel = .179, the cut-off rate R_{01} for the innermost stage was = .179, the capacity C_1 for the inner most stage was = .3226, the rate R for the innermost stage was =.2, and the constrint length for the innermost stage was = 9; R_{02} = .63039, C_2 = .84861, the rate for the next innermost stage was = .65, the constraint length K for this stage was = 30; R_{03} = .92477, C_3 = .9950, and the rate R was = .96153 and the constraint length for this stage was = 55.

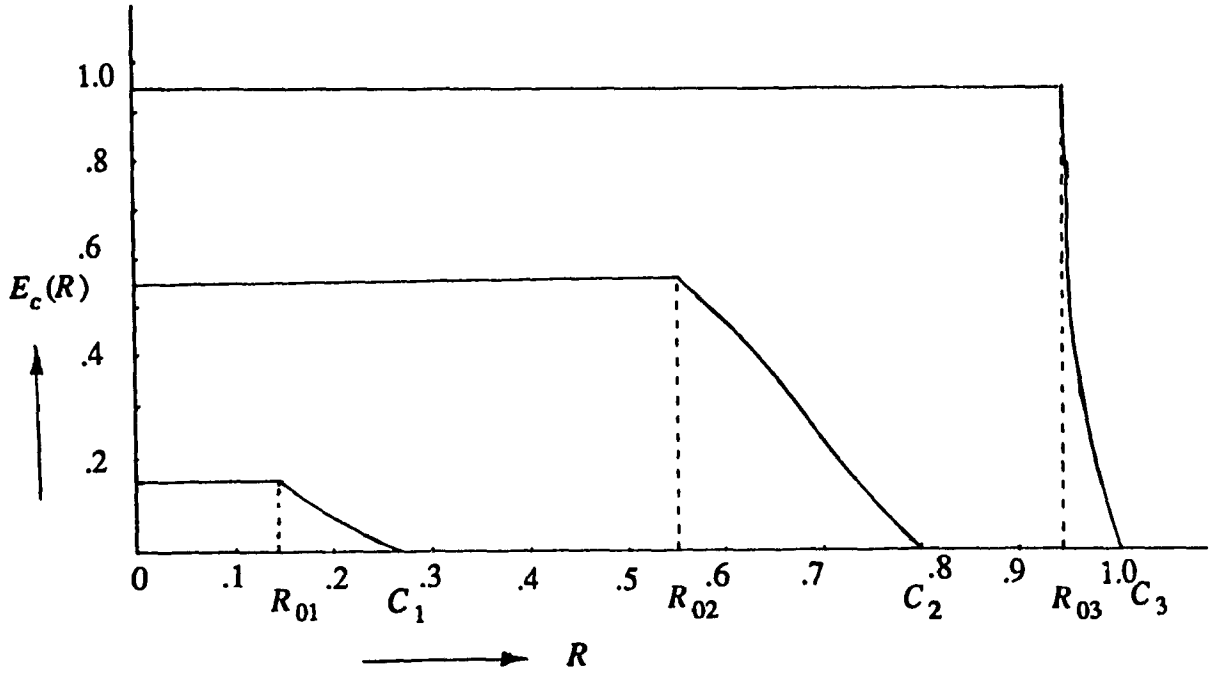

Fig. 4.8 Exponential bound parameter $E_c(R)$ versus rate R, the parameters are M = 8, the number of users U = 20, number of symbols per hop N_s = 5, signal to noise ratio (SNR) = 10. For detemining the above plot the point of operations are as follows: Probability of bit error on the channel = .207, the cut-off rate R_{01} for the innermost stage was = .143, the capacity C_1 for the inner most stage was = .263, the rate R for the innermost stage was =.2, and the constrint length for the innermost stage was = 20; R_{02} = .5653, C_2 = .794, the rate for the next innermost stage was = .65, the constraint length K for this stage was = 50; R_{03} = .946, C_3 = .995350, and the rate R was = .961 and the constraint length for this stage was = 55.

REFERENCES

[4.1] P. Elias, 'Error-Free Coding', IRE, Transactions on Information Theory, Vol. IT-4, pp. 29-37, Sept. 1954

[4.2] G.D. Forney. Jr., 'Concatenated Codes', Cambridge, Mass., M.I.T. Press, 1966

[4.3] A.J. Viterbi, 'Error Bounds for Convolutional Codes an Asymptotically Optimal Decoding Algorithm', IEEE, Trans. on Inf. Theory, Vol. IT-13, pp. 260-269, April 1967

[4.4] Lin-Nan Lee, 'Concatenated Coding Systems Employing a Unit-Memory Convolutional Code and a Byte-Oriented Decoding Algorithm', IEEE, Trans. on Communications, Vol. Com -25, No. 10, pp. 1064-1074, October 1977

[4.5] A. J. Viterbi, J.K. Omura, ' Principles of Digital Communications and Coding', Mc-Graw Hill Book Company, New York.

[4.6] A. J. Viterbi, 'Convolutional Codes and Their Performance in Communications Systems', IEEE, Transactions on Communication Technology, Vol. Com -19, No. 5, pp. 751-772, October 1971

CHAPTER V

CONCATENATED COMBINED MODULATION AND CODING OF FREQUENCY HOPPING MULTI ACCESS SYSTEMS

5.1. Introduction

There is a growing need for reliable transmission of high quality voice and digital data in band limited channel. In conventional communications the two primary communication resources are the transmitted power and the channel bandwidth. A general system design objective would be to use these two resources as efficiently as possible. For example, space communication links are typically power limited. In power limited channels, coding schemes are generally used to save power at the expense of bandwidth, whereas in band-limited channels 'spectrally efficient modulation' techniques would be used to save bandwidth. The primary objective of spectrally efficient modulation is to maximize the bandwidth efficiency, defined as the ratio of data rate to channel bandwidth (in units of bits/Hz.).

On the other hand, in spread spectrum communication the channel bandwidth employed is much larger than that used in conventional communications system. Although the bandwidth of spread spectrum systems are large it is not unlimited and they are limited by allocations [5.1]. In such systems it is most often possible to achieve the desired throughput with either modulation techniques or coding techniques. But instead the integration of a bandwidth efficient modulation scheme with some form of coding will exploit

the best possible attributes of both.

Because, as was discussed in chapter-III, coding is critical to the multi access FH system, we continue in this chapter the search for more powerful codes.

Moreover, in the chapters to follow we are proposing an acquisitionless spread spectrum system, in which reception will be possible by incorporating a number of programmable matched filters at the receiver. Due to Doppler and or fading, etc., one matched filter peak may be lost occasionally (miss), another may be added (false alarm). These timing information (indicating code alignment status) may not be completely reliable. Hence, the forward error correction coding (FEC) has to be reliable for timing information to rely on.

Combined modulation and coding technique has been the subject of intensive research [5.2] at present. However, its applicability has been restricted to coherent PSK, PAM and QAM systems [5.2], [5.3]. In this chapter, we briefly review the combined modulation and coding technique, and we extend the technique to the soft noncoherent demodulation of FH/MFSK in a jamming and multi access environments. The performance of the proposed multi access system using combined modulation and coding technique (trellis) concatenated with Reed-Solomon (RS) codes in partial band jamming is also investigated and the performance compared to that using RS outer/RS inner concatenated codes [5.4], [5.7], all in a noncoherent detection environment.

5.2. Combined Modulation and Coding

In the past, coding and modulation have been treated as separate operations with regard to overall system design. In the traditional approach to

channel coding, encoding is performed separately from modulation in the transmitter. Likewise for decoding and detection in the receiver. Moreover, error control is provided by transmitting additional redundant bits in the code, which has the effect of lowering the information bit rate per channel bandwidth. That is, bandwidth efficiency is traded for increased reliability. Ungerboeck showed in his pioneering paper [5.2] that considerable gains in terms of SNR (signal to noise ratio) can be achieved with respect to sacrificing neither data rate nor bandwidth. He noticed that codes should be designed for maximum free Euclidean distance rather than maximum Hamming distance, and that the redundancy necessary for coding would have to come from expansion. Computing the capacity of channels with AWGN for the case of discrete multilevel modulation at the channel output he observed firstly, that coding gains of about 7-8 db over conventional uncoded modulation are achievable, and secondly, that an expansion of the signal set by a factor of two is sufficient for most cases.

The trellis codes for band limited channels result from combining convolutional coding with modulation. This form of coding has two features:

1. The number of signal points in the constellation used is larger than what is required for the modulation format of interest with the same data rate; the additional points allow redundancy for forward error control coding without sacrificing bandwidth.
2. Convolutional coding is used to introduce a certain dependency between successive signal points such that certain patterns or sequences are permitted.

In the prescence of AWGN, maximum likelihood decoding of trellis codes

consists of finding that path through the trellis with minimum squared Euclidean distance to the received sequence. In the design of trellis codes, the emphasis is on optimizing the minimum Euclidean distance between the code vectors rather than optimizing the minimum Hamming distance of an error correcting code.

To design this type of a trellis code involves partitioning a constellation successively into 2, 4, 8,....., subsets with increasing minimum Euclidean distance between their respective signal points. This mapping rule is called mapping by set partitioning. The partitioning procedure [5.2], [5.3] is illustrated in Fig. 5.1 a. and Fig. 5.1.b by considering a constellation that corresponds to 8-PSK and 16-QAM, respectively. The 2, 4, and 8 subsets resulting from three successive application of the rule are also shown in the same figure (Fig. 5.1). These subsets share the common property that the minimum Euclidean distances between their individual points follow an increasing pattern: $d_0 < d_1 < d_2 \cdots$

It is possible to devise relatively simple and effective coding scheme based on the subsets resulting from successive partitioning of a two dimensional constellation. Fig. 5.2 shows the general structure of encoder/modulator combination for trellis coded modulation. Specifically, to send n *bits/symbol* with quadrature modulation, we start with a two dimensional constellation of 2^{n+1} signal points appropriate for the modulation format of interest.

5.2.1 Asymptotic Coding Gain

The asymptotic coding gain of Ungerboeck's code is given as [5.2], [5.3]

$$G = 10 \log_{10} \left(\frac{d_{free}^2}{d_{ref}^2}\right) \tag{5.1}$$

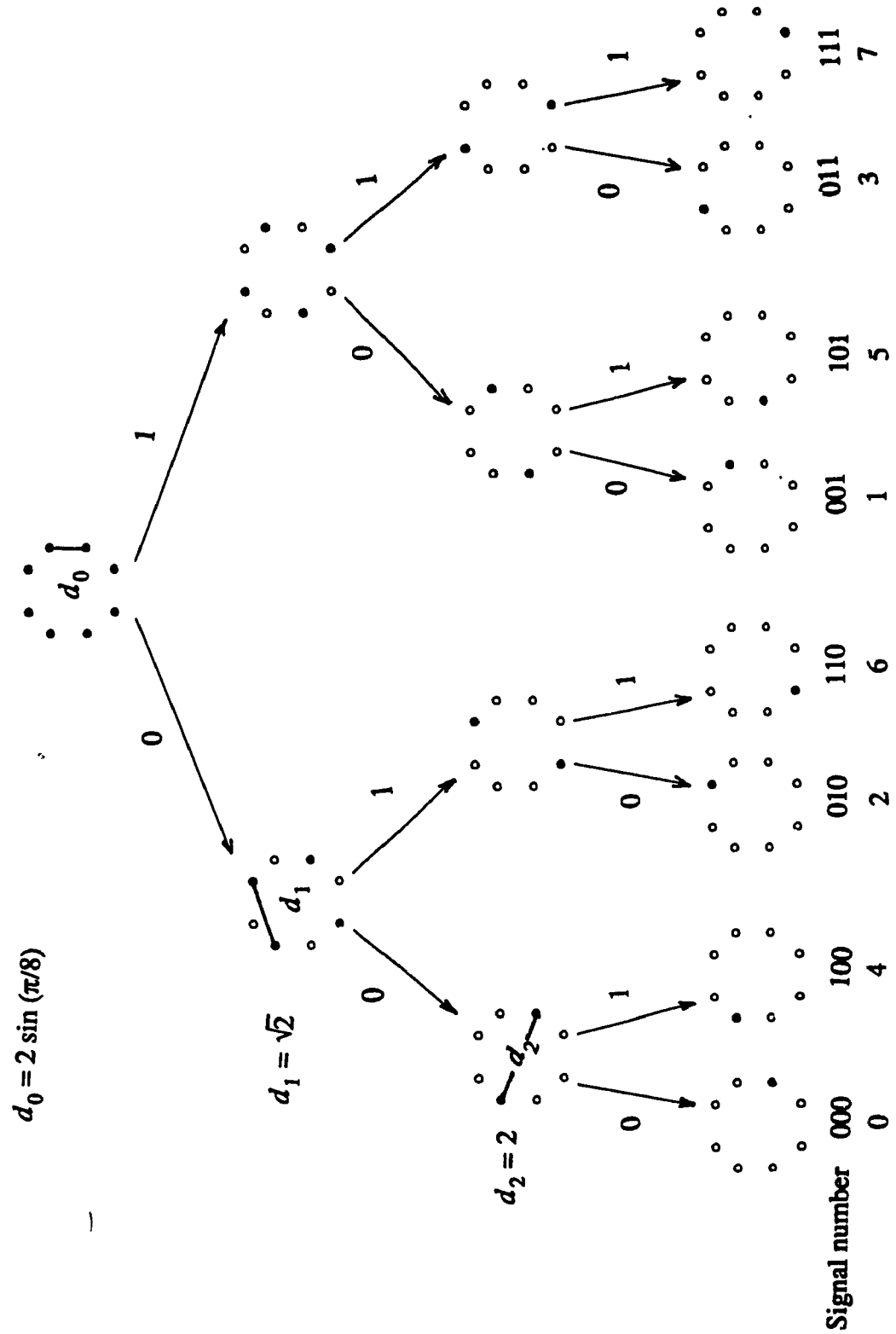

Fig. 5.1.a Partitioning of 8-PSK constellation

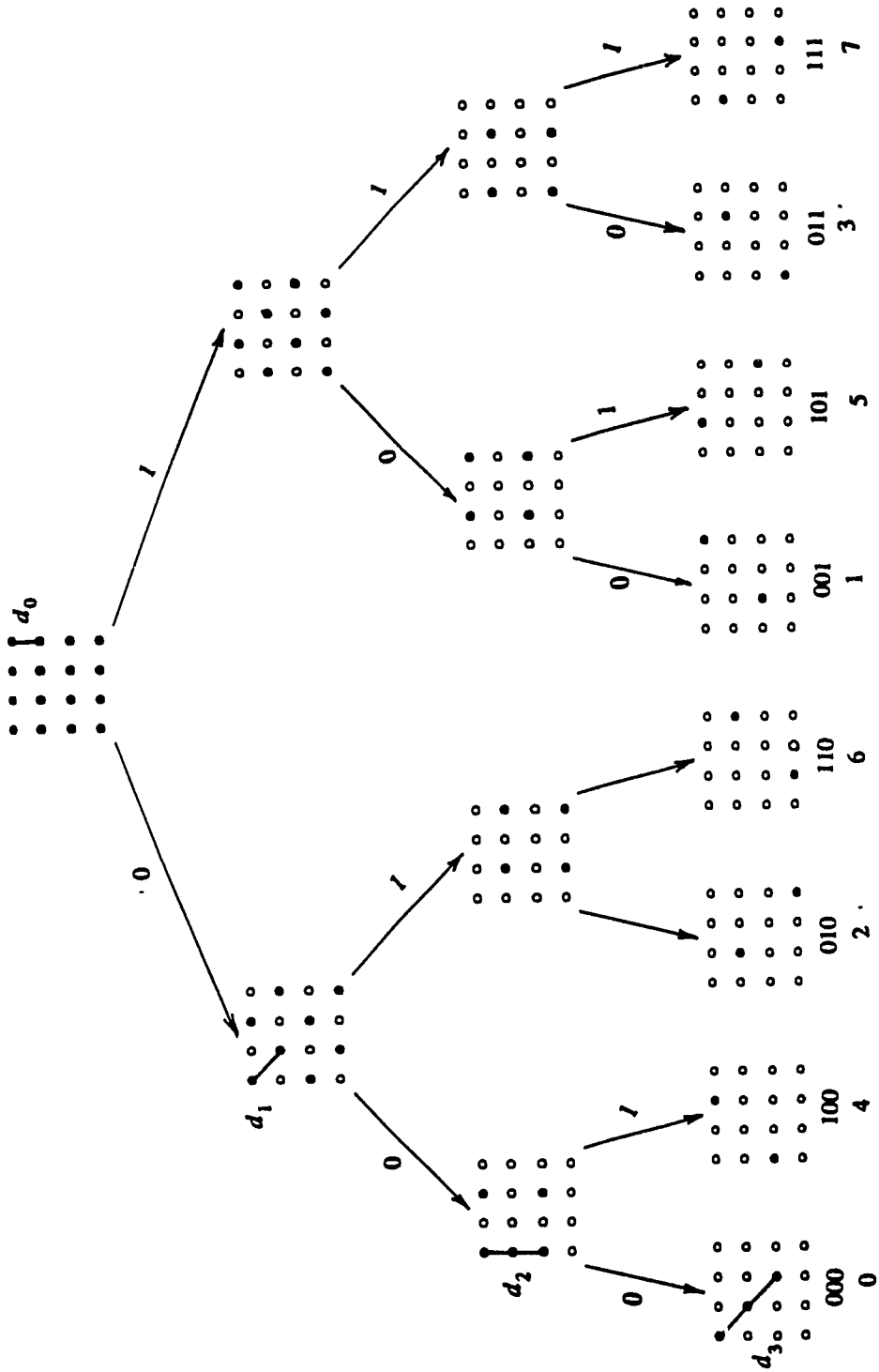

Fig. 5.1.b Partitioning of 16-QAM constellation

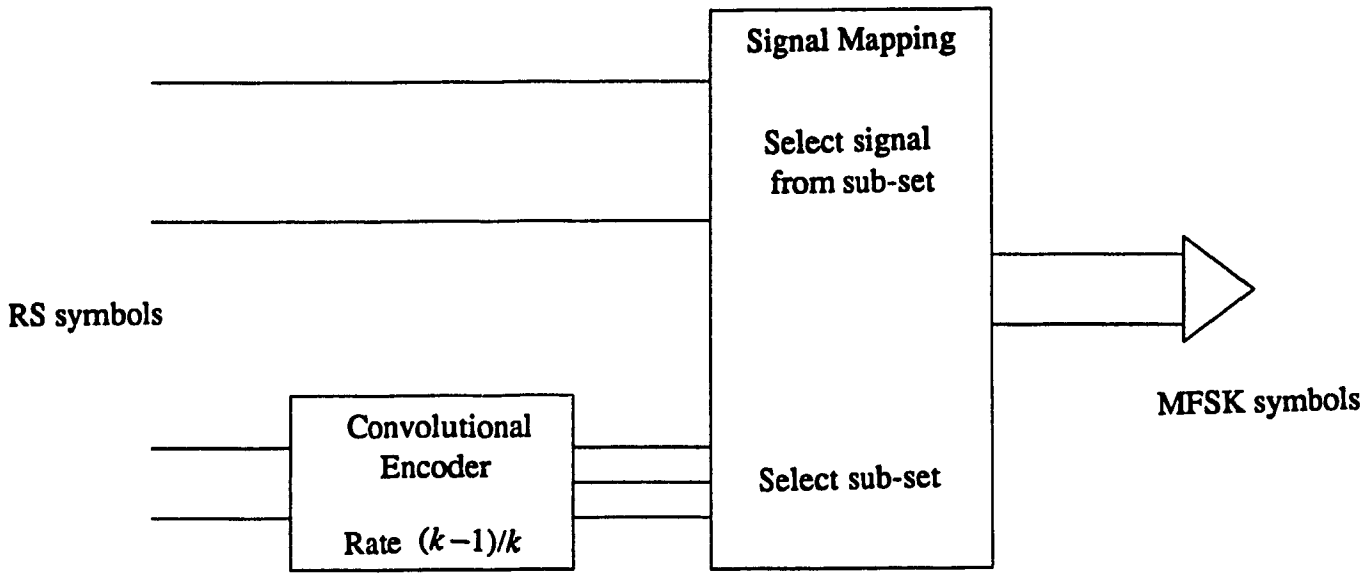

Fig. 5.2 General structure of encoder/modulator for trellis coded modulation

where d_{free} is the free Euclidean distance of the code, and d_{ref} is the minimum Euclidean distance of an uncoded modulation scheme operating with the same energy per bit.

The Ungerboeck's 8-PSK code is as shown in Fig. 5.1.a. The signal constellation has 8 message points and we send 2 bits per message point. The uncoded transmission requires a signal constellation with 4 message points. The uncoded 4-PSK is regarded as the reference for Ungerboeck's 8-PSK code of Fig. 5.3 .

The Ungerboeck's 8-PSK code of Fig. 5.3.a achieves an asymptotic coding gain of 3 db. The free Euclidean distance d_{free} of the code can be no larger than the Euclidean distance d_2 between the antipodal signal points of such a subset is $d_{free} = d_2 = 2$, d_2 is as shown in Fig. 5.3.c. The minimum Euclidean distance of an uncoded QPSK, viewed as a reference operating with the same energy per bit, equals (Fig. 5.3.d) $(d_{ref}) = \sqrt{2}$ and hence the asymptotic coding gain is 3 db.

The asymptotic coding gain of Ungerboeck's code increases with the number of states in the convolutional encoder. Table-1 represents the asymptotic coding gain for increasing number of states. In the table asymptotic coding gain $G_{8\text{-}AM/4\text{-}AM}$ means

$$G_{8\text{-}AM/4\text{-}AM} = 10 \log_{10} \left\{ \frac{d^2_{free}(8\text{-}AM)}{\Delta_0^2(4\text{-}AM)} \right\} \tag{5.2}$$

In Table-1 N_{free} denotes the (average) number of nearest neighbor signal sequences with distance d_{free} that diverge at any state from a transmitted signal sequence and remerge with it after one or more transitions [5.3].

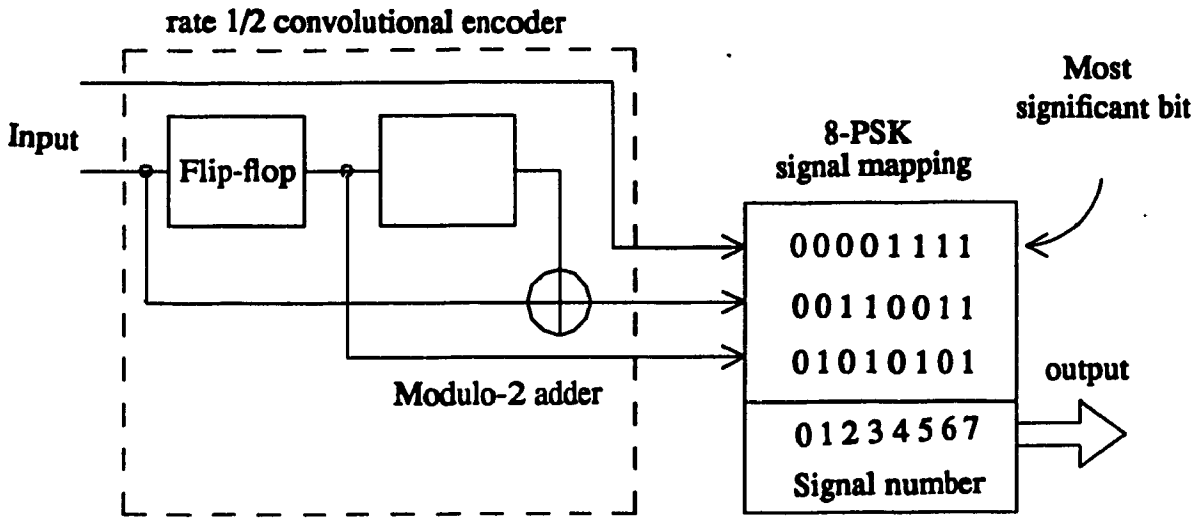

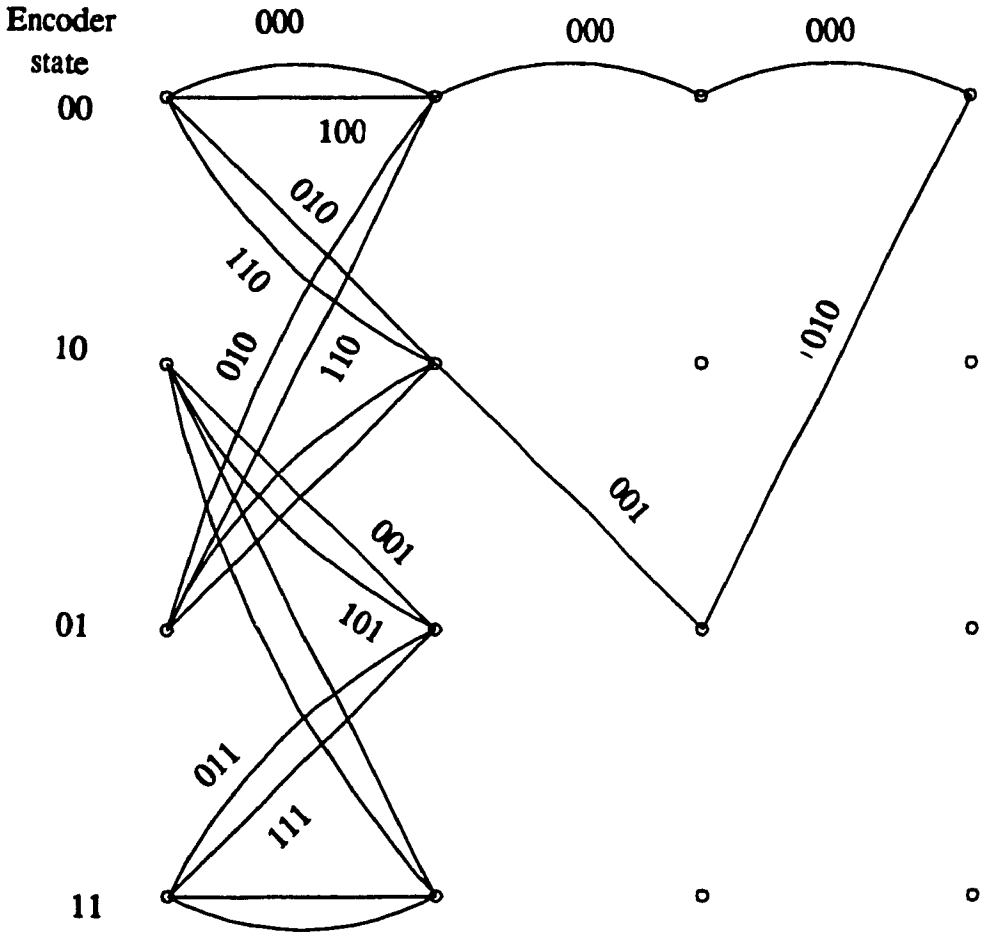

Fig. 5.3. (a) Four-state Ungerboeck code for 8-PSK. (b) Trellis.

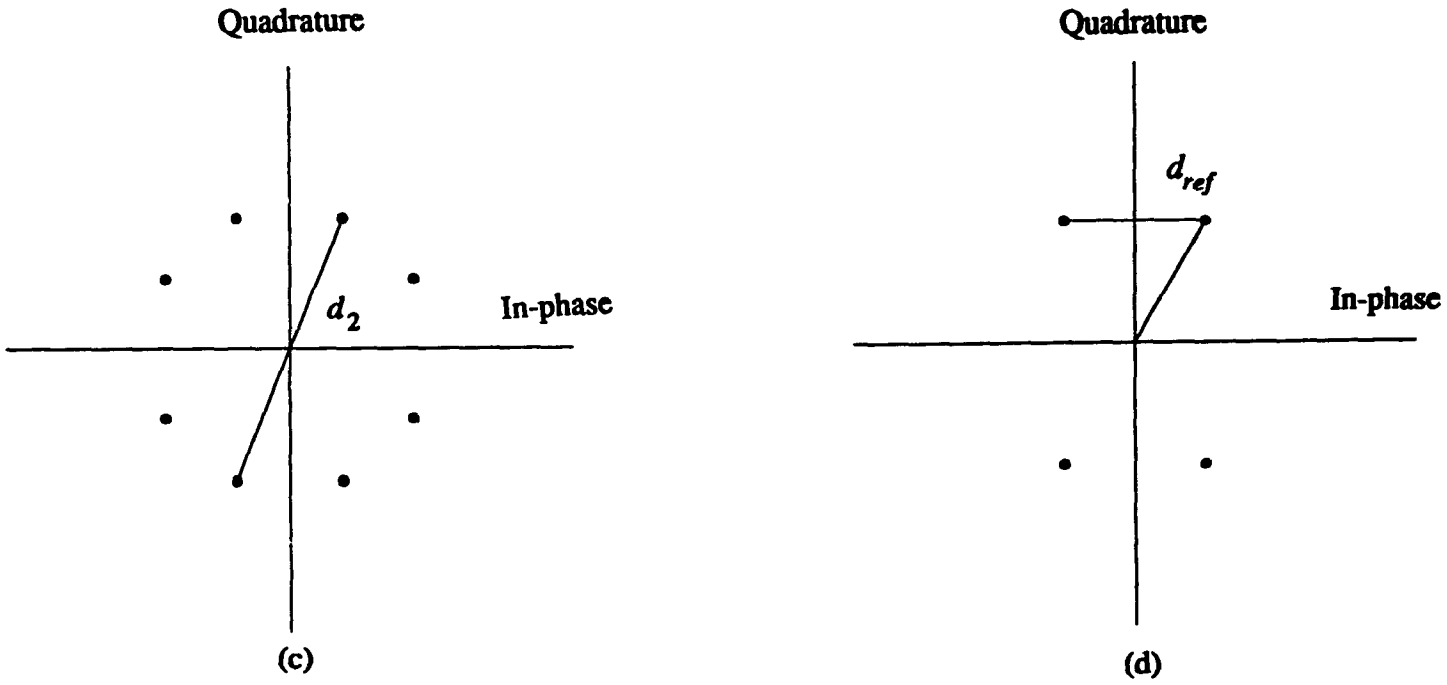

Fig. 5.3. Signal-space diagrams for calculation of asymptotic coding gain

TABLE -1

No. of states 2^{ν}	$\tilde{m}$	Parity check coefficients h^1	h^0	d^2_{free}/Δ^2_0	Asympt. coding gain [db] $G_{4AM/2AM}$ $(m=1)$	$G_{8AM/4AM}$ $(m=2)$	G_{clu} $(m=\infty)$	N_{free} $(m=\infty)$
4	1	2	5	9.0	2.55	3.31	3.52	4
8	1	04	13	10.0	3.01	3.77	3.97	4
16	1	04	23	11.0	3.42	4.18	4.39	8
32	1	10	45	13.0	4.15	4.91	5.11	12
64	1 024	103	14.0	4.47	5.23	5.44	36	
128	1	126	235	16.0	5.05	5.81	6.02	66
256	1	362	515	16.0	-	5.81	6.02	2
256	1	362	515	17.0	5.30	-	-	-

5.3. Combined Modulation Coding Performance for Noncoherent FH/MFSK Multi-access Systems [5.4], [5.7]

The system under consideration is shown in Fig. 5.4. A concatenated coding scheme is used with RS code as an outer code. The inner code can be trellis code (scheme-a) or RS code (scheme-b). $M-ary$ FSK data modulation with noncoherent demodulation is employed. Slow frequency hopping is assumed. N_s $M-ary$ symbols are transmitted during each hop.

It is assumed that in the vicinity of a particular receiver there are U asynchronous transmitted signals, all of which share the same channel; and the receiver can acquire synchronization with the frequency hopping pattern and time of one of the U signals then the other $U-1$ signals interfere with the reception of the signal that was singled out [5.6].

The model for the partial band noise interference is one commonly used in the literature [5.8]. Additive white Gaussian noise (AWGN) is also assumed to be present. If N_j denotes the one sided spectral density of the partial band noise, N_0 denotes that of the AWGN, and ρ $(0 \leq \rho \leq 1)$ is the probability that in a particular dwell time (frequency slot) is jammed, then the one sided spectral density of the Gaussian noise is N_0+N_j/ρ with probability ρ and it is N_0 with probability $(1-\rho)$. The density of the noise remains constant over the duration of the frequency slot [5.6].

Throughout this chapter, it is assumed that the interleaving is perfect so that all errors that the decoder sees are independent.

Two types of concatenated coding schemes are considered. In scheme-a, Reed-Solomon outer code is concatenated with the inner trellis code. For the outer code, we assume that (N, K) RS codes over $GF(2^{km})$ are employed:

thus there are m $M-ary$ symbols in each R-S symbol and each $M-ary$ symbol contains k bits. Pursley and Stark considered (64, 32) RS codes in their work [5.8], similarly, Geraniotis and Gluck considered (64, 32) R-S code over $GF(2^{km})$ where M is the signal constellation size, m is the number of $M-ary$ symbols contained in each RS symbol, and k is the number of bits per $M-ary$ symbol, in their work [5.6]. In this chapter, (64, 32) RS code has been considered as the outer code. The error correction capability of the (64,32) RS code is very large without reducing rate appreciably and encoding and decoding of this code can be accomplished with moderate complexity. Signal set expansion in the inner trellis encoder can be accomplished by a convolutional code encoder (similar to Fig. 5.3.a). For example, the convolutional code encoder (Fig. 5.3.a) will convert the 2 bit/s/Hz input bits into 3 bits/s/Hz output bits for 8-FSK modulation. First, a trellis coded 8-level PAM signal is designed. Then the 8-FSK is generated from the 8-PAM by an one-to-one mapping. Soft decision is used in the the inner decoder of scheme-a.

In scheme-b, R-S outer code is concatenated with R-S inner code. RS codes over $GF(2^{km})$ are employed; thus there are m $M-ary$ symbols in each R-S symbol and each $M-ary$ symbol contain k bits. In scheme-b, for both inner and outer code, (64, 32) R-S codes were employed. Hard decision decoding of RS codes are assumed done in scheme-b.

It was assumed in this chapter, that the data rate r_b, the spread spectrum bandwidth W, and the uncoded bit SNR, are the same for both the scheme-a and for scheme-b.

The received signal at the i-th receiver in the multi access slow Frequency Hop (SFH) /MFSK environment of U users and partial band jamming of power J occupies ρ of the SS bandwidth W, is given by

$$r(t) = \sqrt{2P}\ \cos(w_h^i t + w_l^i t + \phi_l^i) + \sum_{\substack{u=1 \\ u \neq i}}^{U} \sqrt{2P}\ \cos(w_h^u t + w_l^u t + \phi_l^u) + n(t) + J(t) \tag{5.3}$$

where

w_h^i is the hopping frequency of the i-th user during $(j-1)T_h < t < jT_h$

w_l^i is the l-th MFSK symbol frequency of the i-th user during $(l-1)T_s < t < lT_s$

P is the power of each of the U users

ϕ_l^i is the unknown random phase of the i-th user during the l-th symbol

$n(t)$ is the AWGN noise of n single sided density

$J(t)$ is the jammer partial band noise power of band density factor ρ

We assume Slow Frequency Hop (SFH) ($T_h >> T_S$), perfect code acquisition † † and independence of the jammers and user interference, etc. As well, all like users signals have the same power P and the FH processing gain (PG) is high enough to preclude the existence of more than M interferers in the M receiver banks, i.e., one interfering tone per bank (if any). This justifies the small hit probability that will result for high processing gain. † Finally, at the entrance of the MFSK data demodulator of the i-th receiver (Fig's. 5.4, 5.5, 5.7) following down conversion, dehopping, etc., and assuming ideal acquisition, synchronization and demodulation condition, we find one of the following six signals depending on the multi access situation:

† † By the use of a bank of L matched filters, the receiver will be locked to the 'SUGARW' system random code subsections arriving.

† A more accurate analysis can be easily extrapolated by accounting for a higher number of possible interferers per bank thus allowing for moderate and low PG (compared to number of users in the system). In this thesis PG was high enough to justify the above assumption.

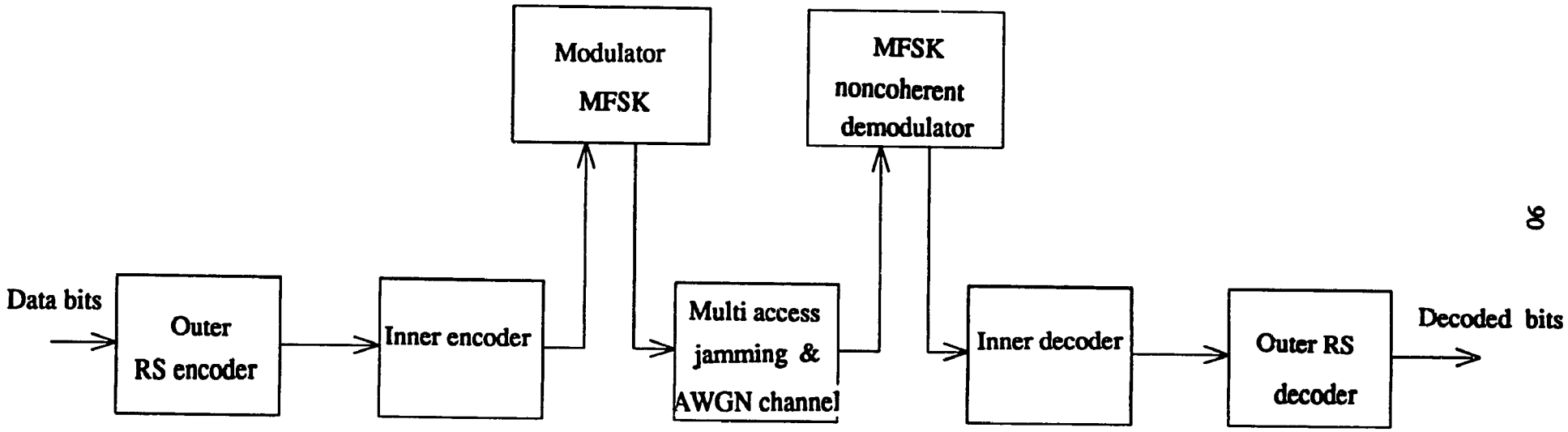

Fig. 5.4 Concatenated coding scheme for FH/MFSK

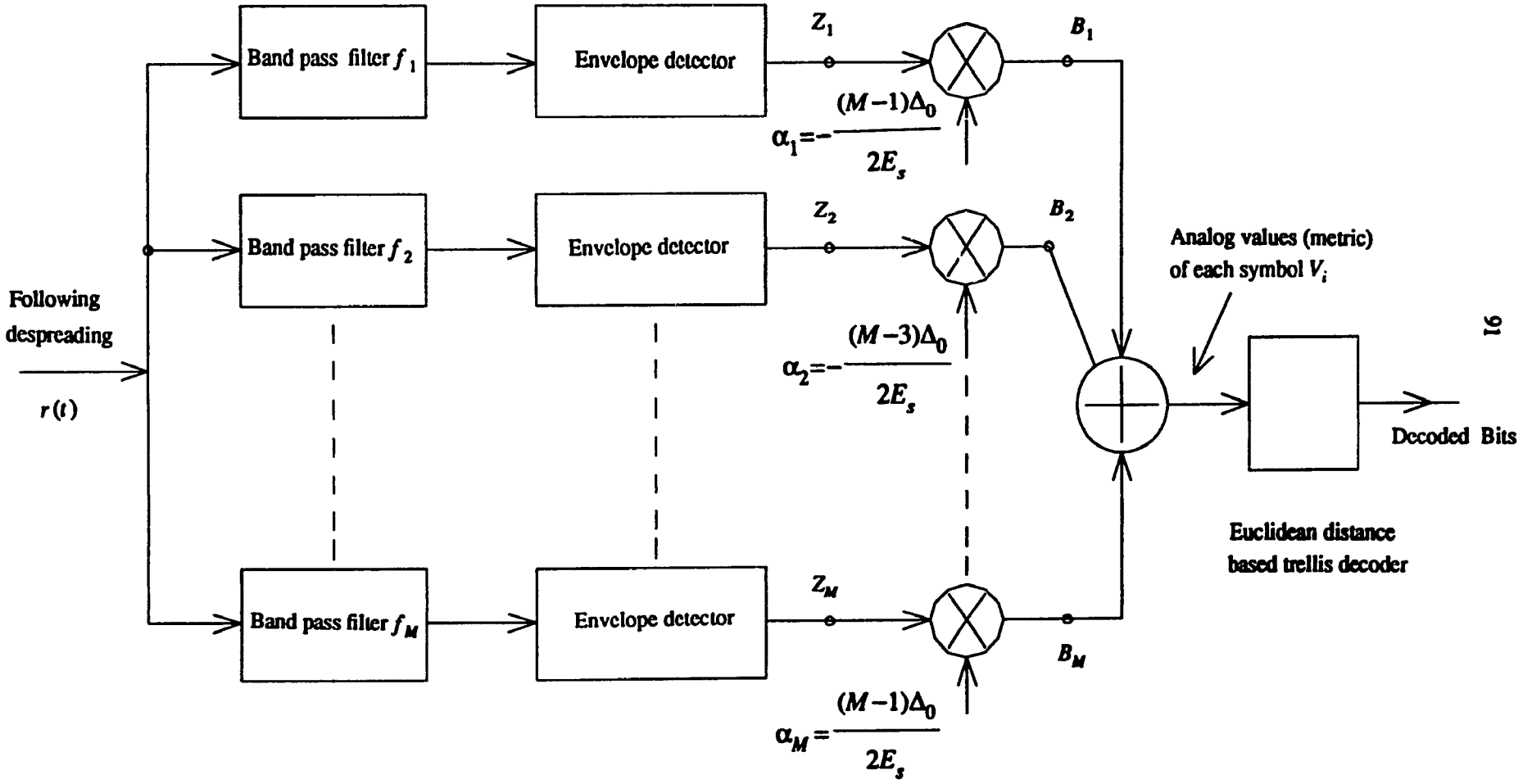

Fig. 5.5 Soft decision noncoherent detection of MFSK signals by mapping to (PAM equivalent) and subsequent trellis decoder

$$r_1^i(t) = \sqrt{2P}\ \cos(w_l^i\, t + \phi_l^i) + n(t) \tag{5.4}$$

occurring with probability

$$p_1 = (1-\rho)\,(1 - \frac{1+1/N_s}{PG})^{U-1} \tag{5.5}$$

(i.e., no partial band jamming, nor like user frequency hit in any of the M banks),

$$N_s = \frac{T_h}{T_s} \tag{5.6}$$

where N_s is the number of symbols per hop, T_h is the hop time and T_s is the symbol time.

$$r_2^i(t) = \sqrt{2P}\ \cos(w_l^i + \phi_l^i) + n(t) + J(t) \tag{5.7}$$

occurring with probability

$$p_2 = \rho\,(1-\frac{1+1/N_s}{PG})^{U-1} \tag{5.8}$$

This is the event of wide band jamming hitting the data band of the i-th user with density equal to

$$N = \frac{J}{W\rho} \tag{5.9}$$

And no like user frequency tone hits any where in the M filter banks of the intended i-th receiver

$$r_3^i(t) = \sqrt{2P}\cos(w_l^i\, t + \phi_l^i) + n(t) + \sqrt{2P}\cos(w_l^u\, t + \phi_l^u) \tag{5.10}$$

This is the event of one of the like users hitting the filter bank containing the signal of the i-th user ($w_l^u = w_l^i$) and no partial band jamming. It happens with probability p_3 where

$$p_3 = (1 - (1 - \frac{1+1/N_s}{PG})^{U-1})\,(1-\rho)\,\frac{1}{M} \tag{5.11}$$

$$r_4^i(t) = \sqrt{2P}\cos(w_l^i + \phi_l^i) + n(t) + \sqrt{2P}\cos(w_l^u + \phi_l^u) \tag{5.12}$$

This is in the event of one or the like users tone hitting in the $(M-1)$ filter bank not containing the signal $(w_l^u \neq u_l^i)$ and no partial band jamming. This occurs with probability p_4, where

$$p_4 = (1 - (1 - \frac{(1+1/N_s)}{PG})^{U-1})(1-\rho)\,(\frac{M-1}{M}) \tag{5.13}$$

$$r_5^i(t) = \sqrt{2P}\cos(w_l^i t + \phi_l^i) + n(t) + J(t) + \sqrt{2P}\cos(w_l^u t + \phi_l^u) \tag{5.14}$$

This is in the event of wide-band jamming plus one of the like user tones hitting in the $(M-1)$ banks not containing the signal $(w_l^u \neq w_l^i)$. This arises with probability,

$$p_5 = (1 - (1 - \frac{(1+1/N_s)}{PG})^{U-1})\,(\rho)\,(\frac{M-1}{M}) \tag{5.15}$$

$$r_6^i(t) = \sqrt{2P}\cos(w_l^i t + \phi_l^i)) + n(t) + J(t) + \sqrt{2P}\cos(w_l^u t + \phi_l^u) \tag{5.16}$$

This is the event of wide-band jamming plus one of the like users tone hitting the filter bank containing the signal $(w_l^u = w_l^i)$ occurring with probability,

$$p_6 = (1 - (1 - \frac{(1+1/N_s)}{PG})^{U-1})\,(\rho)\,(\frac{1}{M}) \tag{5.17}$$

In a typical noncoherent MFSK receiver (Fig. 5.7), one of the six signals $r_1(t)$ through $r_6(t)$ will pass depending on the situation through the conventional non coherent MFSK demodulator. Then the bits of the detected symbols will feed the inner convolutional decoder, which is based on the binary Hamming distance and Viterbi decoding, finally yield the input bits to the next RS

decoder.

However, it is worth trying to see if combined coding and modulation technique (trellis coding) (Fig. 5.4) will work for the noncoherently detected MFSK signals some how in a suboptimal and practical way. This implies that the hard detected MFSK signals (typical in the literature) should be replaced by the PAM equivalent soft detected system of Fig. 5.5, and the inner trellis decoder will work on the test statistics V_i analog values corresponding to the symbol l of user i. Fig. 5.6 shows the normalized phasor diagram of the PAM system equivalent to MFSK.

Following de-spreading and during a certain symbol time, one of the six signals in eqs. (5.4), (5.7), (5.10), (5.12), (5.14), and (5.16) will pass through the various filters, envelope detectors and coefficient multipliers as in Fig. 5.5. Finally, the metrices V_i corresponding to various symbol times (obtained by adding the outputs of the M banks at the end of each data symbol). The subsequent Viterbi kind of decoder will compute the (analog) survivors, etc., and give the most probable path and hence the data signals. The details of this trellis decoding can be found in [5.2], [5.3].

Fig. 5.6 shows the phasor diagram of the PAM equivalent of the received MFSK signals and Fig. 5.2 shows one of the various possible trellis diagrams for this case. Table-1 [5.2],[5.3] gives the possible code generators, distance properties, coding gain, etc., of PAM systems that we used throughout this chapter. The multiplication factors in Fig. 5.5 are given by,

$$\alpha_i = -\frac{(M-(2i-1))\Delta_0}{2E_s} \tag{5.18}$$

where,

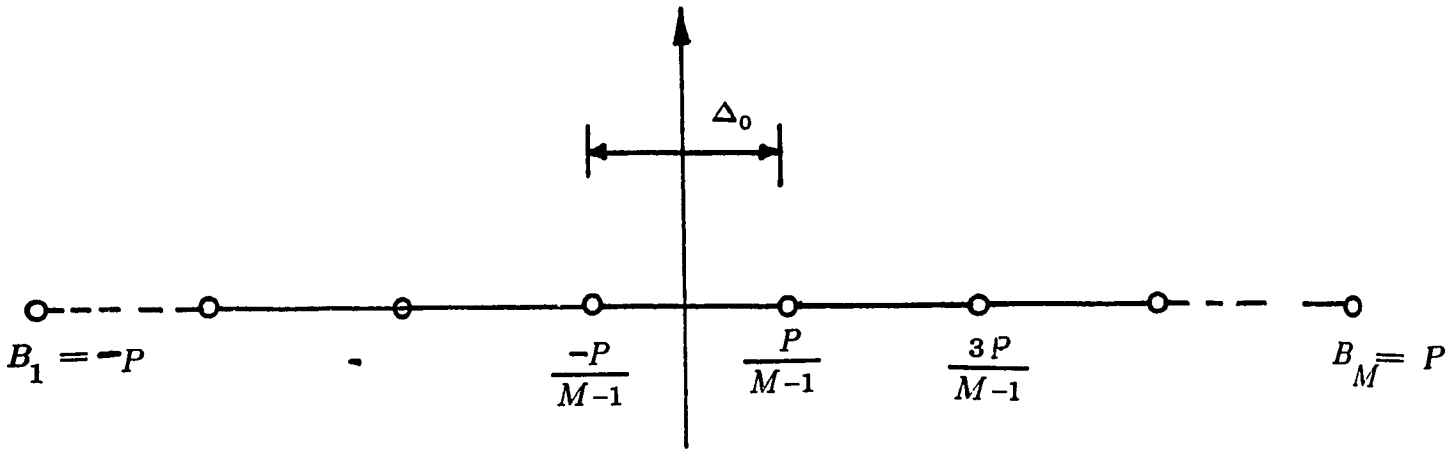

Fig. 5.6 Phasor diagram of the PAM equivalent of the MFSK signal set.

$$\Delta_0 = \frac{2P}{M-1} \quad , \qquad \Delta_i = 2\Delta_{i-1}$$

$$i = 1, 2, \ldots\ldots\ldots\log_2 M$$

$$B_i = \frac{(M - (2i - 1)}{2}\Delta_0 = \frac{-(M - (2i - 1))\,P}{(M - 1)}$$

normalization condition, $P = \sqrt{\frac{3(M-1)}{M+1}}$, $\Delta_0 = \sqrt{\frac{12}{(M^2-1)}}$

$$\Delta_0 = \frac{2P}{M-1} \tag{5.19}$$

is the distance between consecutive signals of the M PAM set. The symbol energy E_s is given by

$$E_s = A^2 T_s / 2 \tag{5.20}$$

Under noise free, jamming free, like user free conditions the signals $Z_1, Z_2, \ldots\ldots, Z_M$ (Fig. 5.5) will have a value E_s or zero depending on which signal was transmitted. It follows that the various PAM signals in this ideal case (B_i's of Fig. 5.5) to be added together is given by,

$$B_i = -\frac{(M-(2i-1))}{2}\Delta_0 = \frac{-(M-(2i-1))P}{(M-1)} \tag{5.21}$$

The factor P above is found from the normalization condition, i.e., average signal power in (5.1) is independent of the alphabet size M, i.e.,

$$P = \sqrt{\frac{3(M-1)}{M+1}}$$

$$\Delta_0 = \frac{2P}{(M-1)} = \sqrt{\frac{12}{(M^2-1)}} \tag{5.22}$$

while the i-th correct decision boundary (lower and upper) (Fig. 5.6) is given by

$$b_i = \left\{ \frac{-(M-2i+2)P}{(M-1)}, \frac{-(M-2i)P}{(M-1)} \right\} \tag{5.23}$$

$$i = 2, 3, \ldots\ldots, (M-1)$$

For i equal to one ($i=1$) the lower limit is replaced by $(-\infty)$

and for i equal to M ($i=M$) the upper limit is replaced by $(+\infty)$

Signals are assigned to the various branches of the trellis [5.2], such that the minimum distance is maximized [5.2]. Set partitioning is used [5.2] such that the distances are given by,

$$\Delta_i = 2\Delta_{i-1}$$

$$i = 1, 2, \ldots\ldots\ldots, \log_2 M \tag{5.24}$$

The resulting decoding symbol error probability at the output of the trellis decoder is given by [5.2]:

$$P_s \doteq N_{free} P_r(d_{free}/2\sigma) \tag{5.25}$$

where P_r denotes the probability of incorrectly decoding a certain symbol by another spaced by d_{free} on the phasor of Fig. 5.6 and N_{free} has been defined earlier.

To evaluate this probability one should find the density (pdf) of the variable V_i of Fig. 5.5, (i.e., the metric) for the cases corresponding to receiving two signals spaced by d_{free} . Under just AWGN, it is known that the (pdf) of Z_i is Rician if it contains the signal and Rayleigh otherwise. The densities of the PAM variables B_i then immediately follow. The summation of B_i's, i. e., V_i follows from the characteristic function techniques. However, in the presence of additional partial band jamming and like user interferences, most of the B_i's will still be distributed Rayleigh or Rician except for that bank which is hit by like user interference. The summation V_i of all B_i 's is assumed Gaussian in this chapter. This is a good approximation if we recall that the constituting distributions are: Rayleigh or Rician derivatives thereof (pdf) stretched or contracted depending on the value of multiplication factor α_i (Papoulis [5.5]). Also, the assumption is justified for larger alphabet size M

and by the mechanism of the Viterbi decoding (decision as to surviving paths is based on symbols at each stage). Also, because of slow FH we can separately find the means and variances of V_i (assumed Gaussian) then combine the six situations previously discussed. And noting that the normalized Rayleigh mean and variance equals $\sqrt{\pi/2}$ and $(2-\pi/2)$, respectively, and the Rice mean equals 1 (one) and the Rice variance equals 1 (one). Assuming signal i, $i = 1, ,2, \ldots\ldots M$ is transmitted we obtain,

$$\mu_1 = \sigma(\sqrt{\frac{\pi}{2}} \sum_{\substack{j=1 \\ j \neq i}}^{M} B_j + B_i A \tag{5.26}$$

The first term is the summation of the $(M-1)$ Rayleigh means of the filters not containing the signal. The second term is the mean of the Rician (R.V.) of the filter containing the signal. σ^2 is the AWGN noise variance and signal amplitude A assumed equal to one.

The variance of V_i corresponding to situation one is given by,

$$\sigma_{1i}^2 = \sigma^2 ((2-\frac{\pi}{2}) \sum_{\substack{j=1 \\ j \neq i}}^{M} B_j^2 + \sigma^2 . B_i^2) \tag{5.27}$$

In the second of the six cases discussed before, the only change from case one is the addition of the wide-band jammer variance in the data band, i.e.,

$$\sigma_J^2 = \frac{J}{\rho W} . W_d . = \frac{J}{\rho W} M . R_s \tag{5.28}$$

It follows that

$$\mu_{2i} = (\sqrt{\sigma^2 + \sigma_J^2} (\sqrt{\frac{\pi}{2}}) \sum_{\substack{j=1 \\ j \neq i}}^{M} B_j + B_i A . 1) \tag{5.29}$$

$$\sigma_{2i}^2 = (\sigma^2 + \sigma_j^2)\,(2-\frac{\pi}{2}) \sum_{\substack{j=1 \\ j\neq i}}^{M} B_j^2 + B_i^2 \cdot (\sigma^2 + \sigma_j^2) \tag{5.30}$$

In the third case, we have signal plus noise plus like user tone in the bank containing the signal. The mean and variance of this bank (containing the signal) are denoted by θ_1 and γ_1^2, respectively based on AWGN variance σ^2. It follows that

$$\mu_{3i} = \sigma(\sqrt{\frac{\pi}{2}}) \sum_{\substack{j=1 \\ j\neq i}}^{M} B_j + B_i \cdot \theta_i \tag{5.31}$$

$$\sigma_{3i}^2 = \sigma^2(2 - \frac{\pi}{2}) \sum_{\substack{j=1 \\ j\neq i}}^{M} B_j^2 + B_i^2 \cdot \gamma_1^2 \tag{5.32}$$

The remaining cases follow from the above, i.e.,

$$\mu_{4i} = \frac{1}{M} \sum_{k=1}^{M} (\sigma(\sqrt{\frac{\pi}{2}}) \sum_{\substack{j=1 \\ j\neq i,k}}^{M} B_j + A \cdot B_i + B_k \cdot A) \tag{5.33}$$

$$\sigma_{4i}^2 = \frac{1}{M} \sum_{k=1}^{M} (\sigma^2\,(2 - \frac{\pi}{2})) \sum_{\substack{j=1 \\ j\neq i,k}}^{M} B_j^2 + \sigma^2 \cdot B_i^2 + \sigma^2 \cdot B_k^2) \tag{5.34}$$

The averaging implied by the summation over k is necessary since the tone interference can hit in any of the M banks.

$$\mu_{5i} = \frac{1}{M} \sum_{k=1}^{M} (\sqrt{\sigma^2 + \sigma_j^2}\,(\sqrt{\frac{\pi}{2}}) \sum_{\substack{j=1 \\ j\neq i,k}}^{M} B_j + A \cdot B_i + B_k \cdot A) \tag{5.35}$$

$$\sigma_{5i}^2 = \frac{1}{M} \sum_{k=1}^{M} ((\sigma^2 + \sigma_j^2)\,(2 - \frac{\pi}{2}) \sum_{\substack{j=1 \\ j\neq i,k}}^{M} B_j^2 + (\sigma^2 + \sigma_j^2) B_k^2 + (\sigma^2 + \sigma_j^2) \cdot B_k^2) \tag{5.36}$$

$$\mu_{6i} = \sqrt{\sigma^2 + \sigma_j^2}\left(\sqrt{\frac{\pi}{2}}\right) \sum_{\substack{j=1 \\ j \neq i}}^{M} B_j + B_i \cdot \theta_2 \tag{5.37}$$

$$\sigma_{6i}^2 = \left(\sqrt{\sigma^2 + \sigma_j^2}\right)\left(2 - \left(\sqrt{\frac{\pi}{2}}\right)\right) \sum_{\substack{j=1 \\ j \neq i}}^{M} B_j^2 + B_i^2 \cdot \gamma_2^2 \tag{5.38}$$

Still, θ_2, γ_2^2 (mean and variance, respectively, of the bank containing the signal) are derived similar to θ_1, γ_1^2. However, they are based on AWGN plus jamming variance ($\sigma^2+\sigma_j^2$) rather than just σ^2 as in the (θ_1, γ_1^2) case.

Averaging the quantities in eqs. (5.26) - (5.38) over the probabilities in eqs. (5.5), (5.8), (5.11), (5.13), (5.15) and (5.17) we obtain the average mean and variance of V_i.

$$\mu_{Vi} = p_1\mu_{1i} + p_2\mu_{2i} + p_3\mu_{3i} + p_4\mu_{4i} + p_5\mu_{5i} + p_6\mu_{6i} \tag{5.39}$$

$$\sigma_{Vi}^2 = p_1\sigma_{1i}^2 + p_2\sigma_{2i}^2 + p_3\sigma_{3i}^2 + p_4\sigma_{4i}^2 + p_5\sigma_{5i}^2 + p_6\sigma_{6i}^2 \tag{5.40}$$

Substituting the various values of B_i of the means and variances of Rayleigh and Rice (pdfs) we get

$$\begin{aligned}\mu_{Vi} = {} & p_1\left[\sigma \cdot \sqrt{\frac{\pi}{2}} \cdot \Delta_i + B_i \cdot A\right] + p_2\left[\left(\sqrt{\sigma^2+\sigma_j^2}\right)\sqrt{\frac{\pi}{2}} \cdot \Delta_i + A \cdot B_i\right] \\ & + p_3\left[\sigma\sqrt{\frac{\pi}{2}}\Delta_i + B_i \cdot \theta_i\right] + p_4\left[\left(\frac{1}{M}\sum_{k=1}^{M}\sigma\sqrt{\frac{\pi}{2}} \cdot \Delta_{i,k}\right) + A \cdot B_i\right] \\ & + p_5\left[\frac{1}{M}\sum_{k=1}^{M}\sqrt{\sigma^2+\sigma_J^2} \cdot \sqrt{\frac{\pi}{2}} \cdot \Delta_{i,k} + A \cdot B_i\right] \\ & + p_6\left[\sqrt{\sigma^2+\sigma_j^2}\sqrt{\frac{\pi}{2}} \cdot \Delta_i + B_i \cdot \theta_2\right]\end{aligned} \tag{5.41}$$

$$\begin{aligned}\sigma_{Vi}^2 = {} & p_1\left[\sigma^2\left(2 - \frac{\pi}{2}\right) \cdot \nabla_i + \sigma^2 \cdot B_i^2\right] \\ & + p_2\left[(\sigma^2 + \sigma_j^2) \cdot \left(2 - \frac{\pi}{2}\right) \cdot \nabla_i + (\sigma^2+\sigma_j^2) \cdot B_i^2\right]\end{aligned} \tag{5.42}$$

$$+ p_3 \left[\sigma^2 \cdot (2 - \frac{\pi}{2}) \nabla_i + B_i^2 \cdot \gamma_1^2\right]$$

$$+ p_4 \left[\frac{1}{M} \sum_{k=1}^{M} \sigma^2 (2 - \frac{\pi}{2}) \cdot \nabla_{i,k} + \sigma^2 \cdot B_i^2 + \sigma^2\right]$$

$$+ p_5 \left[(\sigma^2 + \sigma_f^2) \cdot (2 - \frac{\pi}{2}) \frac{1}{M} \sum_{k=1}^{M} \nabla_{i,k} + (\sigma^2 + \sigma_f^2) \cdot B_i^2 + (\sigma^2 + \sigma_f^2) \cdot 1\right]$$

$$+ p_6 \left[(\sigma^2 + \sigma_f^2) \cdot (2 - \frac{\pi}{2}) \cdot \nabla_i + B_i^2 \cdot \gamma_2^2\right]$$

Now, assuming signal i is transmitted and by the minimum free distance of the taken trellis code given by d_{free} the probability of correctly decoding the i-th signal is

$$P_{ci} = \int_{\varsigma_1}^{\varsigma_2} \frac{1}{\sqrt{2\pi}\sigma_{Vi}} e^{\frac{-(\gamma - \mu_{Vi})^2}{2\sigma_{Vi}^2}} d\gamma \qquad (5.43\text{-A})$$

where ς_1 and ς_2 are given as follows:

$$\varsigma_1 = \frac{-(M-2i+2)P}{M-1} + \frac{1}{2}\left[\frac{d_{free}}{\Delta_0}\right]\Delta_0 \qquad (5.43\text{-B})$$

$$\varsigma_2 = \frac{-(M-2i)P}{M-1} + \frac{1}{2}\left[\frac{d_{free}}{\Delta_0}\right]\Delta_0 \qquad (5.43\text{-C})$$

In (5.43-B) and (5.43-C) integer values of $\left[\frac{d_{free}}{\Delta_0}\right]$ are obtained from reference [5.2], [5.3].

For PAM signals we have now to average over all signal levels, i.e.,

$$P_c = \frac{1}{M} \sum_{i=1}^{M} P_{ci} \qquad (5.44)$$

and P_{ce} is the trellis symbol decoding error and is given by

$$P_{ce} \cong N_{free}(1 - P_c) \qquad (5.45)$$

where P_c is given above (5.44) and N_{free} has been defined earlier.

Now, if concatenated Reed-Solomon/trellis coding (scheme-a) is used then the decoded symbols from the inner decoder (trellis) will feed the outer RS decoder. However, we assume here a (N, K) RS code with symbols taken from the (M^m) possibilities, i.e., each RS symbol encompasses m (MFSK) symbols and it follows that the probability of RS symbol error at the input of the RS decoder is given by (assuming independence)

$$P_{se} = \sum_{l=1}^{m} \binom{m}{l} (P_{ce})^l (1-P_{ce})^{m-l} \tag{5.46}$$

The resulting probability of correct RS symbol decoding at the output of the RS decoder is given by

$$P_{rs} = \sum_{l=e+1}^{N} \binom{N}{l} P_{se}{}^l (1-P_{se})^{N-l} \frac{l+e}{N} \tag{5.47}$$

where e is the RS symbol error correction capability of the (N, K) RS outer code, i.e.,

$$e = \left\lfloor \frac{N-K}{2} \right\rfloor \tag{5.48}$$

Again, an error in one RS symbol does not necessarily mean all m $M-ary$ symbols are in error and an $M-ary$ symbol error does not imply all bits are in error. The first fact reflects itself in a multiplicative factor $(\frac{P_{ce}}{P_{se}})$ and the second in $\frac{M}{2(M-1)}$, the common practice for orthogonal signaling we obtain finally the probability of decoded bit errors, i.e.,

$$P_b = P_{rs} \cdot \frac{P_{ce}}{P_{se}} \cdot \frac{M}{2(M-1)} \tag{5.49}$$

The next step in the analysis is the most natural question. Is trellis coding the most powerful and efficient inner code for noncoherent MFSK/FH in the combined jamming, multi access environment involved ?

It will be instructive to compare the performance obtained from the concatenated RS/trellis code (scheme-a) with a concatenated RS outer/RS inner code (scheme-b). Again, slow FH is assumed, together with the assumptions before and no side information utilized. The partial band jamming and multi access environment remains the same as outlined before. The inner and outer codes have rates k_i/n_i and K_i/N_i, respectively. The inner and outer code symbols contains each m_i, m_i' M-ary symbols, respectively, where

$$m_i = \log_M (n_i + 1) \tag{5.50}$$

$$m_i' = \log_M (N_i + 1) \tag{5.51}$$

Emphasis will be placed on the codes' performance rather than their algebraic structure. While the received signal and the jammer are still described by eqs. (5.3), (5.2) and (5.7), the receiver structure is slightly different than that of Fig's. 5.4, 5.5 and 5.7.

Hard decisions will be used rather than the soft decisions, we associated with the trellis code before. The receiver (Fig. 5.7) is nothing but a bank of M filters and envelope detectors. A subsequent largest of hard decision will yield the MFSK symbol and a subsequent parallel to serial conversion will yield the detected bits. These bits will be fed to the inner and outer RS decoders as in Fig. 5.4.

Now, to find the probability of one Reed-Solomon symbol error we could average over the six conditions of interference on the channel whose

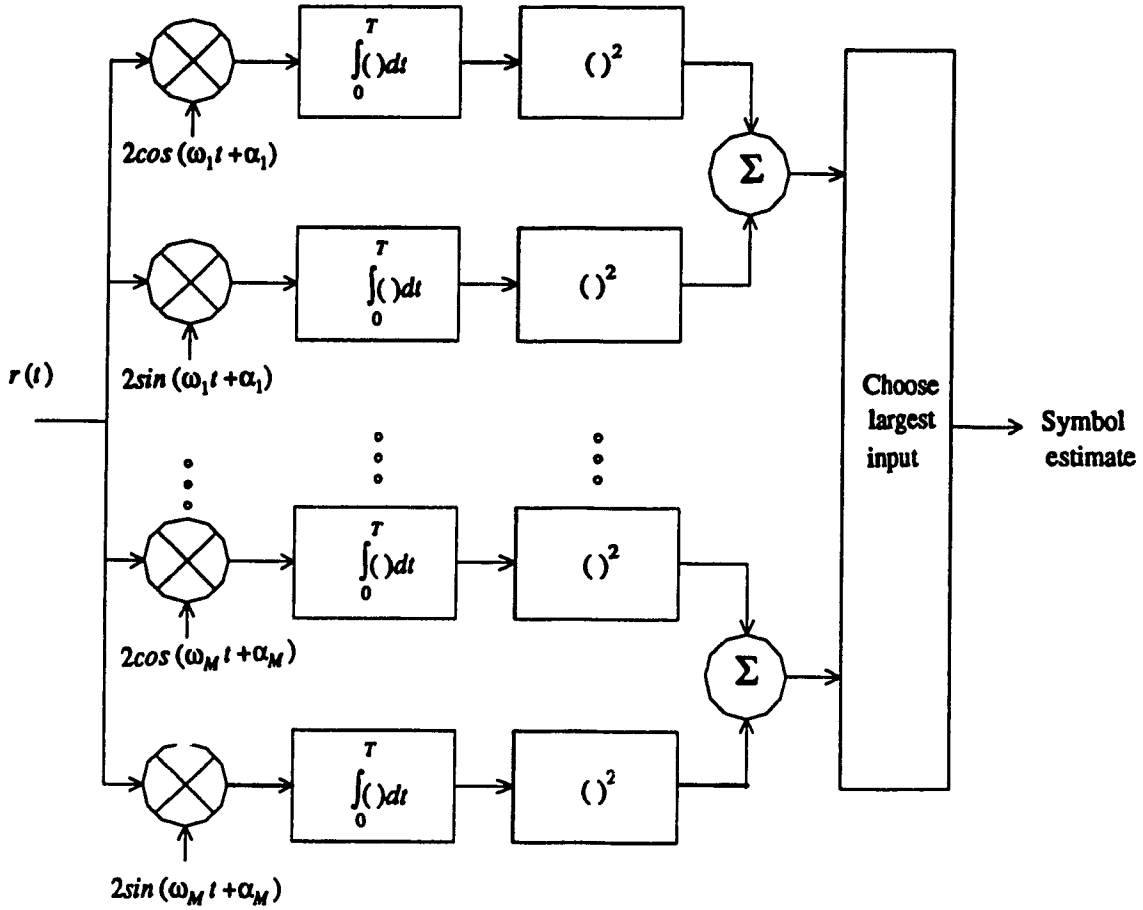

(a)

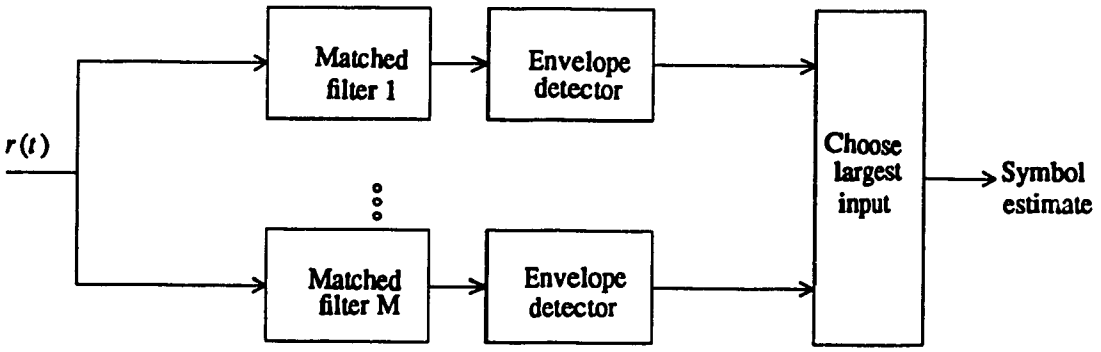

(b)

Fig. 5.7 Noncoherent demodulators for *M–ary* FSK, a.) Correlate and integrate implementation b.) Bandpass filter and envelope detect implementation

probabilities were given by eqs. (5.5), (5.8), (5.11), (5.13), (5.15) and (5.17). However, we choose to obtain a worst case here and thus obtain the probability of symbol demodulation error as

$$P_{se} \leq 1-(1-P_h)^{U-1}\,[(1-\rho)(1-P_0)^{m_i}] + \rho(1-P_{J,0})^{m_i}] + \frac{1}{2M}(1-(1-P_h)^{U-1})$$

where M, K, P_h, ρ, and m_i are the $M-ary$ size, the number of users, the probability of hit, the jammer band ratio (eq. 5.9) and number of $M-ary$ symbols per RS inner code symbol, respectively. Now

$$P_h = (\frac{1+(m_i/N_s)}{PG})\,\frac{n_i}{k_i}\,\frac{N_i}{K_i} \tag{5.53}$$

where N_s is as defined in (5.6), PG is the uncoded Processing Gain (PG) and the multiplication by N_i/K_i, n_i/k_i takes care of the fact that data bandwidth expands by the use of the inner and outer codes thus decreasing the PG and increasing the probability of frequency hit (if we are to keep the effective data rate the same in both cases of coded and uncoded systems).

P_0, P_{J0} are the symbol error probability on a channel affected only by AWGN or (AWGN and partial band jamming), respectively. These will be given shortly.

Eq. (5.52) in fact reflects all six interference situations explained before except for replacing situations (5.10), (5.14), and (5.16) by the last term on the right hand side of (5.52). This reflects a worst case since we are effectively saying than an error will always occur if a like user tone exists anywhere in the intended receiver banks. However, our worst case is more lenient than [5.6] since in one of the situations (with probability, $1/M$) the interference will hit the signal bank and roughly in 50% of these cases the interference will aid the

signal and no error will be made. The probabilities P_0, $P_{J,o}$ in (5.52) will now be given,

$$P(\eta) = \sum_{i=1}^{M-1} \binom{M-1}{i} \frac{(-1)^{i+1}}{1+i+i\,\beta(\eta)} \exp\left(\frac{i\,\delta(\eta)}{i+1+i\,\beta(\eta)}\right) \tag{5.54}$$

Equation (5.54) is just the formula for error probability for noncoherent MFSK modified to include fading. where

$$\beta(\eta) = \Lambda(\eta)/(1+\gamma^{-2}) \tag{5.55}$$

$$\delta(\eta) = \Lambda(\eta)/(1+\gamma^{2}) \tag{5.56}$$

$$\Lambda(\eta) = (E_b \log_2 M/\eta)\frac{K_i\, k_i}{N_i\, n_i} \tag{5.57}$$

where $\Lambda(\eta)$ is the coded symbol SNR and E_b is the uncoded bit SNR, and $\eta/2$ is the double sided noise density,

γ^2 is the (scatter/fading) power ratio,

If γ^2 = zero, this implies $\beta(\eta) = 0$, $\delta(\eta) = \Lambda$-(η) which is the pure AWGN reception case.

If γ^2 = infinity, this implies $\beta(\eta)=\Lambda(\eta)$ and $\delta(\eta) = 0$ which is the Rayleigh fading reception case.

$P_{0,j}$ is simply obtained by replacing η by $(\eta + N_J)$ in (5.54) where N_J is given by equation (5.7), i.e.,

$$P_{0,j} = P_0(\eta + N_J) \tag{5.58}$$

Now, to find the error improvement obtained by using the concatenated RS codes we assume that m_i/m_i' is an integer and we follow the sequence of

events taking place following the M-*ary* noncoherent symbol detection and the associated RS symbol errors given by P_{se} of eq. (5.52). The inner decoder combines n_i (RS symbols) each consisting of m_i MFSK symbols to give $(k_i\, m_i)$ MFSK symbols to the outer decoder. The outer decoder takes $(N_i\, m_i')$ of these symbols and finally give $(K_i\, m_i')$. The probability of one RS symbol being in error following the inner decoder is given by,

$$P_{se}^{in} = \sum_{j=t+1}^{n_i} \frac{j+t}{n_i} \binom{n_i}{j} (P_{se})^j (1-P_{se})^{n_i-j} \tag{5.59}$$

where t is the error correction capability of the inner decoder

$$t = \left\lfloor \frac{(n_i - k_i)}{2} \right\rfloor \tag{5.60}$$

If we now assume $m_i = m_i'$ then every RS symbol decoding error coming out of the inner decoder means one input RS symbol error to the outer decoder in which case the probability of one RS symbol error of this outer decoder becomes,

$$P_{se}^{out} = \sum_{j=t_2+1}^{N_i} \frac{j+t_2}{N_i} \binom{N_i}{j} (P_{se}^{in})^j (1-P_{se}^{in})^{N_i-j} \tag{5.61}$$

where $t_2 = \left\lfloor (N_i - K_i)/2 \right\rfloor$ for the outer code. Now a decoding error in one RS symbol does not necessarily mean every one of the m_i' (MFSK) symbols is in error, also, if orthogonal MFSK is used we obtain for the final decoded bit error

$$P_b = \frac{M}{2(M-1)} \frac{P_{se}''}{P_{se}} P_{se}^{out} \tag{5.62}$$

Where P_{se} is as given in (5.52) and P_{se}'' is equal to P_{se} from (5.52) with

m_i equal to one.

In (5.62), the middle term represents the conditional probability of one MFSK symbol error given one RS symbol error.

5.4 Results

The error performance of the new system has been determined for both the inner trellis code (scheme-a) and inner RS code (scheme-b) cases. The bit error probability for the trellis code has been found to decrease as M is decreased in both cases (Figs. 5.8 and 5.16), keeping all other factors such as jamming/signal power ratio J/P, jamming duty factor ρ, number of users, uncoded processing gain and uncoded bit SNR the same for both cases.

For the inner trellis code and outer RS code case (scheme-a) and for $M = 4$, the bit error probability has been calculated for few selected trellis codes of [5.2,5.3], such as the (state 8, $\frac{d_{free}^2}{\Delta_0^2} = 10$) and (state 32, $\frac{d_{free}^2}{\Delta_0^2} = 13$) codes.

In Fig. 5.8, (for the 8 state trellis code (scheme-a) case), the bit error probability vs. the number of users has been plotted using jamming/signal power ratio J/P and processing gain as parameters. Under the same condition the bit error probability has been plotted for 32 state trellis code (scheme-a) case (Fig. 5.9). It is clear from the two Fig's. 5.8 and 5.9 that the error performance in the environment mentioned is better for the 8 state trellis inner code case (in Fig. 8, for 8-state trellis (scheme-a) and $U = 60$, $PG = 512$, the error probability is 2.10^{-5} and in Fig. 9, for 32-state trellis (scheme-a) under the same condition , the error probability is 5.10^{-4}.

For the same trellis codes (scheme-a)(i.e., 8 state, and 32 state) and for $M=4$ the error probability vs. jamming/signal power ratio J/P has been plotted in Fig's. 10, and 11, respectively, using processing gain as a parameter and keeping the number of users equal to 4 and ρ equal to .9. Whether jamming/signal power ratio J/P changes (Fig. 10), or the number of users (Fig. 8), we generally see that the 8 - state trellis (scheme-a) performs better compared to the 32-state trellis code (scheme-a) case. The 8-state code has been compared with other codes of similar complexity and has been found to perform better.

For the 8- state code (scheme-a) (Fig. 5.8), it is apparent that as the processing gain increases the error probability decreases. In Fig. 5.12, the error probability has been plotted vs. the number of users using jamming/signal power ratio J/P as a parameter.

The performance of the new system has been evaluated for RS inner and RS outer code (scheme-b) case also (Figs. 5.13 and 5.17). It has been found that as the $M-ary$ size is decreased the error probability decreases all other conditions, i.e., processing gain, jamming/signal power ratio J/P, jamming duty factor ρ, uncoded bit SNR remaining the same. For RS inner code case (scheme-b) and for $M=4$ the error probability has been plotted vs. the number of users taking processing gain as a parameter (Fig. 5.13). Increasing the number of users in this case (Fig. 5.13) results in a drastic increase in P_b but with the increase of the processing gain the error probability decreases (in Fig. 13, at $PG = 512$, number of users $U = 9$, the error probability is 10^{-7} and at $U = 12$ the error probability is 2.10^{-2}). In Fig. 5.14 and for RS inner code case (scheme-b) the error probability has been vs. jamming/signal power ratio J/P using processing gain as a parameter. In Fig. 5.15, the error

probability has been plotted vs. the number of users with jamming/signal power ratio J/P as a parameter. Comparing Figs.5.14 and 5.15, we generally see the dominating effect for the number of users as opposed to jamming power. For comparison of the performance of the system under inner trellis code case (8-state) (scheme-a) with inner RS code case (scheme-b) we refer to Fig's. 5.8 and 5.13, respectively. It is apparent from the figures that the inner trellis code case (scheme-a) can handle a larger number of users than the inner RS code cas (scheme-b) keeping the same jamming/signal power ratio J/P, jamming duty same uncoded bit SNR (in Fig. 8 for trellis inner code case (scheme-a) for $PG = 512$, and at bit error probability of 10^{-5} the number of users U that can be handled equals $= 55$ and in Fig. 13 for inner RS code (scheme-b) under the same condition and for the same error probability the number of users U that can be handled equals 10).

Finally, comparing Fig's. 5.10 and 5.14 (i.e., for 8- state trellis inner) code case (scheme-a) and RS inner code case (scheme-b), respectively, it is easily seen that the bit error probability for the trellis code case (scheme-a) is less than that of RS inner code case (scheme-b) keeping other parameters the same (in Fig. 10, for inner trellis code case (scheme-a) at $J/P = 12$ and $PG = 512$ the error probability is 3.10^{-5} and in Fig. 14, for inner RS code case (scheme-b) under the same condition as above the error probability equals 4.10^{-2}).

5.5. Conclusion

A new random SS system has been presented. Concatenated trellis code application to such a system have been tried and comparisons were made with concatenated RS codes (scheme-a and scheme-b) (for the first time in the non-coherent environment). It was found that for 4-*ary* MFSK systems the

concatenated trellis code (scheme-a) outperforms the RS concatenated code (scheme-b) and can withstand six times the number of users than the RS case for moderate bit error probability. This may be due to the soft decision decoding inherent in trellis codes as compared to the hard decision assumed for the RS code case.

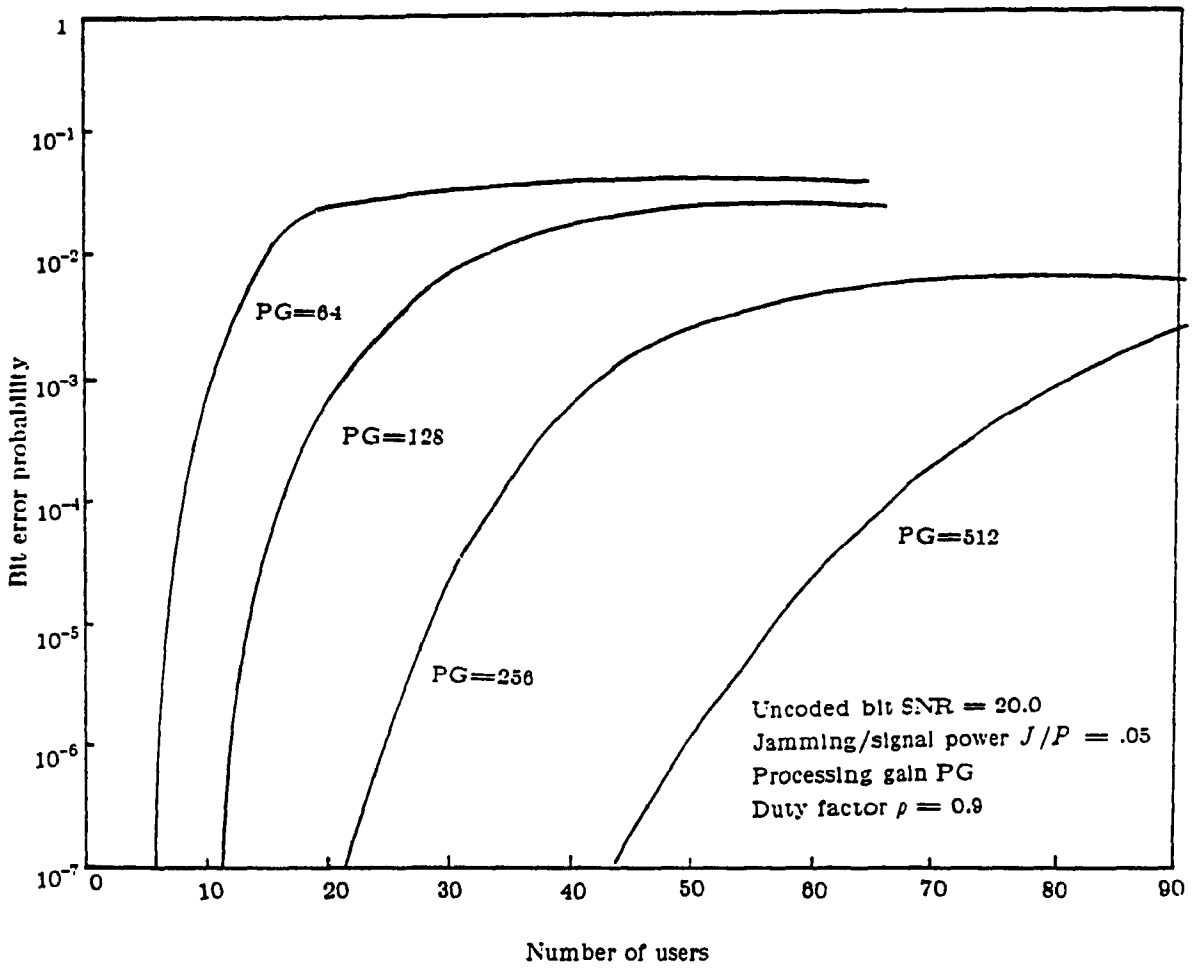

Fig. 5.8 Bit error probability vs. number of users for inner trellis code (8 state) (scheme-a). Uncoded bit SNR = 20. M = 4, jamming/signal power ratio J/P = .05, duty factor ρ = .09

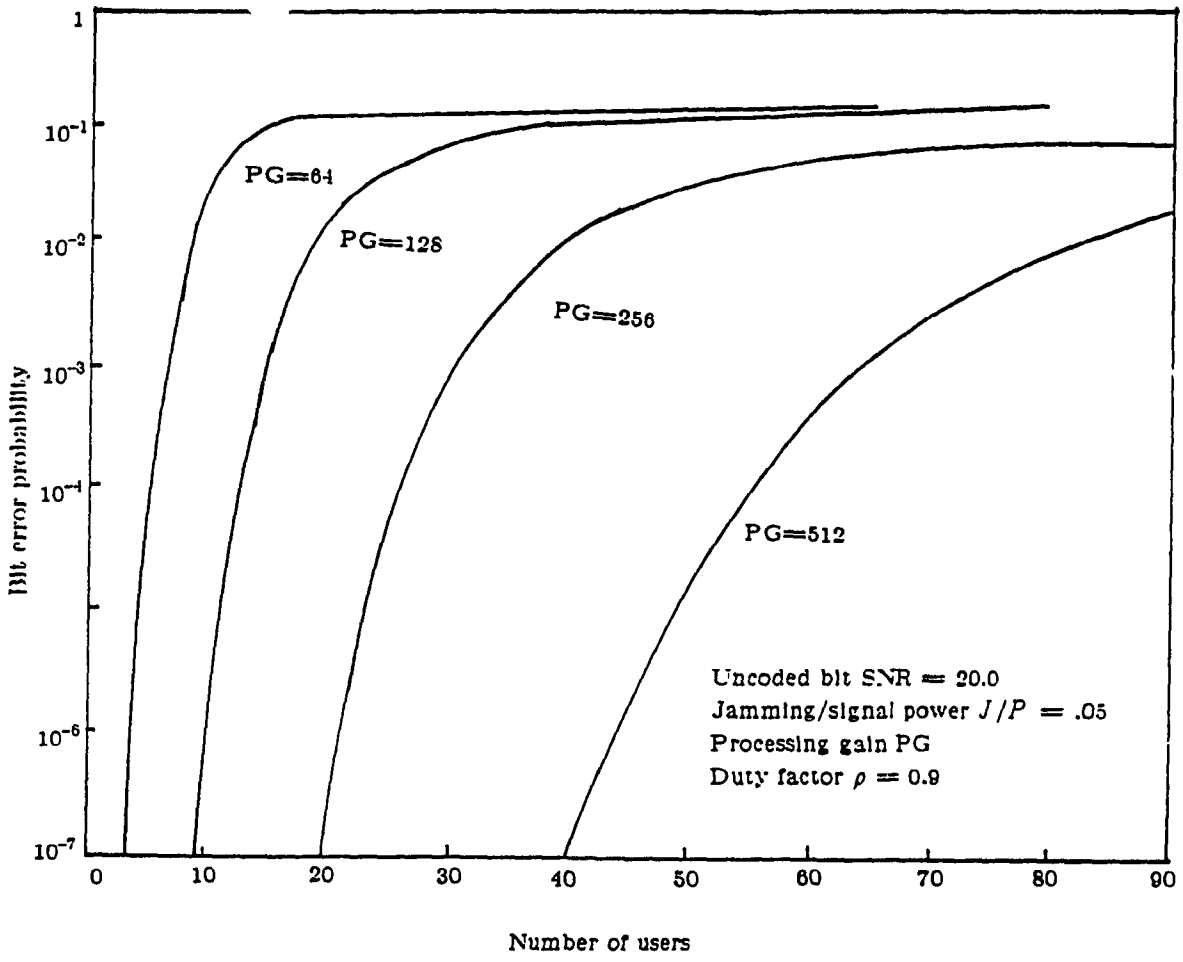

Fig. 5.9 Bit error probability vs. number of users for inner trellis code (32 state) (scheme-a). Uncoded bit SNR = 20., M = 4, Jamming/signal power ratio J/P = .05, duty factor ρ = 0.9

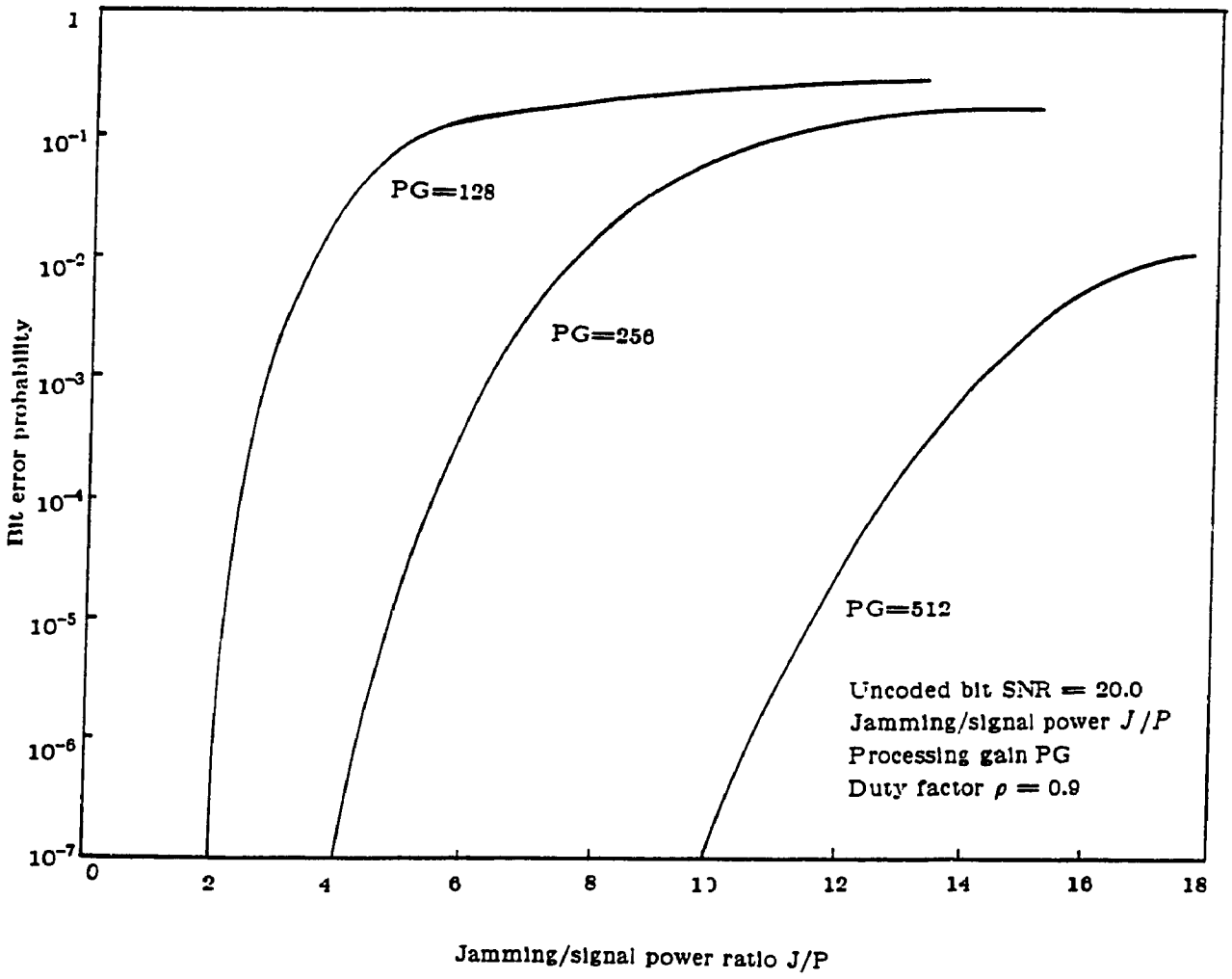

Fig. 5.10 Bit error probability vs. jamming/signal power ratio J/P for inner trellis code (8 state) (scheme-a). $M = 4$, uncoded bit SNR = 20.0, number of users in the system = 4, duty factor $\rho = 0.9$

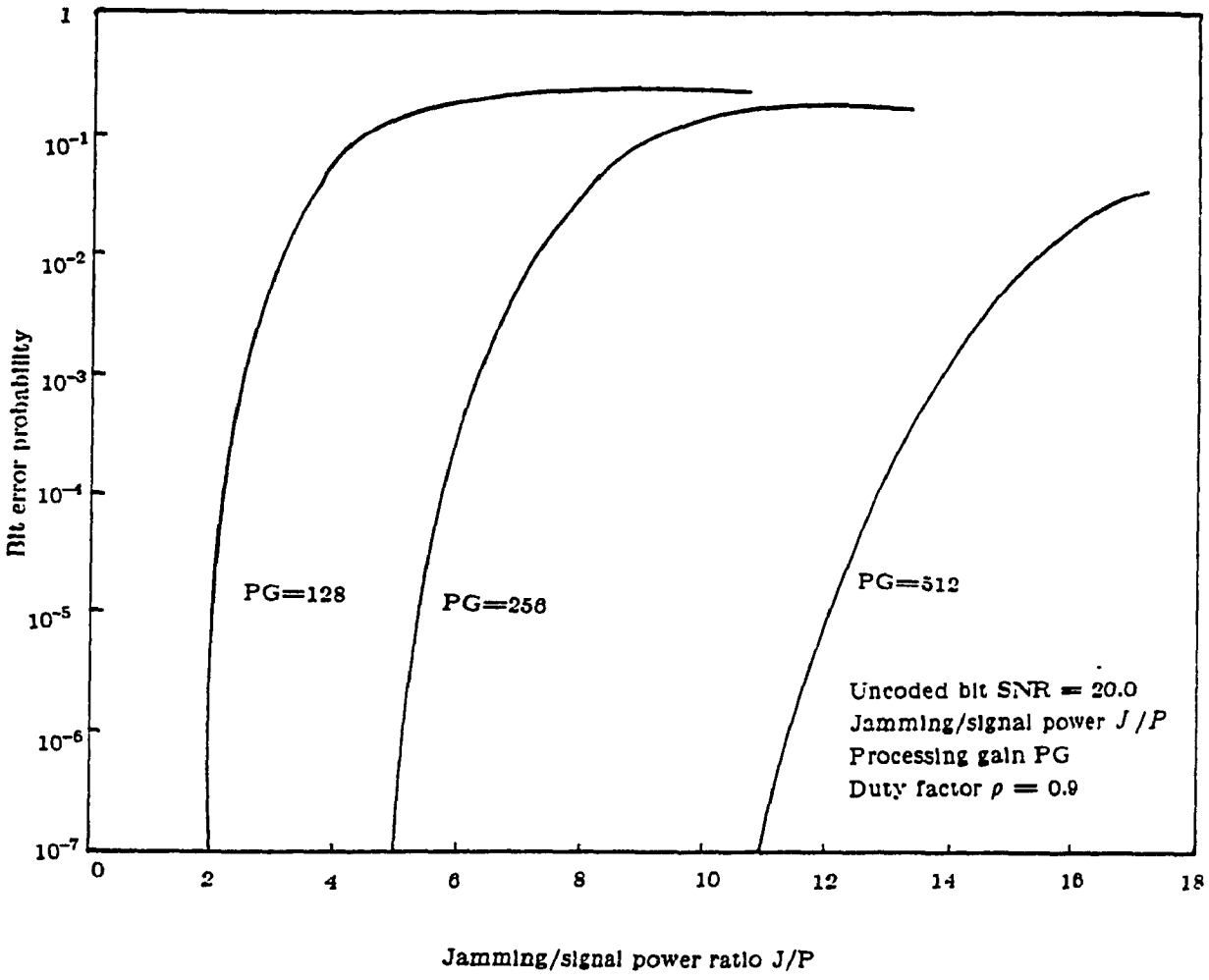

Fig. 5.11 Bit error probability vs. jamming/signal power ratio J/P with processing gain (PG) as a parameter for inner trellis code (32 state) (scheme-a), M = 4, uncoded bit SNR = 20.0, duty factor ρ =0.9.

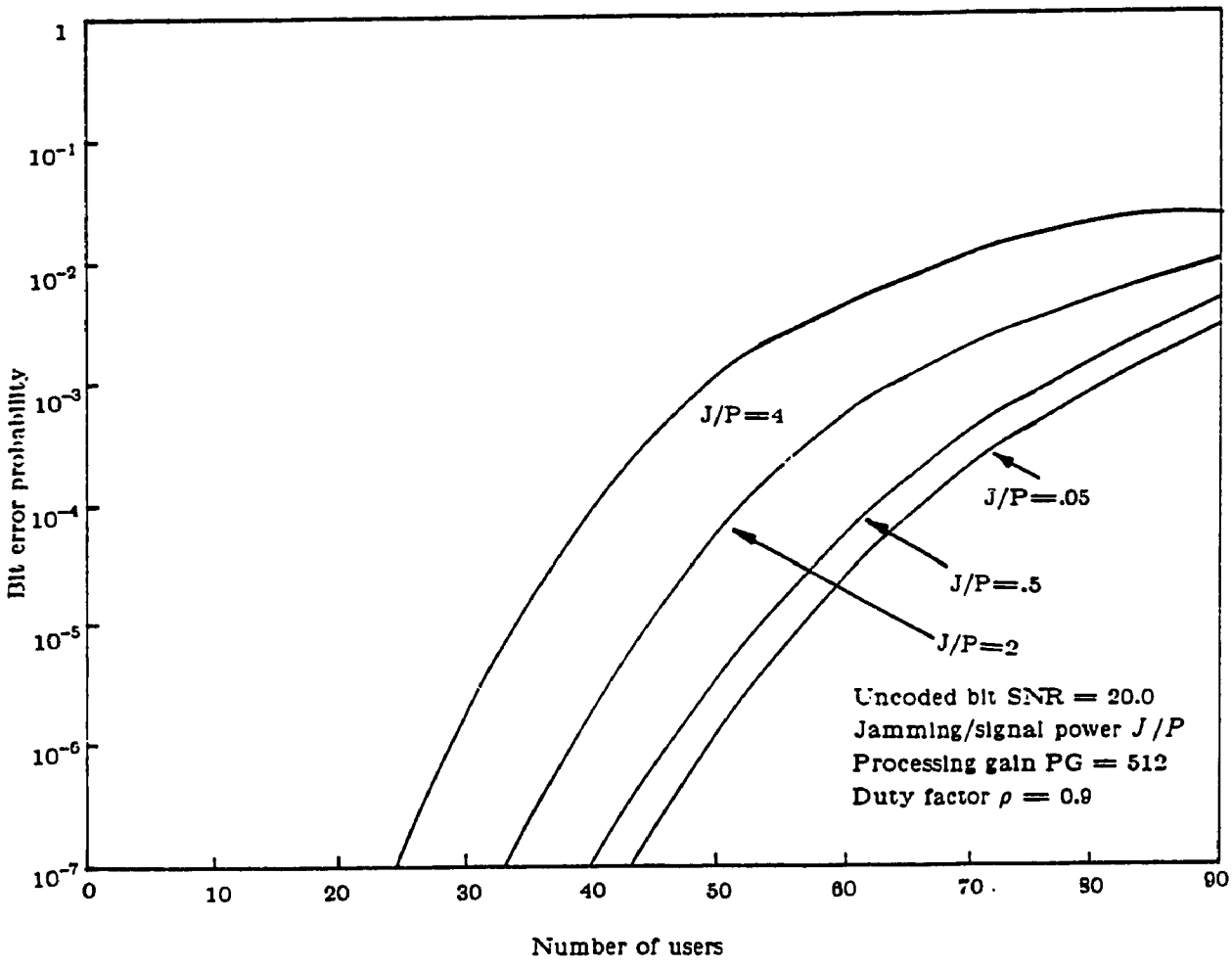

Fig. 5.12 Bit error probability vs. number of users with signal/jamming power J/P as a parameter for inner trellis code (8 state) (scheme-a), $M = 4$, uncoded bit SNR = 20.0, processing gain PG = 512, duty factor $\rho = 0.9$

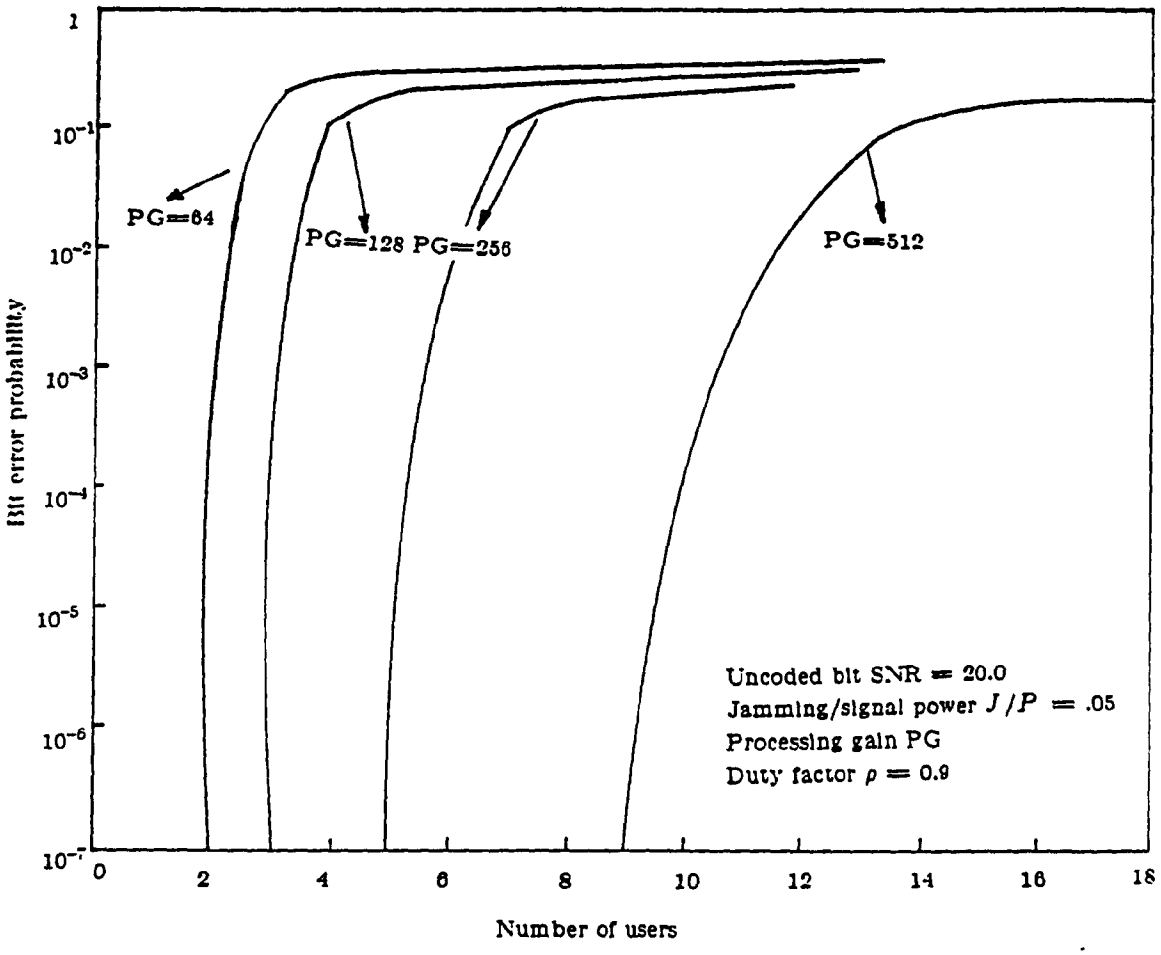

Fig. 5.13 Bit error probability vs. number of users with processing gain (PG) as a parameter for RS inner code (scheme-b). M = 4, uncoded bit SNR = 20.0, jamming/signal power ratio J/P = .05, duty factor ρ = 0.9.

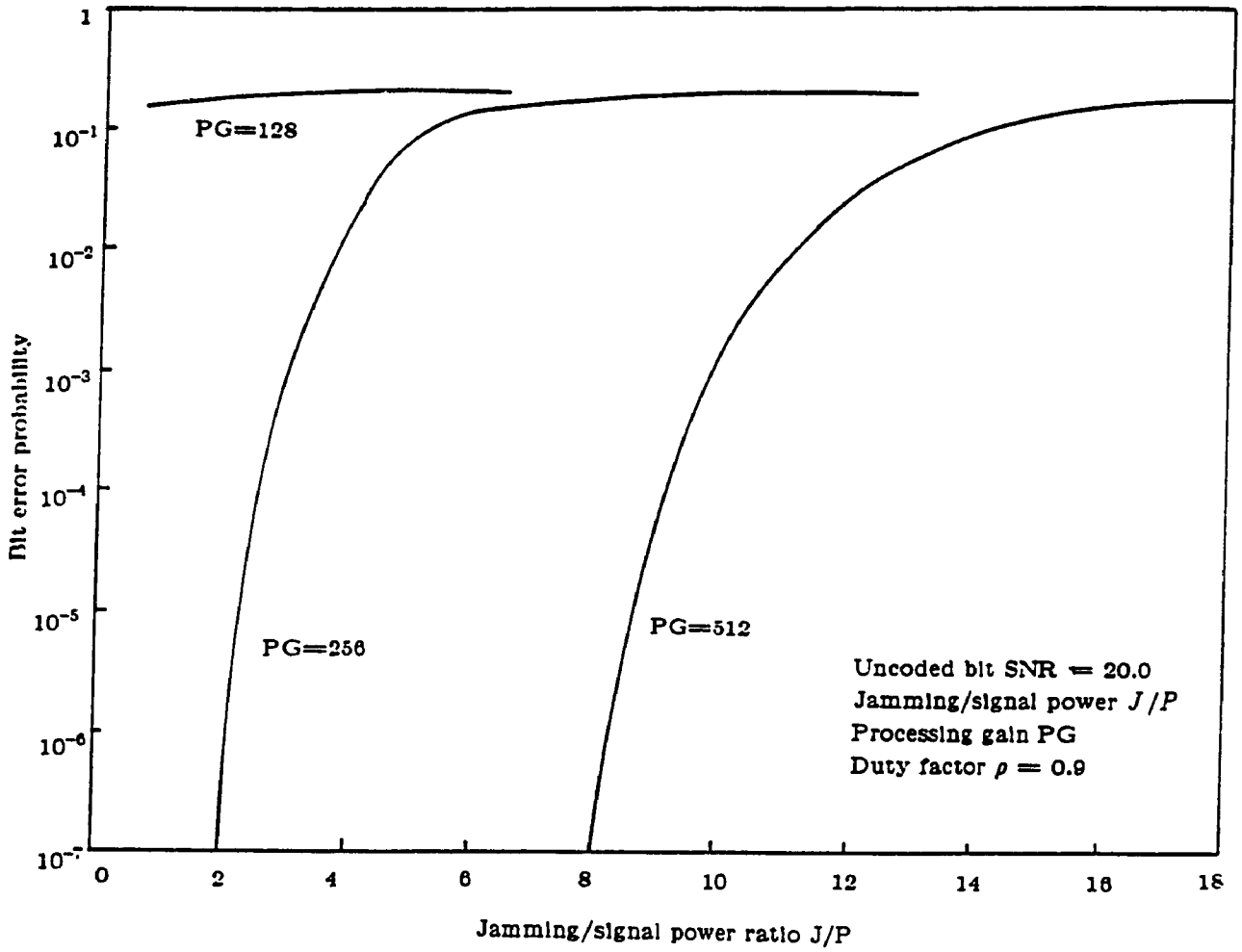

Fig. 5.14 Bit error probability vs. jamming/signal power ratio J/P for RS inner code (scheme-b). $M = 4$, uncoded bit SNR = 20.0, number of users in the system = 4, duty factor $\rho = 0.9$.

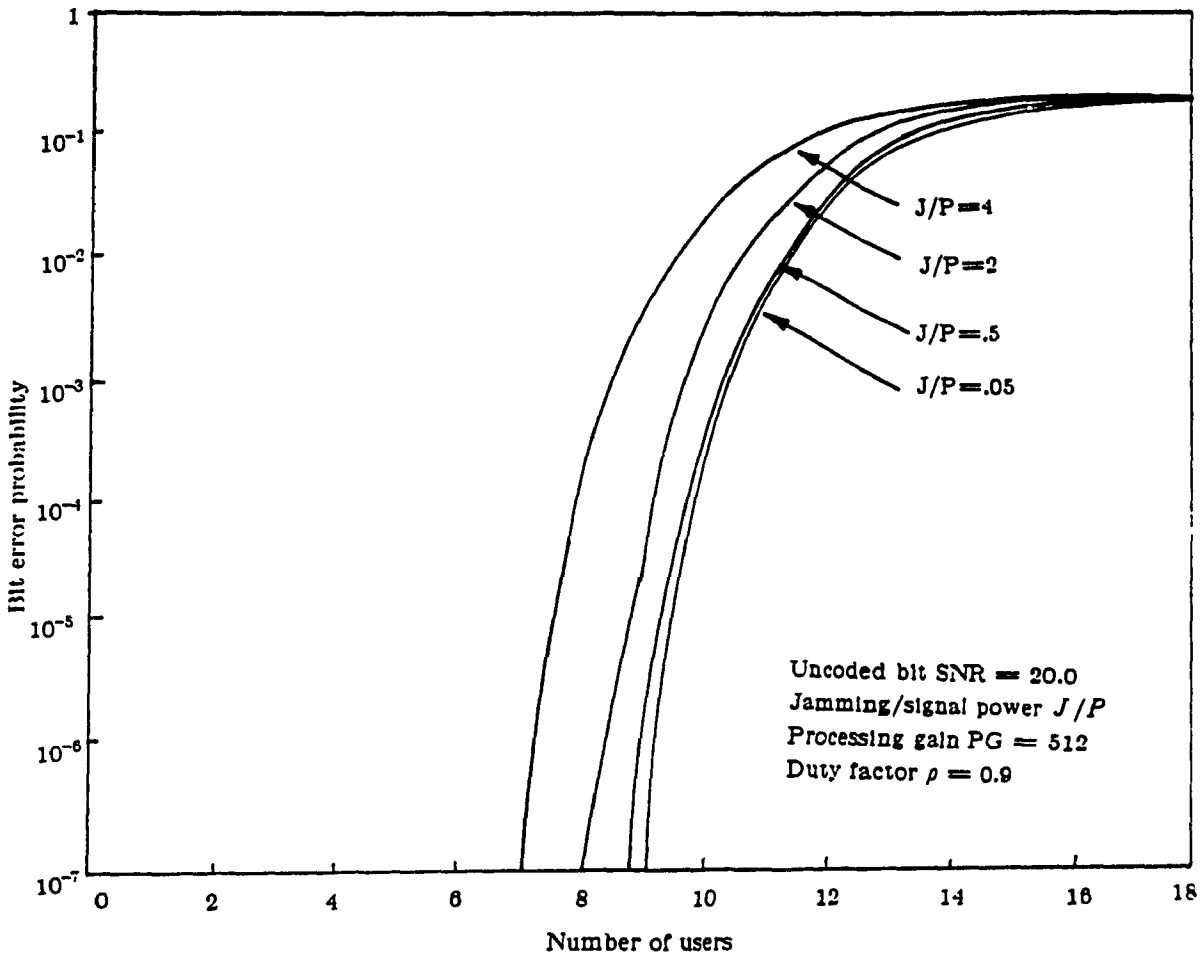

Fig. 5.15 Bit error probability vs. number of users for inner RS code (scheme-b) M = 4, uncoded bit SNR = 20.0, processing gain of the system = 512, duty factor $\rho = 0.9$.

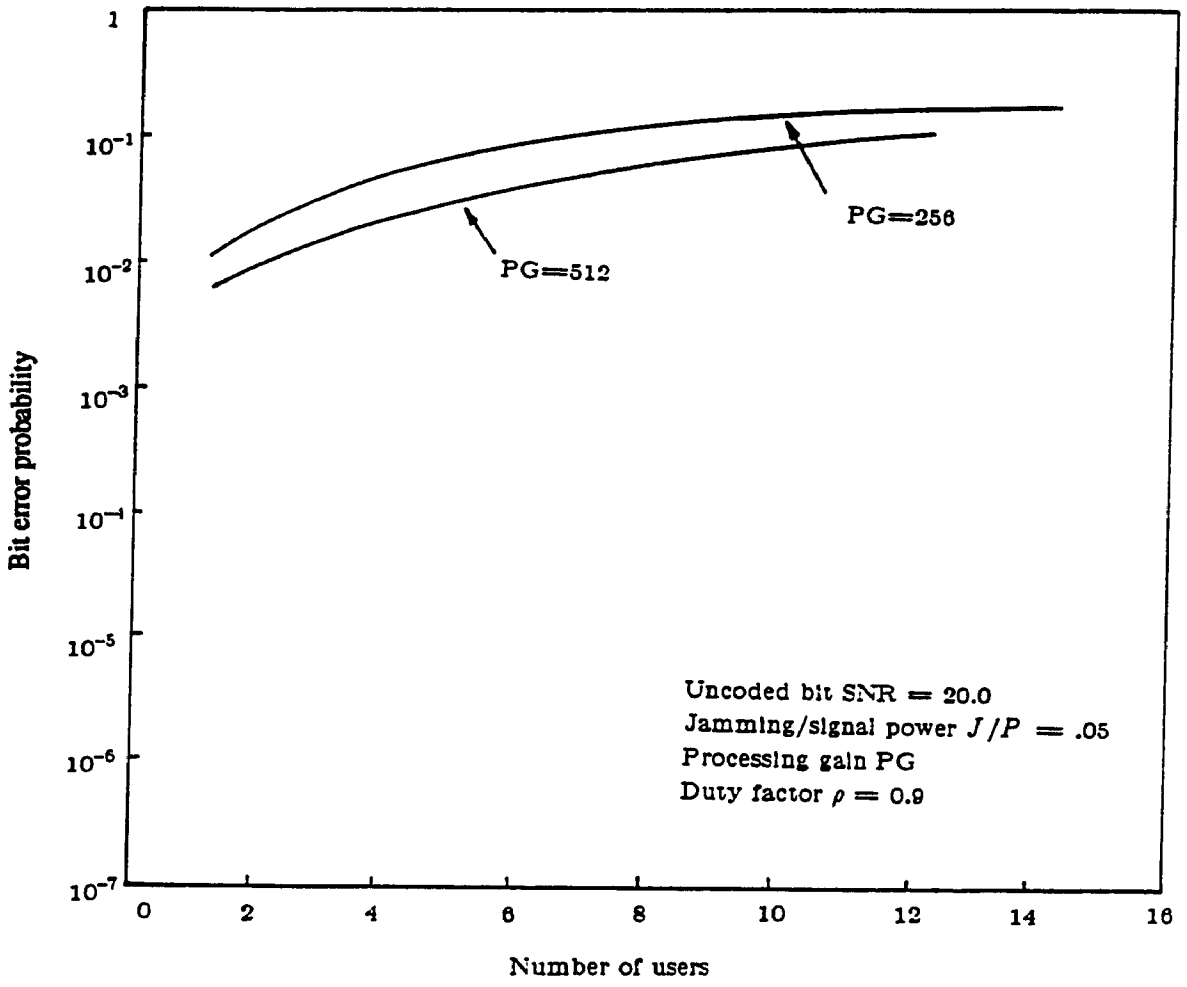

Fig. 5.16 Bit error probability vs. number of users for inner trellis code (8 state) (scheme-a), $M = 8$, uncoded bit SNR = 20.0, jamming/signal power ratio $J/P = .05$, duty factor $\rho = 0.9$.

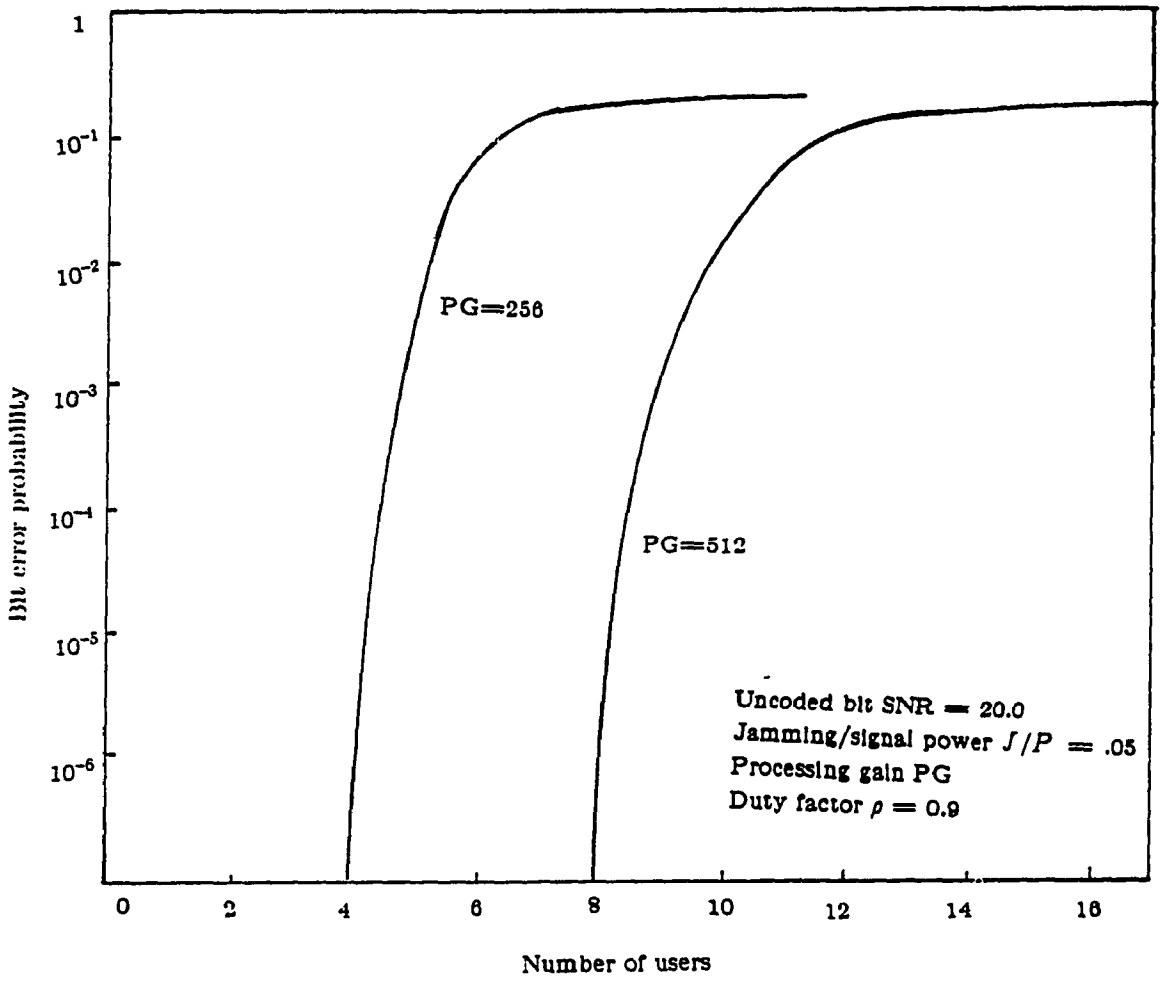

Fig. 5.17 Bit error probability vs. number of users Inner RS code (scheme-b). M = 8, uncoded bit SNR = 20.0, jamming/signal power ratio J/P = .05, duty factor $\rho = 0.9$.

REFERENCES

[5.1] Andrew J. Viterbi, 'Spread Spectrum Communications Myths and Realities', IEEE Communications Magazine, pp. 11-18, May 1979

[5.2] G. Ungerboeck, 'Channel Coding with Multilevel/Phase Signals', IEEE, Transactions on Information Theory', Vol. IT-28, No-1, pp. 55-67, January 1982.

[5.3] G. Ungerboeck, 'Trellis Coded Modulation with Redundant Signal Sets, Part II: State of the Art', IEEE, Communications Magazine, Vol. 25, No. 2, pp. 12-21, February 1987.

[5.4] M.A. Rahman, A.K. Elhakeem, 'Concatenated Combined Modulation and Coding of Frequency Hopping Multi Access Systems', IEEE, Journal on Selected Areas in Communications, Vol. 8, No. 4, pp. 650-662, May 1990

[5.5] A. Papoulis, 'Probability, Random Variables and Stochastic Processes', 2nd. edition, Mc-Graw Hill Book Company, New York.

[5.6] E. Geraniotis, J.W. Gluck, 'Coded FH/SS Communications in the Prescence of Combined Partial-Band Noise Jamming, Rician Non-selective Fading, Multiuser Interference', IEEE Journal of Selected Areas in Communications, Vol. SAC-5, No. 2, pp. 194-213, February 1987

[5.7] M.A. Rahman, A.K. Elhakeem, 'Noncoherent Trellis Coding for Frequency Hopping SUGARW Spread Spectrum Multi Access Systems', AEU, German Journal of Electronics and Communications, Band 44. Heft-1, Jan./Febr. 1990, Selten 1-64, pp. 23-31.

[5.8] M. B. Pursley, W. E. Stark, 'Performance of Reed-Solomon Coded Frequency-Hop Spread-Spectrum Communications in Partial-Band Interference', IEEE, Trans. on Comm., Vol. Com-33, No. 8, pp. 767-773, August 1985.

CHAPTER VI

THROUGHPUT ANALYSIS OF THE 'SUGARW' ACQUISITIONLESS SPREAD SPECTRUM SYSTEM IN MULTI ACCESS AND TONE JAMMING ENVIRONMENTS

6.1 Introduction

Pseudorandom codes have typically been used for the Direct Sequence (DS), the Frequency Hopping (FH) and the Time Hopping spread spectrum (SS) systems [6.1]. It was not possible for a SS receiver to synchronize to a completely random spreading code and the acquisition stage in the SS receiver emerged as the most important component [6.2] in the system. Acquisition time ranges from milliseconds to few seconds in both military and domestic systems [6.3]. Moreover, the inconvenience of plugging in the (time of the day) in some secure systems makes such system inappropriate for real time and/or short mission time applications not to mention the vulnerability to jamming during the acquisition stage, the use of short preamble codes, etc. It would be productive to have a spread spectrum system that does not go from acquisition to verification then to tracking and then to demodulation and back to verification from time to time, etc., [6.4].

To find a system satisfying the acquisitionless requirements the 'SUGARW' SS system was proposed [6.5]. The 'SUGARW' spread spectrum (SS) system does not go from acquisition to verification then to tracking and then to demodulation again from time to time, etc., as in a conventional SS systems. In the DS system preliminary study [6.5] employs Gold codes,

uniform random number generators for the random transmission of one of the few composite Gold Walsh words as the basic spreading waveform of a multi access system with minimum users correlation. The notion of quasi random (as opposed to pseudo-random) code is achieved by a uniform random variate which is used to select the applicable Gold codes (pseudo random) for transmission. Though the effective code length is very long (semi-infinite) the basic constituting Gold codes are short but those basic codes could be changeable in real time on a less frequently basis thus achieving effectively very long quasi random codes. Reception will be possible by incorporating programmable matched filters at the receiver. Due to Doppler and or fading, etc., one matched filter peak may be lost occasionally (miss), another may be added. The FEC status and the control box will be tied by an algorithm that will minimize or cancel these misses and false alarm situations. In the mean time the system will never stop demodulation or switch to acquisition, even under missing few matched filter peaks, the system continues detecting, few information bits will be corrected by decoding, others will be lost. However, the next matched filter output will put things back into prospective and the appropriate Automatic Repeat Request (ARQ) will occasionally be asking for retransmission.

In the following we introduce the new system for Frequency Hopping and we describe the algorithmic detection for this system. In this chapter, the throughput performance of the new acquisitionless spread spectrum (SS) "SUGARW' system has also been evaluated and compared against the conventional SS systems that require code acquisitions for their operations.

6.2 New Acquisitionless System for Frequency Hopping (FH)

To find a system satisfying the acquisitionless requirements a new system has been proposed. The system employs Gold codes [6.6], Walsh functions, uniform random number generators for random transmission of four composite Gold words in DS/PSK and DS/DPSK multi-access systems [6.5]. The technique is slightly modified and applied to the noncoherent FH/MFSK multi-access systems. The generic block diagram of the transmitter of the proposed system is shown in Fig. 6.1.

The uniform number generator of Fig. 6.2, or alternately a large variance Gaussian noise, source is sampled and held every $N_h T_h$ sec where N_h is the number of hops per sub code and T_h is the FH duration. This sample selects one of L stored (short or medium length) Gold codes for controlling the frequency synthesizer (Fig. 6.1). The output of this synthesizer is mixed with the MFSK modulator output after which the signal is up converted and transmitted. The timing box in Fig. 6.1 controls the duration of each involved block. In one example, the Fast Frequency Hopping (FFH) is used meaning that each MFSK symbol ($T_s = \gamma_s T_h$) encompasses one or more frequency hops. However, in this thesis the Slow Frequency Hopping (SFH) is considered and $T_h = N_s T_s$ where N_s is an integer. Before moving to the receiver details it is easy to see that

$$N_h L = PG.M \tag{6.1}$$

where PG is the processing gain, i.e. ratio of the SS bandwidth to the data bandwidth, M is the size of the signal constellation and L is the number of subcode in the total code (number of matched filter banks in each receiver).

$$PG = \frac{W}{MR_b}(log_2 M) \tag{6.2}$$

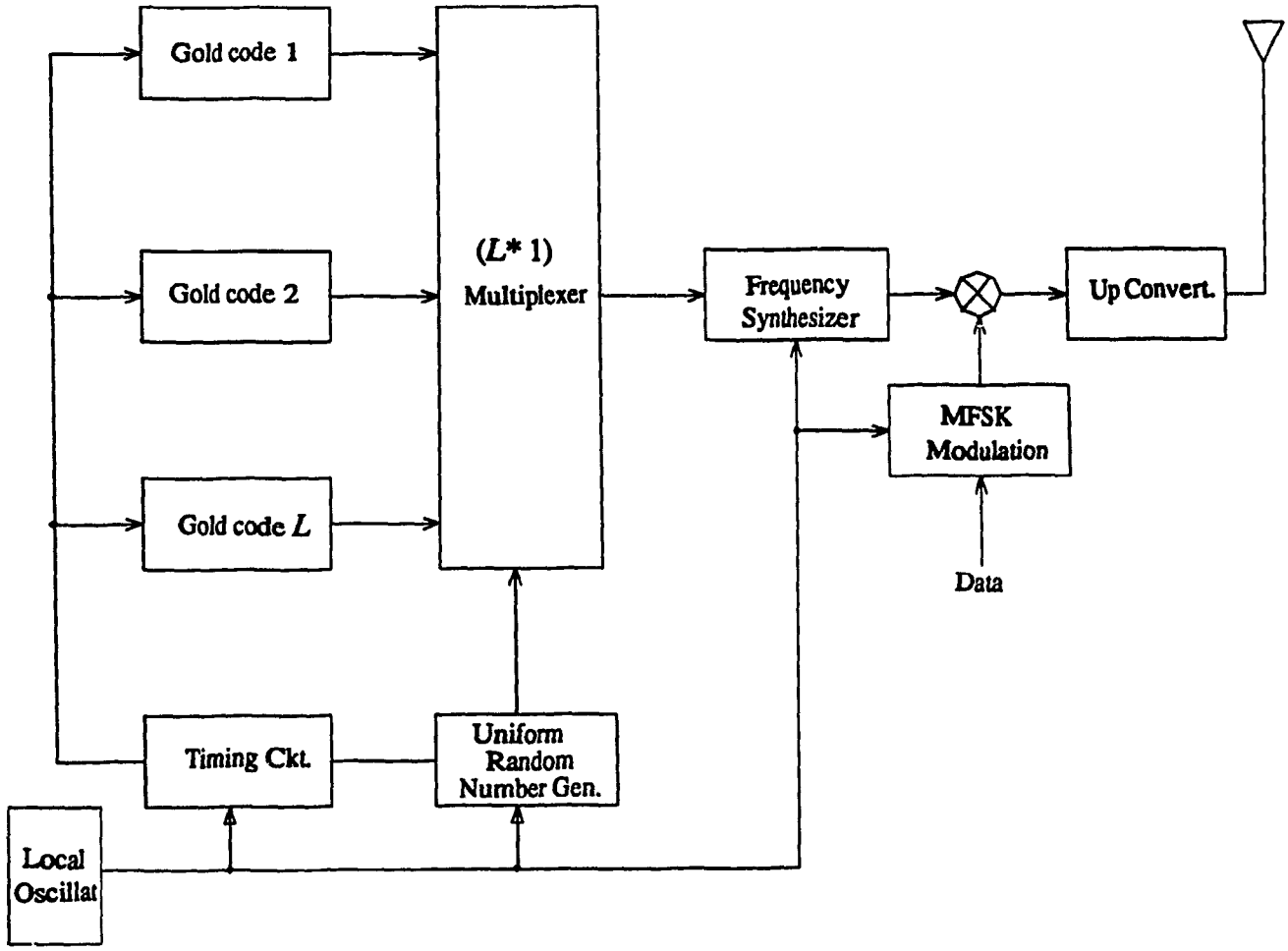

Fig. 6.1. **A novel FH/MFSK transmitter**

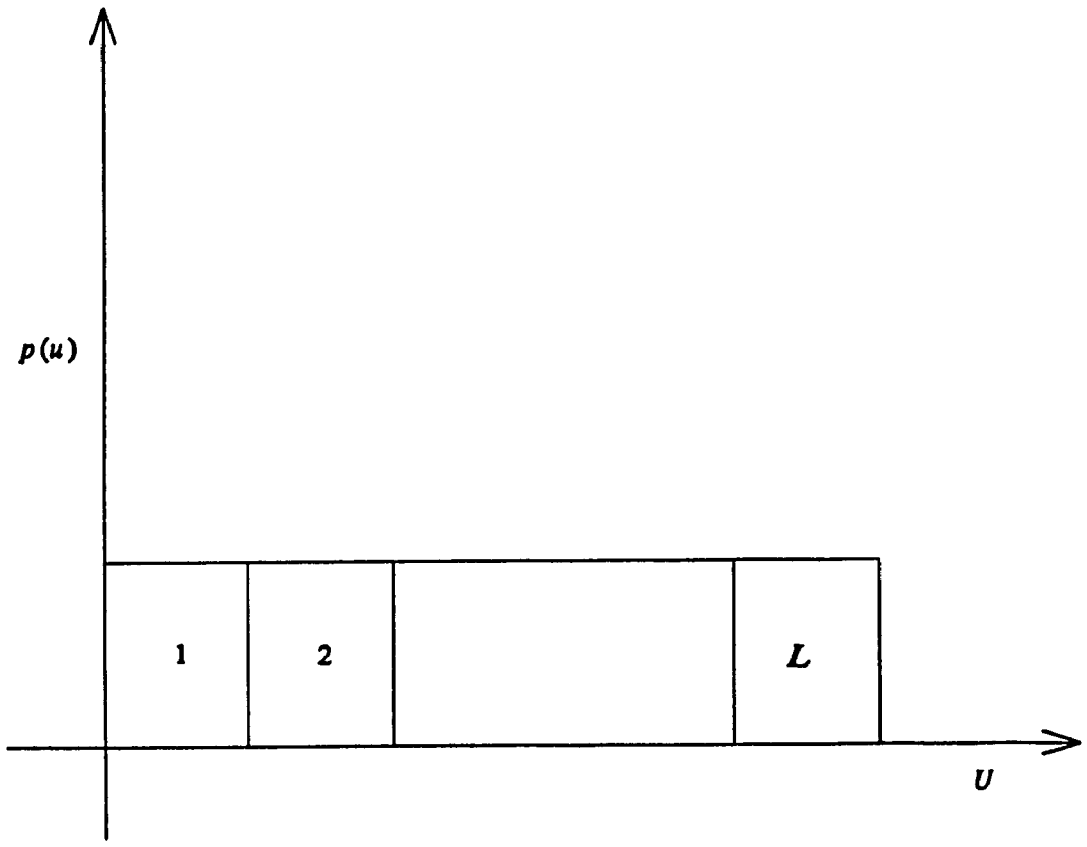

Fig. 6.2 Uniform number generator. Multiplexer selects Gold code number i if the output of the random number generator lies in the range $\frac{i-L}{L} < U < \frac{i}{L}$. Alternately Gaussian noise can be used.

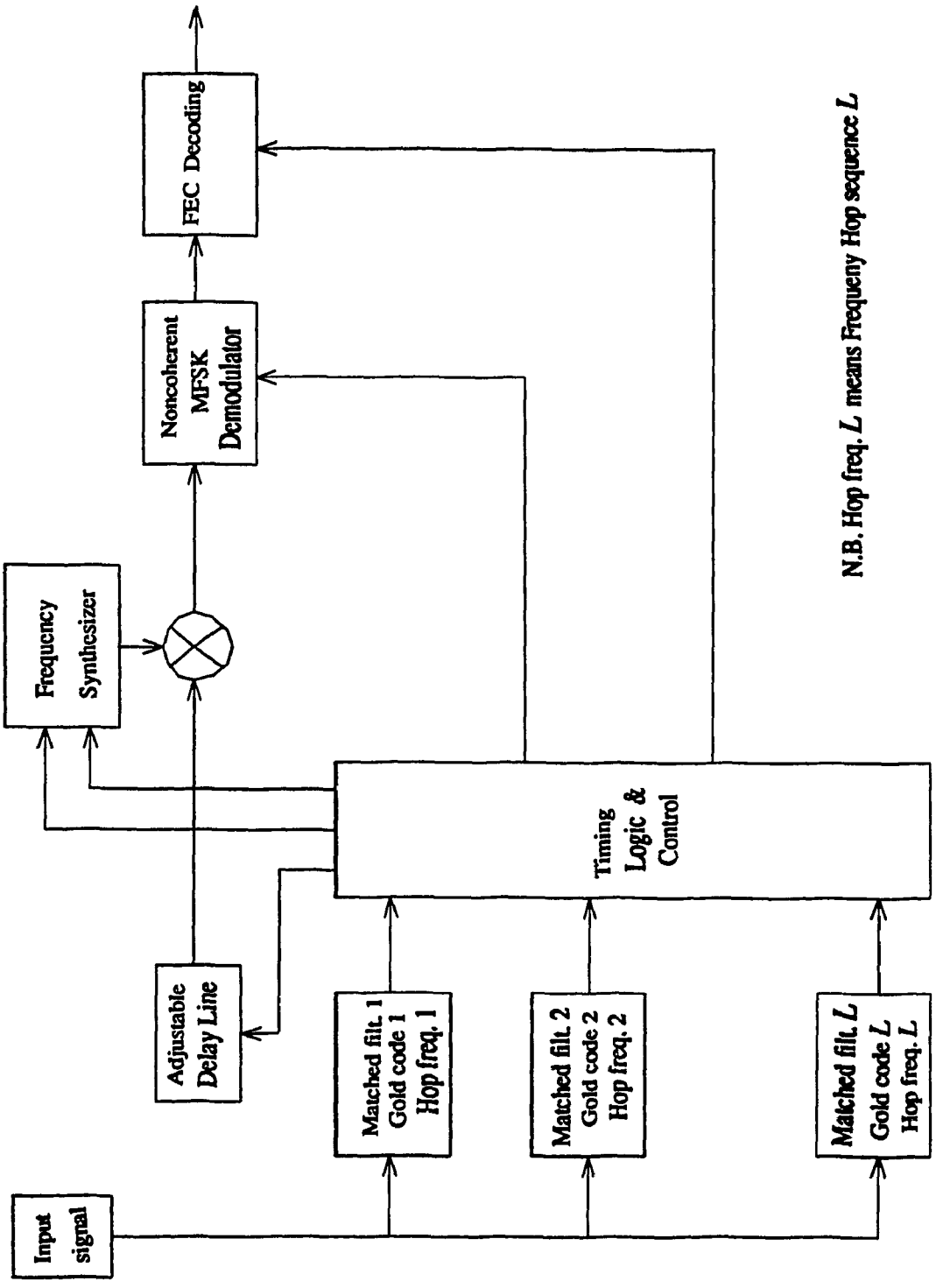

Fig 6.3 Block diagram of the receiver of the proposed system

where W is the SS bandwidth and R_b is bit rate of the system.

The down converted received signal (Fig. 6.3) feeds L matched filters. Each of these filters is matched to the hopping frequencies, transmitted under the control of the applicable Gold code. The received signal is also fed to an adjustable analog delay line that effectively stores the received signal while the timing, logic and control box tries to find the best estimate of the code epoch. The control box selects the appropriate de-hopping frequencies, to mix with the arriving signal. The subsequent MFSK noncoherent detection and concatenated decoding finally give the decoded bits.

For the convenience of analysis we assume operation of the system in the steady state conditions. By the steady state we mean that peaks from the L matched filters will be separated by $N_h T_h$ seconds. This way and following each incoming peak, the control box easily adjusts the delay and the frequency synthesizer will be effectively programmed to match the hopping frequencies that caused the specific matched filter to peak. Due to Doppler and/or fading, etc., one matched filter peak may be lost occasionally (miss), another may be added (false alarm). The error correction has to be reliable for timing information to rely on. In any case, our system will never stop demodulation and move to acquisition, even under missing few matched filter peaks, the system continues detecting, few information bits will be corrected by decoding, others will be lost. However, the next matched filter output will put back things into prospective and the appropriate automatic repeat request will occasionally be asked for retransmission. Needless to say, that the conventional SS systems using pseudorandom codes and acquisition techniques will have to ask for retransmission any how, the difference is eliminating the frequent shuttling between the acquisition and the demodulation modes of operation.

6.3. Systems Description for Algorithmic Detection

The transmitter and receiver of the proposed acquisitionless system [6.6] are shown in Fig's. 6.4 and 6.4.b respectively. In the schematic we have two receivers each consisting of a number of matched filters banks (L). The number of banks in each receiver will depend on the length of the total code and the length of each sub-code. Both of these receivers will demodulate the received FH/MFSK signal. One according to an old code epoch (i.e., a code based on previously synchronized code phase). The other receiver bank uses a new updated code epoch which the receiver tries to find (using a set of parallel matched filters and loading the second local code generator according to the phase of matched filter that peaks). Demodulation is duplicated in the two branches (Fig's. 6.4 and 6.4.b) according to both the new and old code epochs and the branches yield the weights w_1, w_2 every code period. These weights are computed based on the quality of the code epoch and the data decoding according to some preset rule (to follow). Finally, actual data bits will be sampled from the receiver branch that has the highest weight.

It should be noted that we employ Frequency Hopping (FH) in this chapter and so the L matched filters should be matched to the right sequence of Frequency Hopping.

We assume operation of the 'SUGARW' system in the steady state conditions. Steady state † implies that the peaks from the L matched filters will be separated by $N_h T_h$ seconds. Where $LN_h T_h$ is the code length, N_h is the number of hops per sub code and T_h is the hop duration except for the fact

† The fading, multi access, tone jamming, environments, signal power natures and parameters are slowly varying.

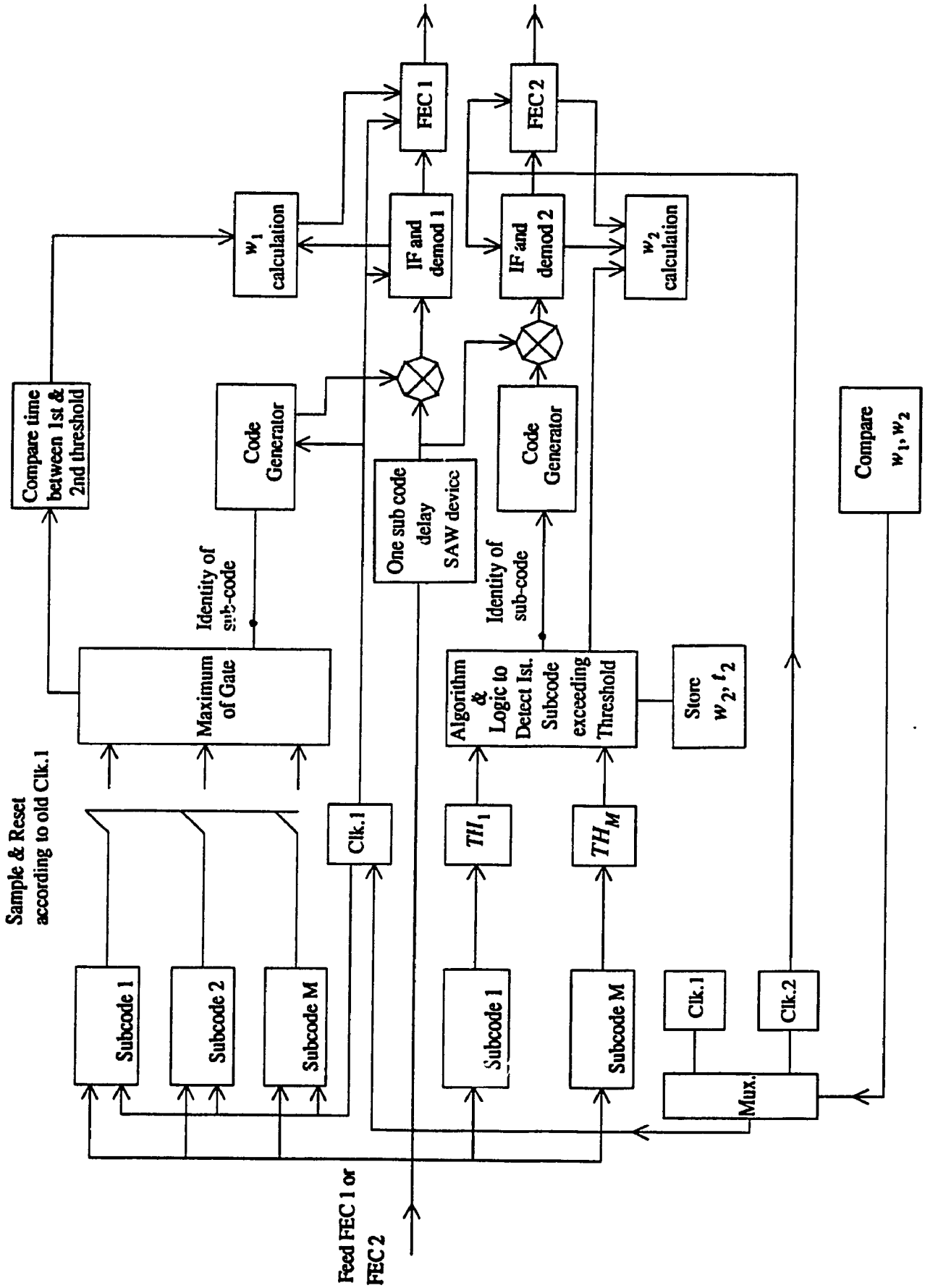

Fig. 6.4 Receiver for algorithmic detection

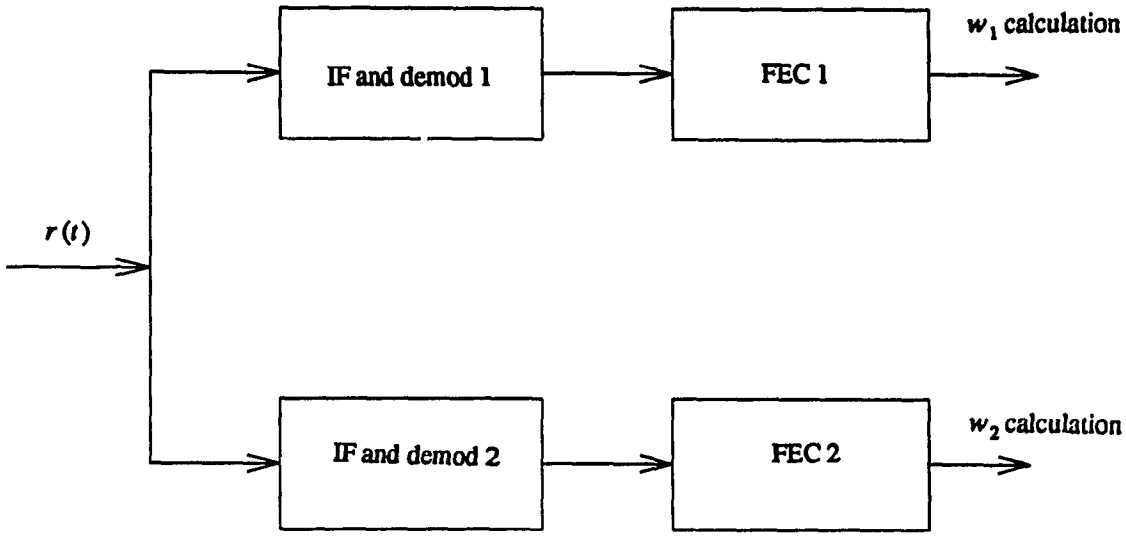

Fig. 6.4.b. Schematic of the simplified receiver

that due to Doppler and/or fading, etc., one matched filter peak may be occasionally lost (missing), another may be added (false alarm). The forward error correction (FEC) condition and the control box will be tied by an algorithm that will minimize or cancel these misses and false alarm situations.

At the receiver turn on, the code generator of the first receiver is loaded with any initial condition corresponding to sub-code-1 phase for example. The received signal passes through both the so called new and the old receiver sets. The old receiver operates according to the stored clock (code epoch), the upper branch of Fig's. 6.4 and 6.4.b. The new receiver (the lower branch of Fig. 6.4.) is continuously trying to find a new clock (code epoch) within a certain observation period (one code length). Short code lengths are preferred for implementation (However, the effective code length seen by the unauthorized listener is semi infinite). The new code phase is that epoch of the first sub-code matched filter that exceeds its threshold (in the 2nd (called new) receiver bank). Immediately after finding this new epoch (it may be identical to the old clock in most of the cases, if interference, Doppler, multi access jamming, etc., are of smaller magnitudes), the first code generator in the first branch and which is used for the actual data demodulation by active correlation is loaded according to this newly found epoch (clock). The Data will be demodulated and forward error correction FEC executed in the two separate demodulators and the FEC decoders and the corresponding weights w_1 and w_2 found from the two receivers banks are compared at the end of the observation period. The first receiver banks weight w_1 (based on the old epoch) will depend on the result of FEC-1 and the number of sub-code matched filters peaking in order following the first one that peaked in this observation period. In the system we assume the existance of wide-band analog storage devices equal to one sub-code length

(easily implemented by SAW delay lines). As one sub-code record of the received signal passes through the two receiver banks which will in their turn to identify the sub-code corresponding to this record (which matched filter peaks). The same record will be delayed through the SAW device and as soon as the right sub-code is identified in both banks the code generators in both banks will be loaded by the discovered sub-code and appropriate despreading will be done at the two banks (Fig. 6.4). In short we operate the two banks and SAW delay line in a pipeline fashion. The data from the bank one corresponding to higher weight is selected, if weight w_2 of receiver-2 is greater than w_1 then data from receiver-2 will be selected). Also, if $w_2 > w_1$ then the code generator 1 of the old epoch (of the previous frame) will be replaced by the old clock-2 for the next observation period (next frame). However, if $w_1 > w_2$, the old clock-1 is retained in the first receiver (bank) and the second branch runs freely in the next observation period trying to find a new better clock (if there is one). Added if $w_2 > w_1$ we may need to fill the vacant data bits from the second FEC decoder bank with decoded bits coming from the first FEC (see Figs. 6.4-6.5). This is the reason why as a worst case we subtract one sub-code data from the stream of correct throughput data of the system as in eq. (6.41).

Now the next observation period starts according to the newly found epoch-2 and again the second bank runs freely trying to find a different new epoch in each new observation period. While the first bank using the old code epoch.

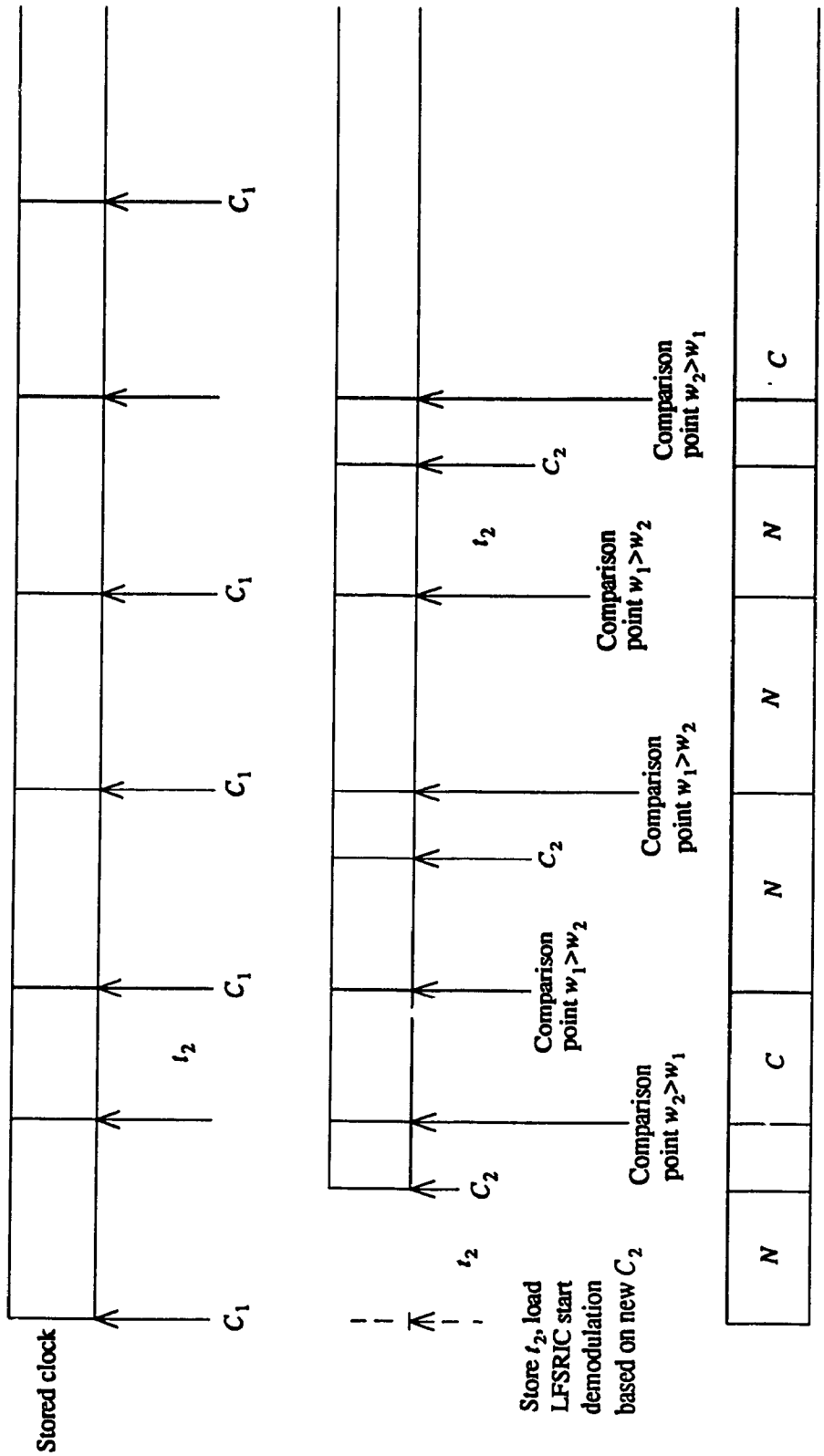

Fig. 6.5. Timing diagram for algorithmic detection

6.4. Analysis of the Weight Distributions w_1, w_2 of the Receiver 1 and 2 and the Clocks Steady State Probabilities.

For finding the weight distribution (the measure of correct code epoch and data demodulation) of the receiver bank-1 and the receiver bank-2 we start with the probability of weight distribution of sub-code matched filters peakings.

Assuming that there are L sub-codes in the total code. If we define the probability distribution of acquisition of the sub-codes in the demod-1 using correct clock (i.e., under signal present) in the following manner

$P(a=0)$ represents the probability of less than C_1 matched filters peaking in order or any order during an observation period of L sub-codes.

Where C_1 is a threshold which is typically equal to $L/2$ or more.

$P(a=1)$ represents the probability of C_1 or more matched filter peaking not necessarily in order (i.e., not separated by the appropriate time).

$P(a=2)$ represents the probability of C_1 or more matched filters peaking in the right time and right order.

Now, these probabilities can be represented by the following equations.

$$P(a=0) = \sum_{i=0}^{C_1-1} \binom{L}{i} \alpha^i (1-\alpha)^{L-i} \tag{6.3}$$

where α is equal to the probability of one matched filter output exceeding its threshold (i.e., probability of detection P_D under signal present in the different interference situations outlined in previous chapter-II) and L equals to the number of sub-codes (i.e., number of matched filter banks in each receiver)

$$P(a=2) = \sum_{j=C_1}^{L} \alpha^j (1-\alpha)^{L-j} \tag{6.4}$$

and

$$P(a=1) = \sum_{j=C_1}^{L} \binom{L}{j} \alpha^j (1-\alpha)^{L-j} - P(a=2) \tag{6.5}$$

where $P(a=2)$ has been defined earlier.

Similarly, when the codes are not aligned (i.e., no signal present), the distribution of the probabilities (denoted by $P(a'=i)$ $i=0,1,2,.....$) is similar to $P(a=i)$ $i=1,2,3.....$ But the probability α in this case will represent the probability of false alarm under no code alignment and no signal present defined in earlier chapter-II (eq. (2.20)) (i.e., false alarm P_{FA} in the different cases of single user, multi access and tone interference cases).

Next, we find the effect of FEC (on the weight distribution) as follows:

We assume that the error detection and the correction occurs per record (part of a sub-code, i.e., code word).

Now, whether FEC is Reed-Solomon (RS) or convolutional code we assume N information symbols per code word or records if convolutional codes are used.

So, the number of FEC block records per L sub-code observation period m' is represented as below

$$m' = \frac{S_L}{S_B} \tag{6.6}$$

where S_L indicates the number of symbols in the L sub-code observation period and S_B indicates the number of symbols in each code block (record).

The number of hopping frequencies, the hopping rate and the processing gain of course enter indirectly into the calculation of total number of bits corresponding to the L sub-code.

In our case m' indicates the number of RS code words per sub-code.

For FEC weight calculation, we define the following three probability distribution for the case when there is signal present.

γ_3 equals the probability of no RS symbol error in a block of N RS symbol

$$\gamma_3 = (1-P_{RS})^N \tag{6.7}$$

where P_{RS} is the RS symbol error probability on the channel eq.(6B-10) for the multiple access case, eq. (6B-11) for single user case with tone jamming and for the single user case (only) eq. (6B-1) with ρ_j equal to zero and U equal to one. The evaluations of these error probabilities has been shown in Appendix-6B.

γ_2 equals the probability of up to t or less errors corrected and detected, where t is the error correction capability of the code.

$$\gamma_2 = \sum_{j=1}^{t} \binom{N}{j} P_{RS}^j (1-P_{RS})^{N-j} \tag{6.8}$$

where t for RS code $= \lfloor (N-K)/2 \rfloor = \left\lfloor (d_{\min}-1)/2 \right\rfloor$.

γ_1 equals the probability that the number of errors exceeds the error correction capability but within the detection capability of the code.

$$\gamma_1 = \sum_{j=t+1}^{D} \binom{N}{j} P_{RS}^j (1-P_{RS})^{N-j} \tag{6.9}$$

where $D = N-K+1$

γ_0 equals the probability of no error detected nor corrected

$$\gamma_0 = 1-(\gamma_1+\gamma_2+\gamma_3) \tag{6.10}$$

Similarly, for the case when there is no signal present these probabilities will be represented as γ_3' , γ_2' , γ_1' and γ_0' , respectively. Which are based on P_{RS}' i.e., RS symbol error under no signal present (P_{RS}' is a very high error based on no code epoch matching between the received signal and the local code, eq. (B-10) for the multiple access, eq. (6B-11) for the single user with tone jamming and eq. (6B-1) with ρ_j equal to zero and U equal to one for single user (only) case. For the case of no code alignment in these equations P_o is given by eq. (6B-9)).

Now the status of the FEC in the first receiver banks under the condition of code alignment (i.e., signal present case) can be represented by using the probabilities γ_3, γ_2, γ_1 and γ_0 defined earlier as follows:

$P(b=0)$ represents the probability of all m' FEC blocks constituting one sub-code had errors, not detectable not correctable

$$P(b=0) = \gamma_0^{m'} \tag{6.11}$$

$P(b=1)$ represents the probability of one FEC block out of m' FEC block not correctable (which can occur in any order) and the rest not detectable not correctable

$$P(b=1) = m' \gamma_1 \gamma_0^{m'-1} \tag{6.12}$$

$P(b=2)$ represents the probability of two FEC blocks detectable but not correctable and the rest not detectable not correctable.

+ probability of one FEC block detectable and correctable and the rest $(m'-1)$ not detectable not correctable.

$$P(b=2) = \begin{pmatrix} m' \\ 2 \end{pmatrix} \gamma_1^2 \gamma_0^{(m'-2)} + \begin{pmatrix} m' \\ 1 \end{pmatrix} \gamma_2 \gamma_0^{(m'-1)} \tag{6.13}$$

$P(b=3)$ is the probability of one FEC block detected and corrected probability of one FEC block detected but not corrected, probability of the rest $(m'-2)$ FEC blocks neither detected nor corrected.

+ probability of three FEC blocks detected but not corrected and of the rest of $(m'-3)$ FEC block neither detected nor corrected.

+ probability of one FEC block out of m' FEC block corrected and the rest $(m'-1)$ block neither detected nor corrected

$$P(b=3) = \binom{m'}{2}\gamma_1^1\gamma_2^1\gamma_0^{m'-1} + \binom{m'}{3}\gamma_1^3\gamma_0^{m'-3} + \binom{m'}{1}\gamma_3\gamma_0^{m'-1} \quad (6.14)$$

$P(b=4)$ is the probability of four FEC block out of m' FEC block detected but not corrected and the rest $(m'-4)$ FEC block neither detected nor corrected.

+ probability of few errors detected and corrected in one FEC block out of $(m'-1)$ block, and the probability of few errors detected but not corrected in two FEC block, and the probability of the rest $(m'-3)$ FEC block neither detected nor corrected.

+ probability of no errors in one FEC block out of $(m'-1)$ block, and the probability of few errors detected but not corrected in one FEC block, and the probability of the rest $(m'-2)$ FEC block neither detected nor corrected.

+ probability of no errors detected nor corrected in two FEC block out of $(m'-2)$ FEC block

$$P(b=4) = \binom{m'}{4}\gamma_1\gamma_0^{m'-4} + \binom{m'}{3}\gamma_2\gamma_1^2\gamma_0^{m'-3}$$

$$+\binom{m'}{2}\gamma_3\gamma_1\gamma_0^{m'-2} + \binom{m'}{2}\gamma_2^2\gamma_0^{m'-2} \quad (6.15)$$

Having defined the probability distribution of the acquisition and FEC status, we now combine these two distributions ($P(a)$, $P(b)$) to define the probability of weight distribution w_1 (assuming demod-1 and FEC-1 are having the correct clock, i.e., codes are aligned).

$P(w_1=0)$ is the probability of threshold C_1 for acquisition not exceeded and probability that FEC could not detect and could not correct one or more errors that occurred

$$P(w_1)= P(a=0).P(b=0) \tag{6.16}$$

and $P(w=1)$, $P(w=2)$, $P(w=3)$, $P(w=4)$ and $P(w=5)$; defined as

$$P(w_1=1) = P(a=1)P(b=0) + P(a=0)P(b=1) \tag{6.17}$$

$$P(w_1=2) = P(a=0)P(b=2) + P(a=1)P(b=1) + P(a=2)P(b=0) \tag{6.18}$$

$$P(w_1=3) = P(a=0)P(b=3) + P(a=1)P(b=2) + (a=2)P(b=1) + P(a=3)P(b=0) \tag{6.19}$$

$$P(w_1=4) = P(a=0)P(b=4) + P(a=1)P(b=3) + P(a=2)P(b=2) \tag{6.20}$$

$$P(w_1=5)= P(a=0)P(b=5) + P(a=1)P(b=4) + P(a=2)P(b=3) \tag{6.21}$$

Similarly, we define the probability of weight distribution w_2 (wrong clock) assuming FEC-2, demod-2 under the absence of signal (i.e., no code alignment)

$$Q(w_2=0) = P(a'=1)P(b'=0) \tag{6.22}$$

a', b' bear similar meaning to those of a, b except they are evaluated under no signal presence (no code alignment) and $Q(w_2=1)$,

$Q(w_2{=}2)$, $Q(w_2{=}3)$, $Q(w_2{=}4)$ and $Q(w_2{=}5)$ defined as

$$Q(w_2{=}1) = P(a'{=}1)P(b'{=}0) + P(a'{=}0)P(b'{=}1) \tag{6.23}$$

$$\begin{aligned} Q(w_2{=}2) = {} & P(a'{=}2)P(b'{=}0) \\ & + P(a'{=}1)P(b'{=}1) + P(a'{=}0)P(b'{=}2) \end{aligned} \tag{6.24}$$

$$\begin{aligned} Q(w_2{=}3) = {} & P(a'{=}2)P(b'{=}1) \\ & + P(a'{=}1)P(b'{=}2) + P(a'{=}0)P(b'{=}3) \end{aligned} \tag{6.25}$$

$$\begin{aligned} Q(w_2{=}4) = {} & P(a'{=}2)P(b'{=}2) \\ & + P(a'{=}1)P(b'{=}3) + P(a'{=}0)P(b'{=}4) \end{aligned} \tag{6.26}$$

$$\begin{aligned} Q(w_2{=}5) = {} & P(a'{=}2)P(b'{=}3) + P(a'{=}1)P(b'{=}4) \\ & + P(a'{=})P(b'{=}5) \end{aligned} \tag{6.27}$$

Changes in the clock status (the system selecting good or bad clock) can be represented by a state transition change in the steady state. †

The transition state probabilities of the clocks reflecting the better code and its associated receiver bank selected at any time out of either bank one (assumed to have good clock) and two (assumed to have bad clock) can be defined as in Fig. 6.6.

P_{11} represents the probability of keeping clock-1 in the next L subcodes given clock one was used.

P_{12} represents the probability of switching from clock-1 used during the part of L sub-codes to clock-2.

---

† Steady state still means random changes in the system between good and bad clocks. But, means under steady and slowly varying jammer, multi access, other environments we get a steady state probability for the good and bad clock in a stricter sense.

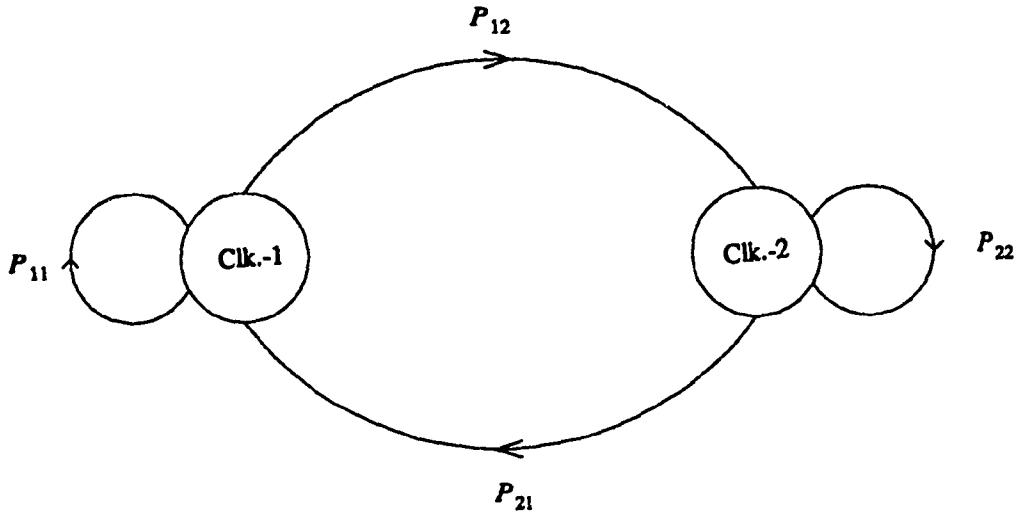

Fig. 6.6. Schematic of the state probabilities of the clock

P_{21} represents the probability of switching clock -1 in the next L subcode for demodulation given that clock-2 was used.

P_{22} represents the probability of using clock-2 in the next L sub codes for demodulation given that clock-2 was used.

For our system the probabilities as defined earlier can also be expressed as follows:

P_{11} represents the probability of a synchronized demod plus FEC-1 weight w_1 remains higher than the probability of an unsynchronized demod-2 + FEC-2 weight w_2

P_{12} represents the probability of an unsynchronized demod, FEC-2 weight w_2 remains greater than the weight w_1 of a synchronized demod-1 and FEC-1.

These steady state probabilities can be explained physically as follows. Assume stored clock-1 was used and is a good clock, the newly found clock-2 is a false one due to fading or like user interference, etc,. So the move P_{12} is a bad one (leaving the good stored clock and using a new false clock). P_{22} is a bad move, P_{11} and P_{21} are good moves. Now the question might arise as how can demod -1, FEC-1 weights go down ? Actually these can go down by the prescence of jamming, like user interference in matched filters, fading, etc., thus decreasing the effective acquisition weight.

Now, the probability of transition from clock-1 to clock-2 can be defined as follows.

P_{12} represents the probability of combined acquisition (demod-2) + FEC-2 weight greater than probability of combined acquisition (demod-1) + FEC-1 weight

Similarly,

P_{21} represents the probability of combined acquisition (demod-1) + FEC-1 weight greater than the probability of combined acquisition (demod-2) + FEC-2 weight.

$$P_{21} = P(w_1 > w_2) = Q_0(P_1+P_2+P_3+P_4+P_5) + Q_1(P_2+P_3+P_4+P_5) + Q_2(P_3+P_4+P_5)+Q_3(P_4+P_5) + Q_4(P_5) \quad (6.28)$$

$$P_{12} = P(w_2 > w_1) = P_0(Q_1+Q_2+Q_3 + Q_4+Q_5) + P_1(Q_2+Q_3+Q_4+Q_5) + P_2(Q_3+Q_4+Q_5) + P_3(Q_4+Q_5) + P_4(Q_5) \quad (6.29)$$

Now, the probability of remaining in clock-1 or clock-2 can be found by solving the set of state equations (at equilibrium),

$$P_A = P_{21}P_B + P_{11}P_A \quad (6.30)$$

$$(1-P_{11})P_A = P_{21}P_B$$

$$P_{12}P_A = P_{21}P_B$$

$$P_1+P_2=1 \quad (6.31)$$

$$P_A = \frac{P_{21}}{P_{21}+P_{12}} \quad (6.32)$$

Similarly,

$$P_B = \frac{P_{12}}{P_{21}+P_{12}} \quad (6.33)$$

Up to now the distributions of weights w_1 and w_2 were based on equal weights (importance) of acquisition (code alignment) and FEC weight.

If now the acquisition (effective code alignment) carries more information than the FEC information then we may assign more weight say θ to

Similarly,

P_{21} represents the probability of combined acquisition (demod-1) + FEC-1 weight greater than the probability of combined acquisition (demod-2) + FEC-2 weight.

$$P_{21} = P(w_1 > w_2) = Q_0(P_1+P_2+P_3+P_4+P_5) + Q_1(P_2+P_3+P_4+P_5) + Q_2(P_3+P_4+P_5)+Q_3(P_4+P_5) + Q_4(P_5) \quad (6.28)$$

$$P_{12} = P(w_2 > w_1) = P_0(Q_1+Q_2+Q_3+Q_4+Q_5) + P_1(Q_2+Q_3+Q_4+Q_5) + P_2(Q_3+Q_4+Q_5) + P_3(Q_4+Q_5) + P_4(Q_5) \quad (6.29)$$

Now, the probability of remaining in clock-1 or clock-2 can be found by solving the set of state equations (at equilibrium),

$$P_A = P_{21}P_B + P_{11}P_A \quad (6.30)$$

$$(1-P_{11})P_A = P_{21}P_B$$

$$P_{12}P_A = P_{21}P_B$$

$$P_1+P_2=1 \quad (6.31)$$

$$P_A = \frac{P_{21}}{P_{21}+P_{12}} \quad (6.32)$$

Similarly,

$$P_B = \frac{P_{12}}{P_{21}+P_{12}} \quad (6.33)$$

Up to now the distributions of weights w_1 and w_2 were based on equal weights (importance) of acquisition (code alignment) and FEC weight.

If now the acquisition (effective code alignment) carries more information than the FEC information then we may assign more weight say θ to

case the distribution of w_1 becomes, the quantities $P(a=...)$ at the left side of eq's.(6.34),(6.35) are the new distribution values of θ while those on the right hand are the original distribution ($\theta=0$, $\delta=0$)

TABLE II

$\theta=1$	$\theta=2$	$\theta=3$
$P(a=0)=0$	$P(a=0)=0$	$P(a=0)=0$
$P(a=1)=P(a=0)$	$P(a=1)=0$	$P(a=1)=0$
$P(a=2)=P(a=1)$	$P(a=2)=P(a=0)$	$P(a=2)=0$
$P(a=3)=P(a=2)$	$P(a=3)=P(a=1)$	$P(a=3)=P(a=0)$
$P(a=4)=P(a=3)$	$P(a=4)=P(a=2)$	$P(a=4)=P(a=1)$
$P(a=5)=P(a=4)$	$P(a=5)=P(a=3)$	$P(a=5)=P(a=2)$

Similarly, if the FEC information carries more weight than the acquisition then we may assign more weight say δ to FEC as compared to acquisition in the process of calculating the weights in which case the distribution of w_1 becomes,

TABLE III

$\delta=1$	$\delta=2$	$\delta=3$
$Q(a=0)=0$	$Q(a=0)=0$	$Q(a=0)=0$
$Q(a=1)=Q(a=0)$	$Q(a=1)=0$	$Q(a=1)=0$
$Q(a=2)=Q(a=1)$	$Q(a=2)=Q(a=0)$	$Q(a=2)=0$
$Q(a=3)=Q(a=2)$	$Q(a=3)=Q(a=1)$	$Q(a=3)=Q(a=0)$
$Q(a=4)=P(a=3)$	$Q(a=4)=Q(a=2)$	$Q(a=4)=Q(a=1)$
$Q(a=5)=Q(a=4)$	$Q(a=5)=Q(a=3)$	$Q(a=5)=Q(a=2)$

In the previous sections we have computed the steady state probabilities of the system remaining in clock-1 or clock-2. Using these clock probabilities we formulate a generalized throughput to compare the 'SUGARW' SS system with the conventional system. In the conventional SS system we will consider the time lost in the acquisition mode. However, the performance during demodulation will be better because of low bit errors. On the other hand in the 'SUGARW' system there is no time lost during the acquisition which is running in parallel with the demodulation. However, we lose data from time to time during clock transition and the tradeoff becomes now clear.

6.5. Throughput Comparison of the Classic and the 'SUGARW' Spread Spectrum Systems

In the spread spectrum (SS) multiple access system where there is no synchronization necessary between the different receivers a large number of users may subscribe to such a system while system performance (error rate) depends only on the number of simultaneous users.

The throughput of a conventional SS system can be defined by the following relationships [6.11], [6.12]

$$EFFC = \frac{U*R_b\,(1-P_b)}{W}\left[1-\frac{T_{ACQ}}{T_t\,(P_{ACQ})}\right]\rho \tag{6.38}$$

$$= \frac{U*R_b\,(1-P_b)}{W}(1-\frac{\Delta}{P_{ACQ}})\rho \tag{6.39}$$

where

ρ is the duty factor, i.e., traffic load,

Δ is the ratio of average acquisition time to data transmission time,

i.e., $\Delta=\frac{T_{ACQ}}{T_t}$ which may vary from .1 to .9,

W is the spread spectrum bandwidth,

U represents the number of users in the system,

R_b is the bit rate, and

P_b is the probability of decoded bit error (which can be obtained from eq. (6B-8) the derivation given in Appendix-6B).

The term $(1-\frac{\Delta}{P_{ACQ}})$ represents the effect of the average time lost due to repeated serial acquisition trials in the conventional systems. Assuming

geometric distribution, this is given by,

$$1 - \Delta \sum_{i=1}^{\infty} i \ (1 - P_{ACQ})^{i-1} P_{ACQ} = (1 - \frac{\Delta}{P_{ACQ}}) \qquad (6.40)$$

as above

The probability of acquisition P_{ACQ} can be obtained from eq's.(6A-6, 6A-7, 6A-8) in Appendix- A (the probability of acquisition for the single dwell system). Similarly, the probability of bit error can be found from eq. (6B-9) of the relationships developed in Appendix-6B (error probabilities of multi access and tone jamming cases).

On the other hand, the efficiency of the new 'SUGARW' SS system can be defined as

$$EFFN = \frac{U*R_b}{W} \left[(1-P_{bg})\rho P_A + \rho P_B (\frac{L-2}{L})(1-P_{bb}) \right] \qquad (6.41)$$

where

P_{bg} is the probability of bit error using good clock (which is the same as P_b in eq. (6B-9) of Appendix-6B)

P_{bb} is the probability of bit error using bad clock (which is assumed equal to .5 because the detected bit may be right or wrong with 50% probability in the case of (worst case) code misalignment)

P_A is the steady state probability of the good clock

P_B is the steady state probability of the bad clock

$(L-2)/L$ is a factor reflecting the data loss due to switching between the good and bad clocks.

Equation (6.41) assumes the existance of wide-band analog storage devices

of length equal to one sub -code length (easily implemented by SAW delay lines).

The main difference between the efficiency relationship of the conventional SS system and the new SS system is that in the new system we detect some data even when the system is in clock-2 (i.e., bad clock that means no code alignment). But, some data will be lost in the transition. In the conventional SS system when the codes are not aligned (no acquisition), data for that period is completely lost.

6 6. Results

The steady sta. probabilities of the bad and good clocks, the efficiencies of the conventional SS and the 'SUGARW' SS system have been computed in the different single user, multi tone jamming and multiple access environments involved.

In the single user case Fig's. 6.7, 6.8 increasing the number of subcodes and keeping everything otherwise fixed (i.e., SNR =10., C_1=2 in both cases) will result in reducing the probabilities of good clock and increasing the probabilities of bad clock acquisition due to less integration time per sub code. Moreover, it was found that states with less weights have higher probabilities. This became true for multiple access cases and also for tone jamming cases. However, the above is true only for high SNR . At low SNR the situation reverses i.e., the nigher is the L the better is the performance (Figs. 6.9, 6.10 for the single user case), similarly for the multiple access case and the tone jamming case).

In the single user case, changing the acquisition weight θ did not result in

a noticeable change in the clocks probabilities (Fig's. 6.7 for $L=4$, $C_1=2$, $SNR=10$, and Fig. 6.11 for $L=8$, $C_1=4$, $SNR=10$) and changing the FEC weight δ up to three did not result in noticeable change in the clocks probabilities (Fig. 6.12). However, as the SNR decreases we see a noticeable change in the clocks probabilities as FEC weight δ increases (Fig. 6.13) and if θ increases the clock probability maintains a steady value (Fig's. 6.9, 6.14)

Also, by decreasing the threshold C_1 with fixing L, SNR and all other parameters otherwise we note a deterioration in the clock probabilities (Fig's. 6.9, 6.14). We get similar results in the multiple access and tone jamming cases.

The good and bad clock probabilities has been plotted vs. SNR for the single user case, the multi access case and the single user tone jamming cases in Fig's. 6.15-6.17. For the single user case the clock probability remains more or less constant up to certain SNR then changes and attains a steady value (Fig. 6.15), these trend can be seen in the other cases also. Comparing Fig. 6.15 (for single user case) and Fig. 6.16 (for multiple access case) we can see that the clock probability saturates more quickly in the single user case than the multiple access case for the same operating condition (i.e., $L=4$, $C_1=3$ in both cases).

The steady state probabilities of the bad and good clock has been plotted vs. the acquisition threshold C_1 for the single user case, the multi access case and the single user tone jamming case both for high and low SNR in Fig's. 6.18-6.19. From these figures it is evident that if the acquisition threshold is increased the good clock probability increases and the bad clock probability decreases.

The throughput efficiency of the new 'SUGARW' SS system has been plotted vs. ρ (duty factor) in Fig's. 6.20-6.23. The efficiency of the conventional SS system has also been plotted vs. ρ with Δ the ratio of average acquisition time to data transmission time as a parameter. In all these cases the performance of the new 'SUGARW' SS system is better than the conventional SS system if the Δ the ratio of average acquisition time to data transmission time is greater than .001. The new SS system throughput has been plotted for two different circumstances, i.e., assuming in one case that in the transition between the clocks one sub-code data is lost and in the other case it is assumed that two sub-code data is lost. So when L is small this affects the performance of the new SS system considerably as is clear from Fig. 6.20 and Fig. 6.21.

6.7 Conclusions

It is possible to have a SS system that does not need acquisition. In this paper we have introduced such a system and proved that in many cases, the throughput of the 'SUGARW' system is higher than a conventional system. It was found in the 'SUGARW' SS system that the clocks probabilities deteriorates if the acquisition threshold is decreased keeping number of subcode and SNR fixed. Moreover, increasing number of subcode keeping everything fixed have resulted in deteriorating receiver performance. In formulating demodulation decision at the receiver coding has been found to be more critical than acquisition at high SNR, at low SNR there is no relative importance of the thresholds δ and θ but still increasing δ makes more sense. The performance of the new 'SUGARW' SS system has been found better than the conventional SS system if Δ the ratio of average acquisition time to data transmission time is greater than .001.

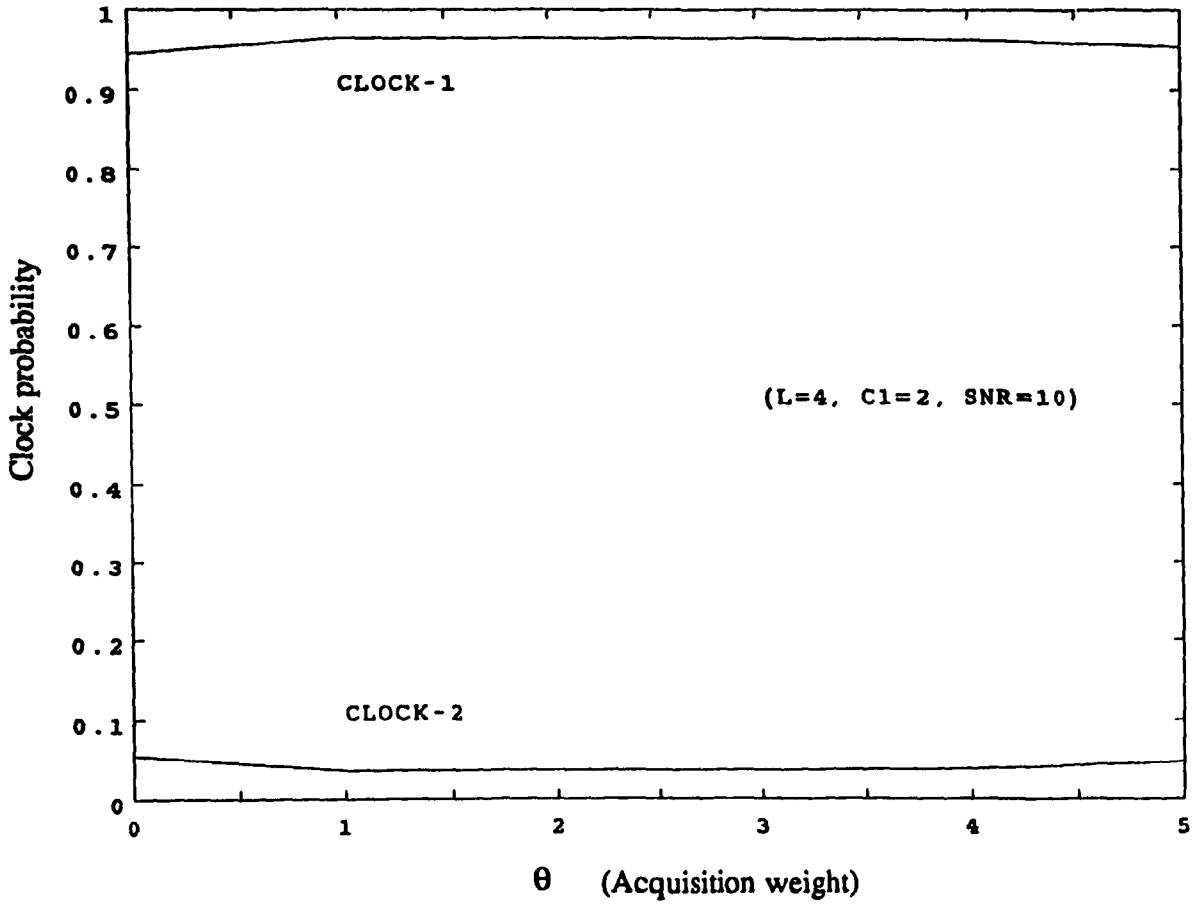

Fig. 6.7 Clock probability versus acquisition weight θ for single user case, parameters are; spread spectum bandwidth = 7.68 Mhz., bit rate = 2Kbps., *M–ary* system of $M = 4$, Reed Solomon code (64, 32), number of subcode $L = 4$, threshold setting $C_1 = 2$, signal to noise ratio = 10.

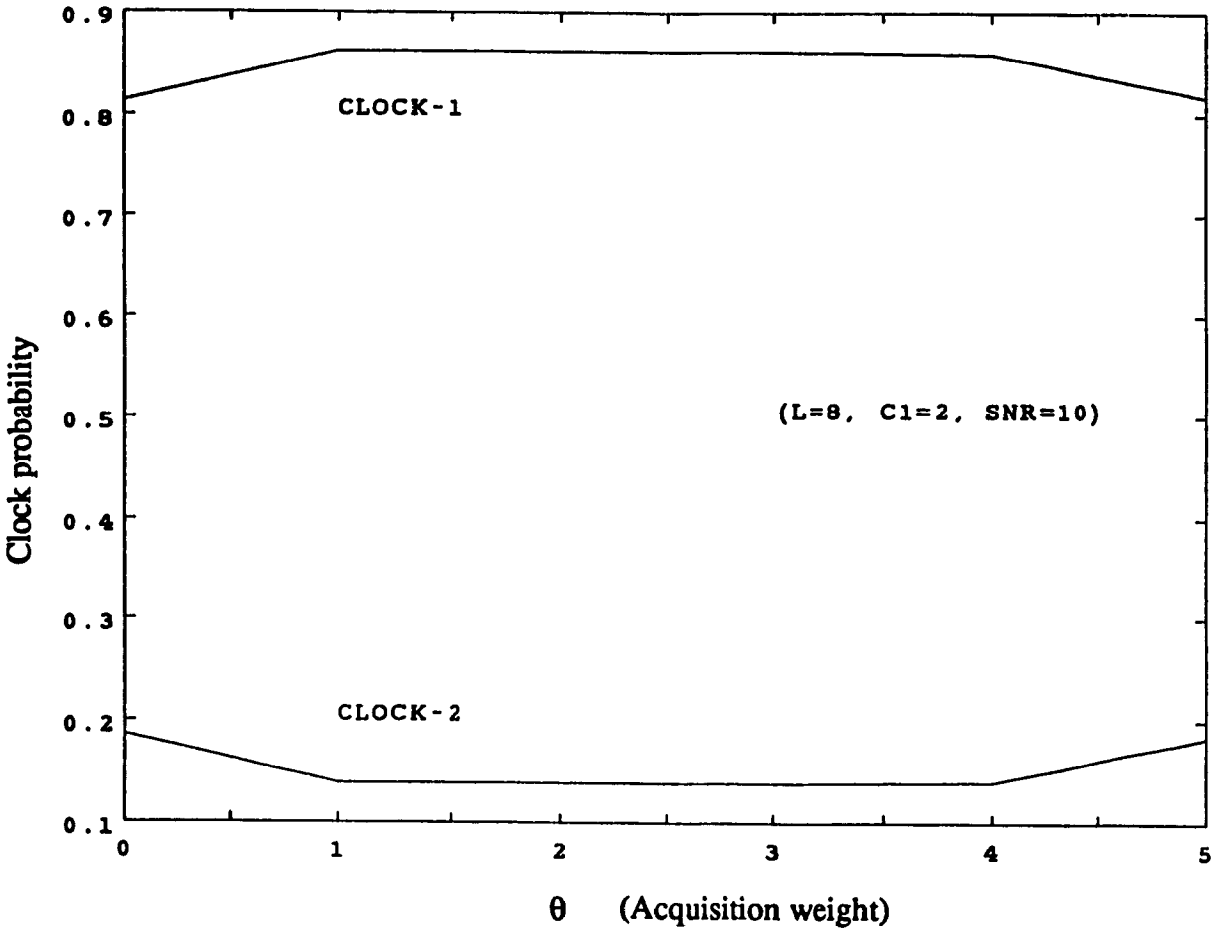

Fig. 6.8 Clock probability versus acquisition weight θ for single user case, parameters are; spread spectum bandwidth = 7.68 Mhz., bit rate = 2Kbps., *M−ary* system of $M = 4$, Reed Solomon code (64, 32), number of subcodes $L = 8$, threshold setting $C_1 = 2$, signal to noise ratio = 10.

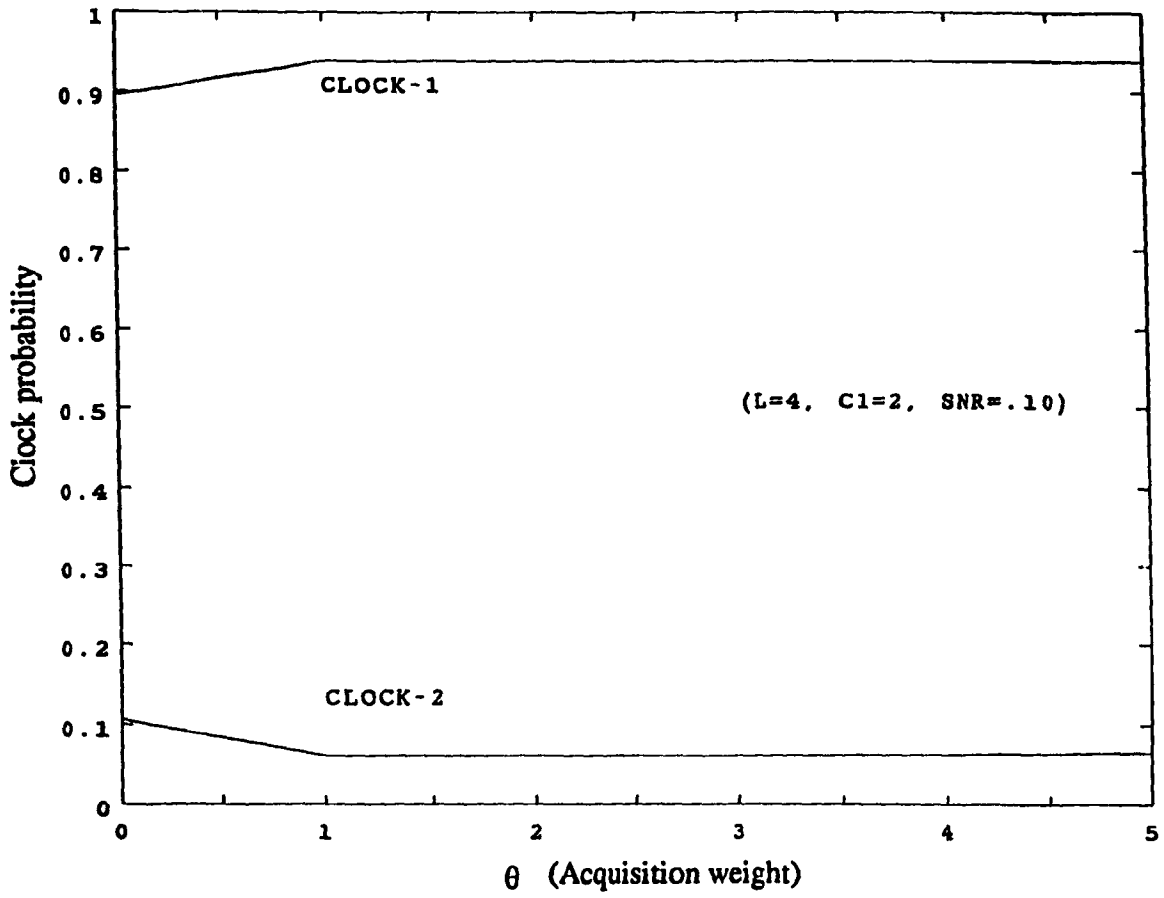

Fig. 6.9 Clock probability versus acquisition weight θ for single user case, parameters are; spread spectum bandwidth = 7.68 Mhz., bit rate = 2Kbps., *M-ary* system of $M = 4$, Reed Solomon code (64, 32), number of subcodes $L = 4$, threshold setting $C_1 = 2$, signal to noise ratio = 0.1

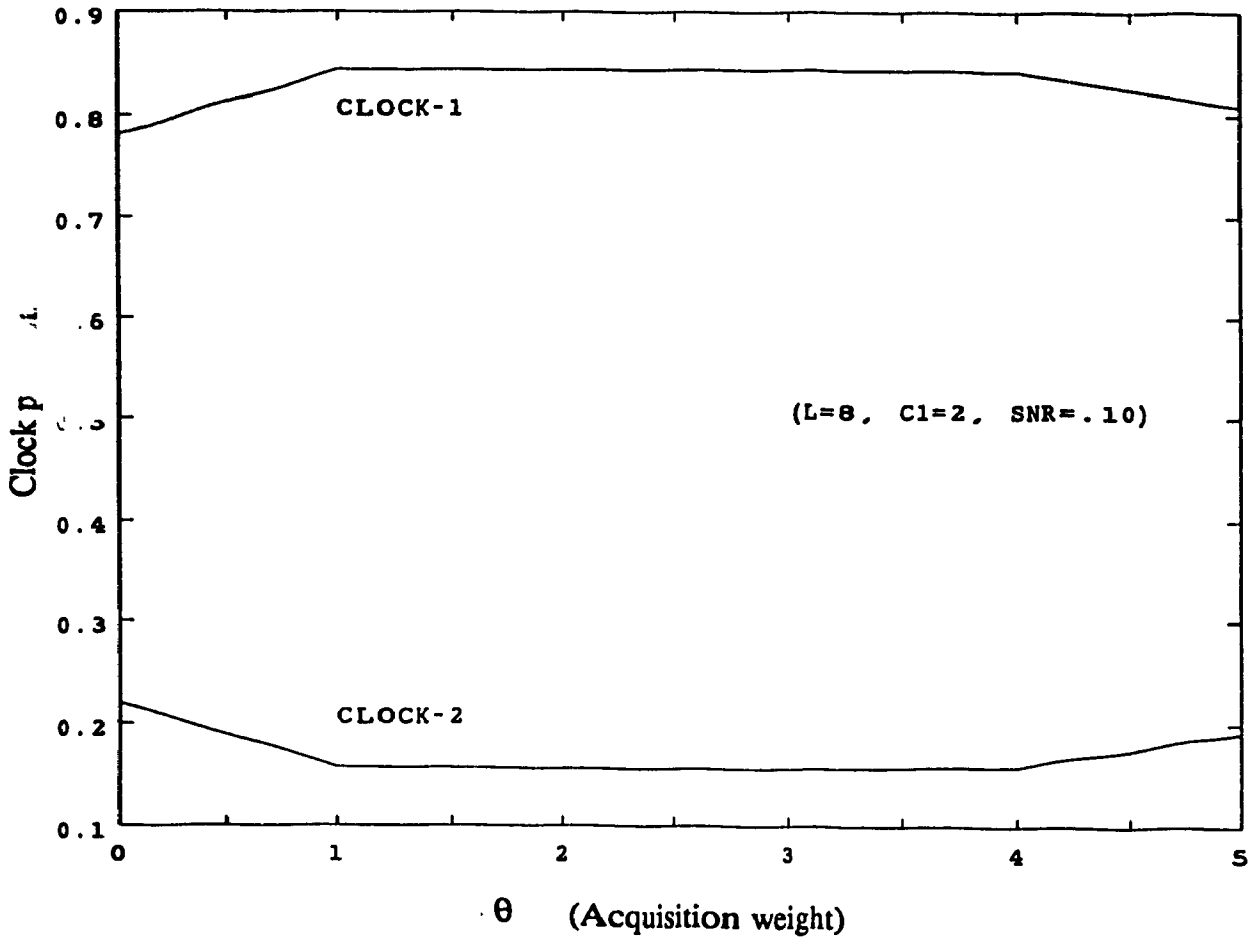

Fig. 6.10 Clock probability versus acquisition weight θ for single user case, parameters are; spread spectum bandwidth = 7.68 Mhz., bit rate = 2Kbps., *M –ary* system of M = 4, Reed Solomon code (64, 32), number of subcodes L = 8, threshold setting C_1= 4, signal to noise ratio = 10.0

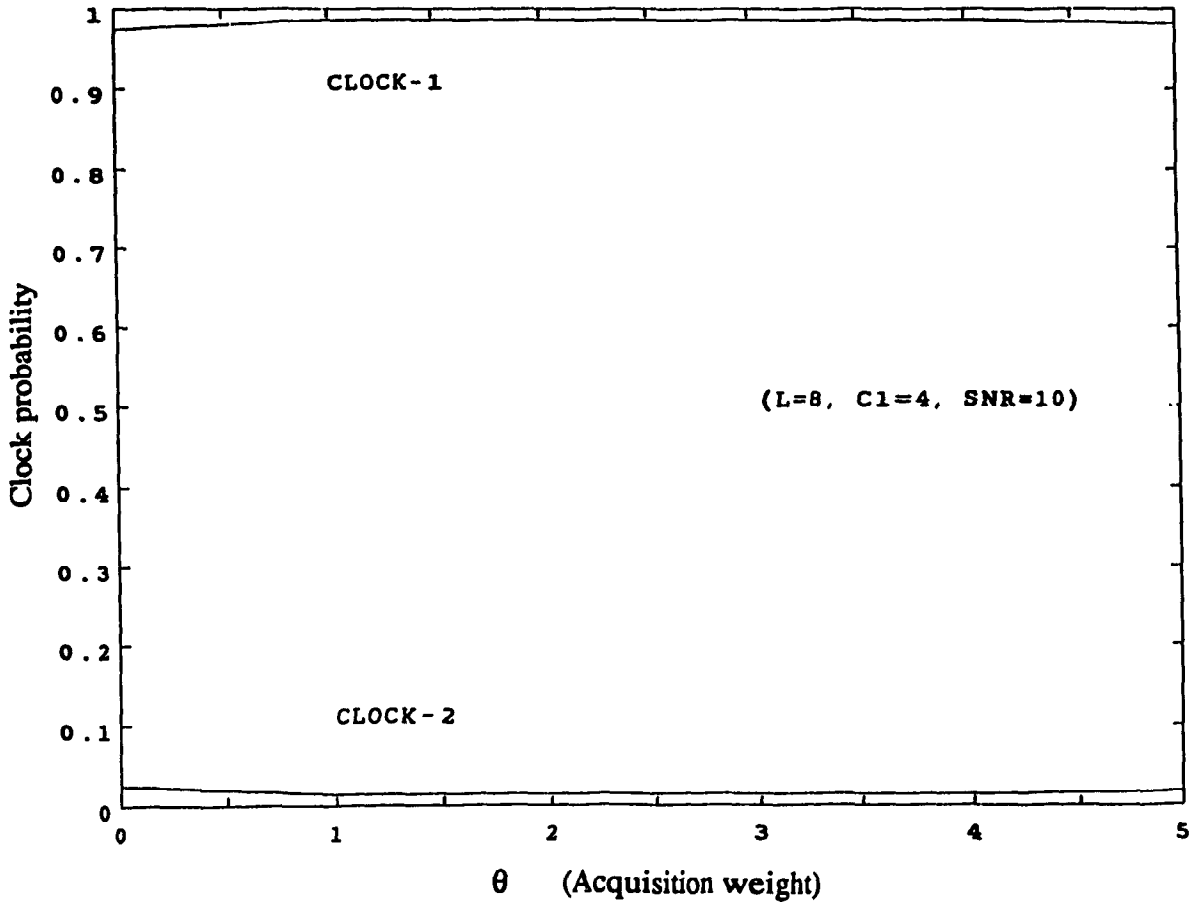

Fig. 6.11 Clock probability versus acquisition weight θ for single user case, parameters are; spread spectum bandwidth = 7.68 Mhz., bit rate = 2Kbps., $M-ary$ system of M = 4, Reed Solomon code (64, 32), number of subcodes L = 8, threshold setting C_1 = 2, signal to noise ratio = 0.1

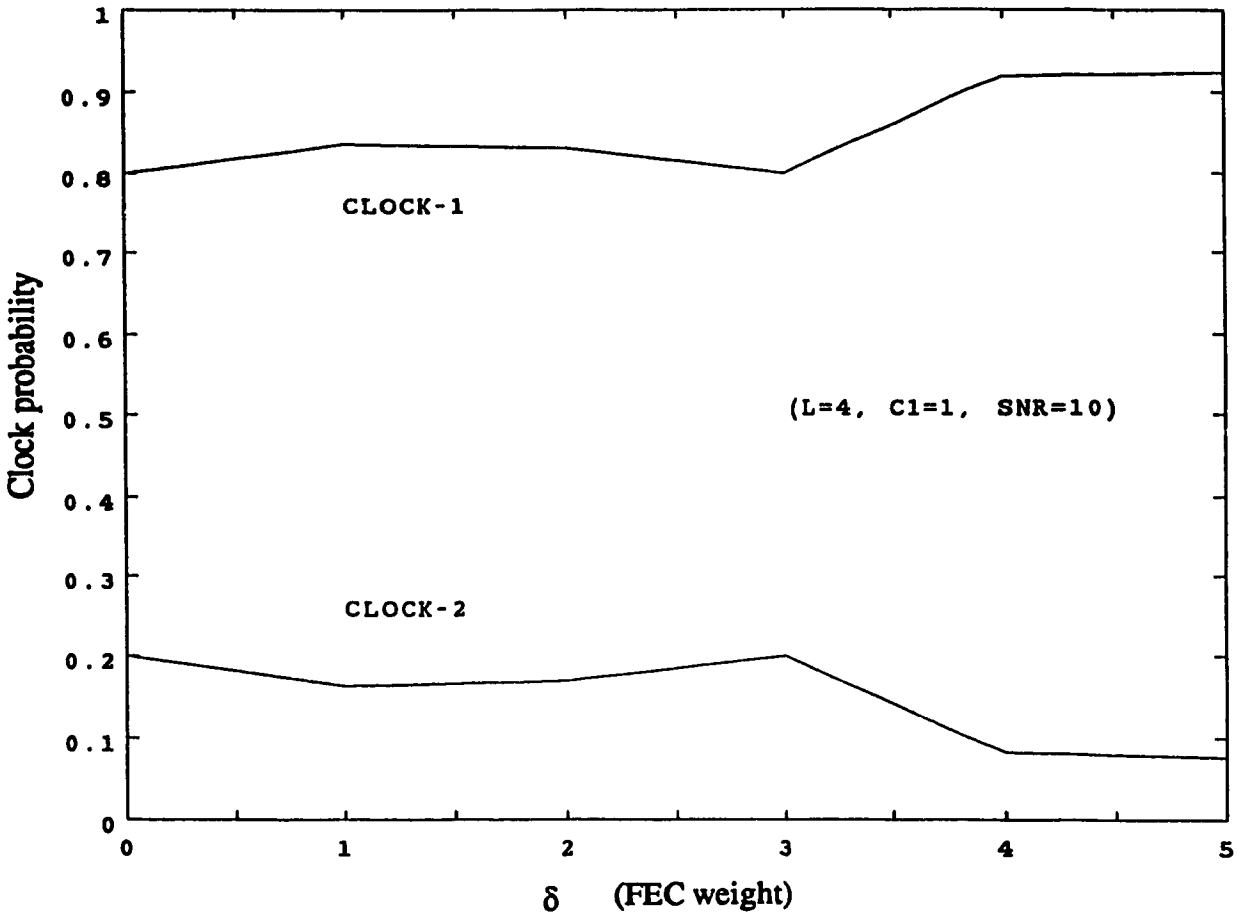

Fig. 6.12 Clock probability versus FEC weight δ for single user case parameters are; spread spectum bandwidth = 7.68 Mhz., bit rate = 2Kbps., $M-ary$ system of $M = 4$, Reed Solomon code (64, 32), number of subcodes $L = 4$, threshold setting $C_1 = 1$, signal to noise ratio = 10.0

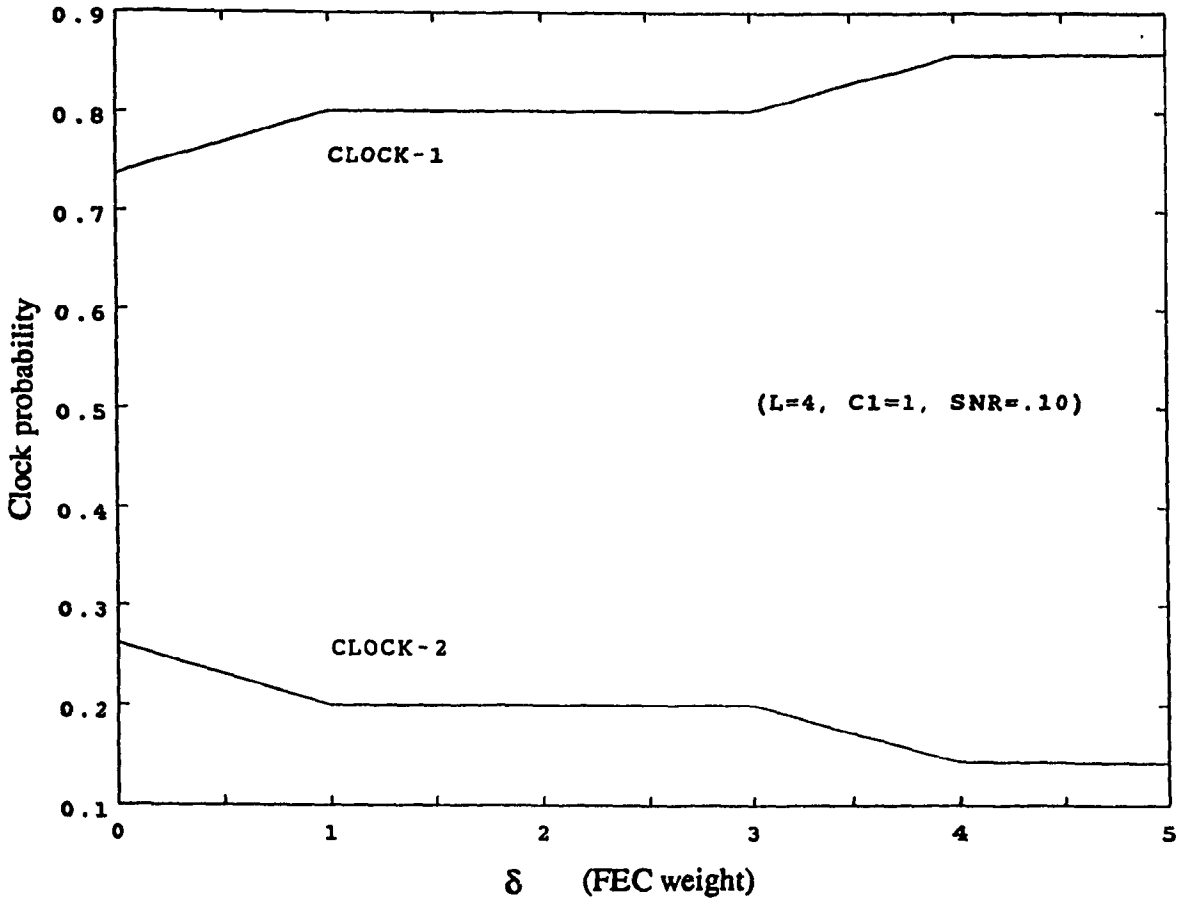

Fig. 6.13 Clock probability versus FEC weight δ for single user case, parameters are; spread spectum bandwidth = 7.68 Mhz., bit rate = 2Kbps., *M –ary* system of $M = 4$, Reed Solomon code (64, 32), number of subcodes $L = 4$, threshold setting $C_1 = 1$, signal to noise ratio = 0.10

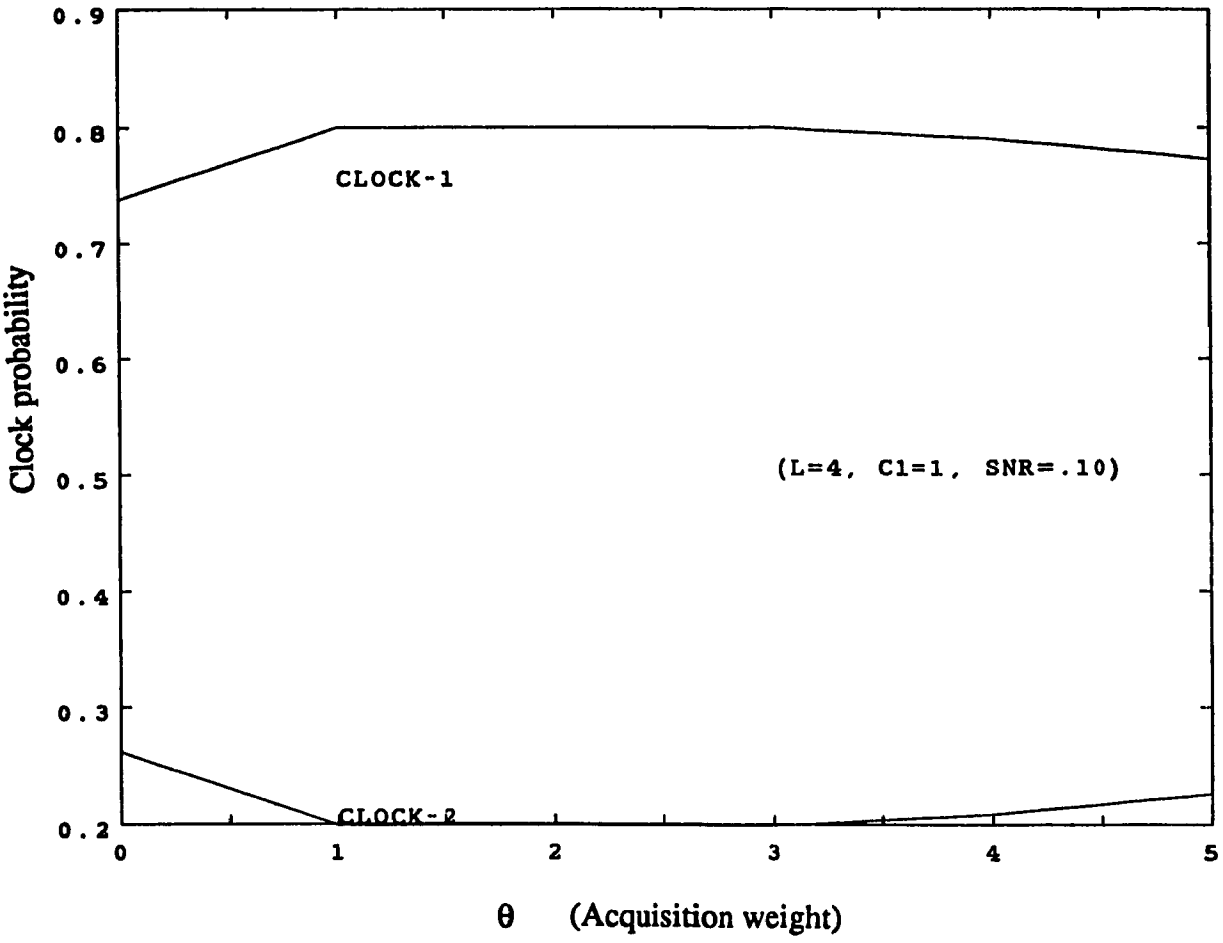

Fig. 6.14 Clock probability versus acquisition weight θ for single user case, parameters are; spread spectum bandwidth = 7.68 Mhz., bit rate = 2Kbps., *M−ary* system of M = 4, Reed Solomon code (64, 32), number of subcodes L = 4, threshold setting C_1= 1, signal to noise ratio = 0.10

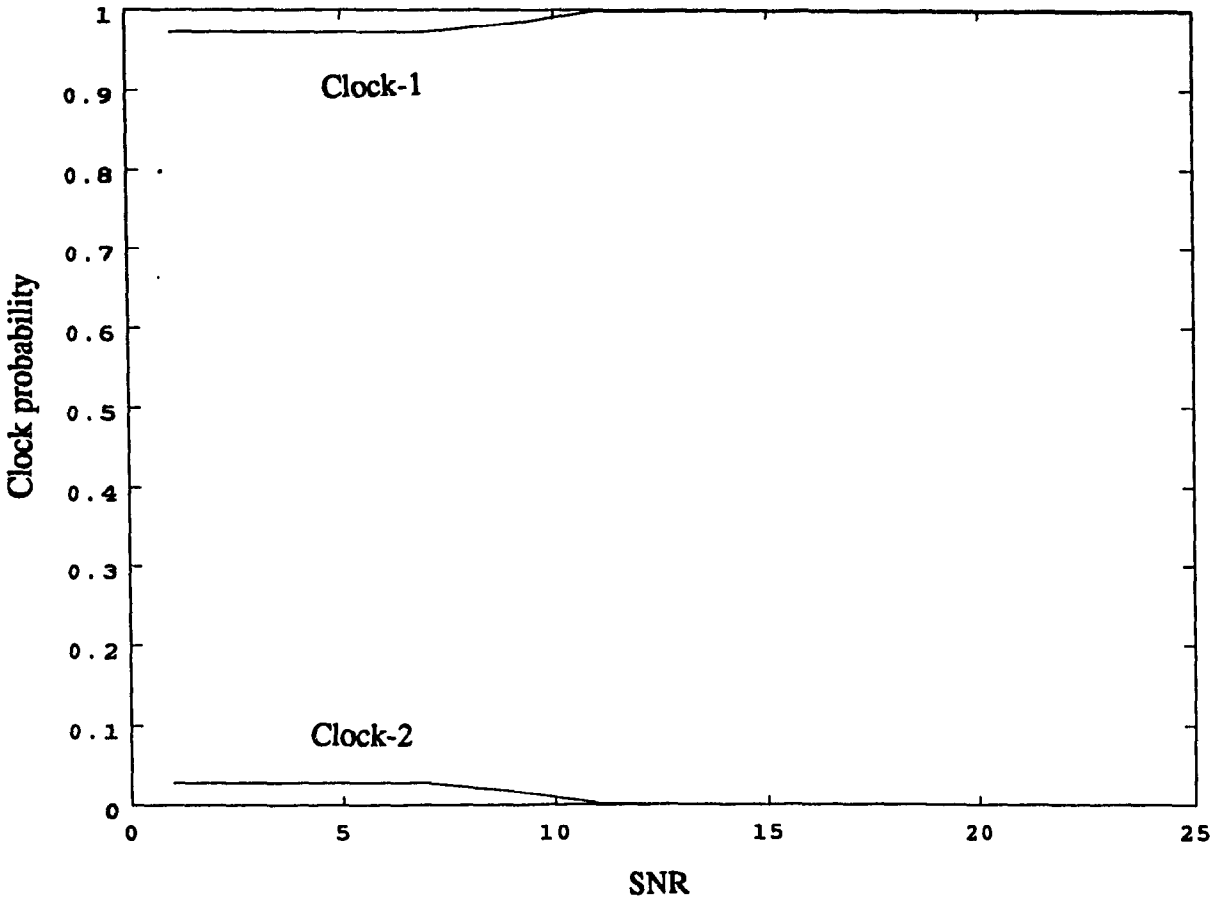

Fig. 6.15 Clock probability versus signal to noise ratio (SNR) for single user case, parameters are; spread spectum bandwidth = 7.68 Mhz., bit rate = 2Kbps., *M−ary* system of $M = 4$, Reed Solomon code (64, 32), number of sub-codes $L = 4$, threshold setting $C_1 = 3$

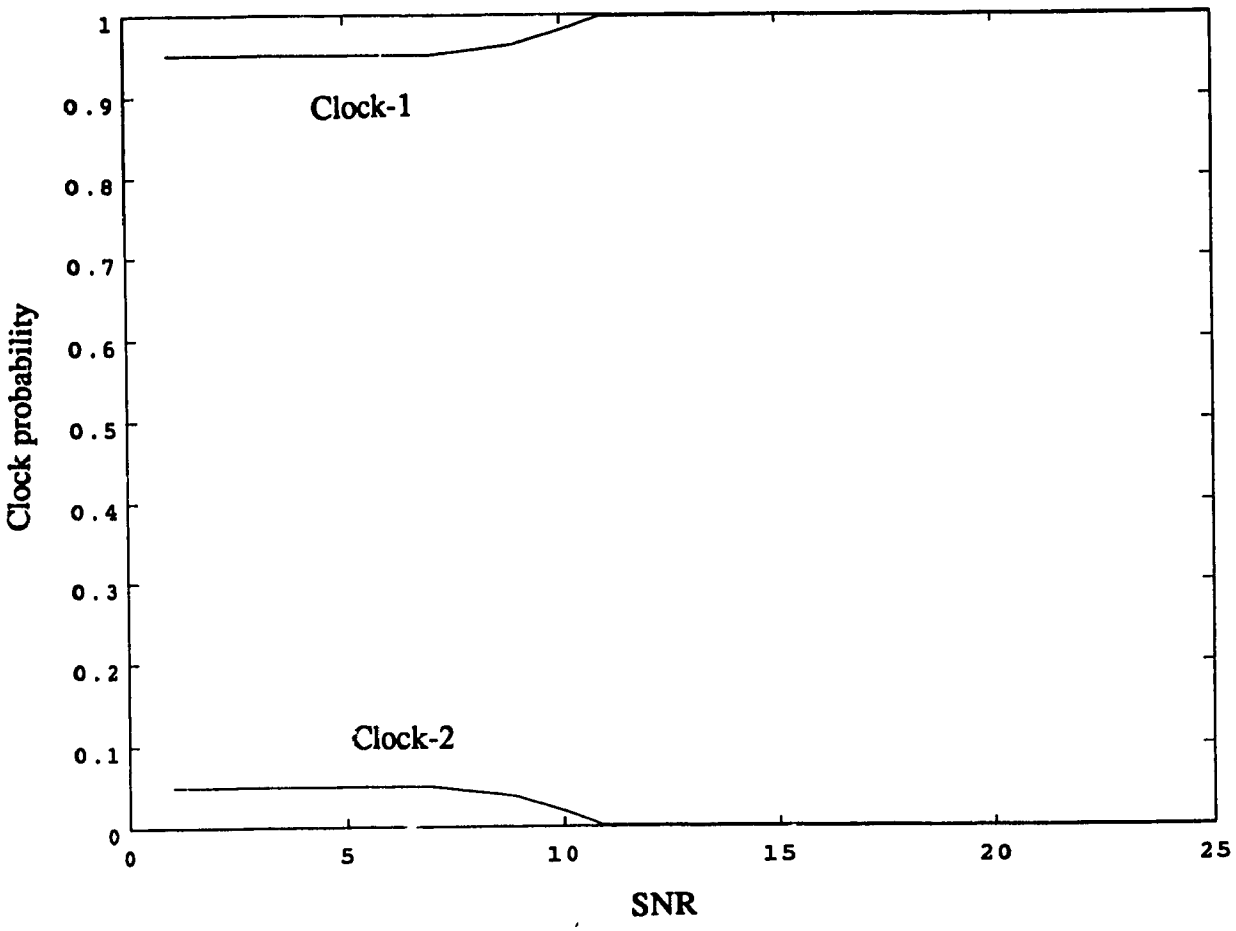

Fig. 6.16 Clock probability versus signal to noise ratio (SNR) for multi access case, parameters are; spread spectum bandwidth = 7.68 Mhz., bit rate = 2Kbps., *M-ary* system of $M = 4$, Reed Solomon code (64, 32), number of sub-codes $L = 4$, threshold setting $C_1 = 3$

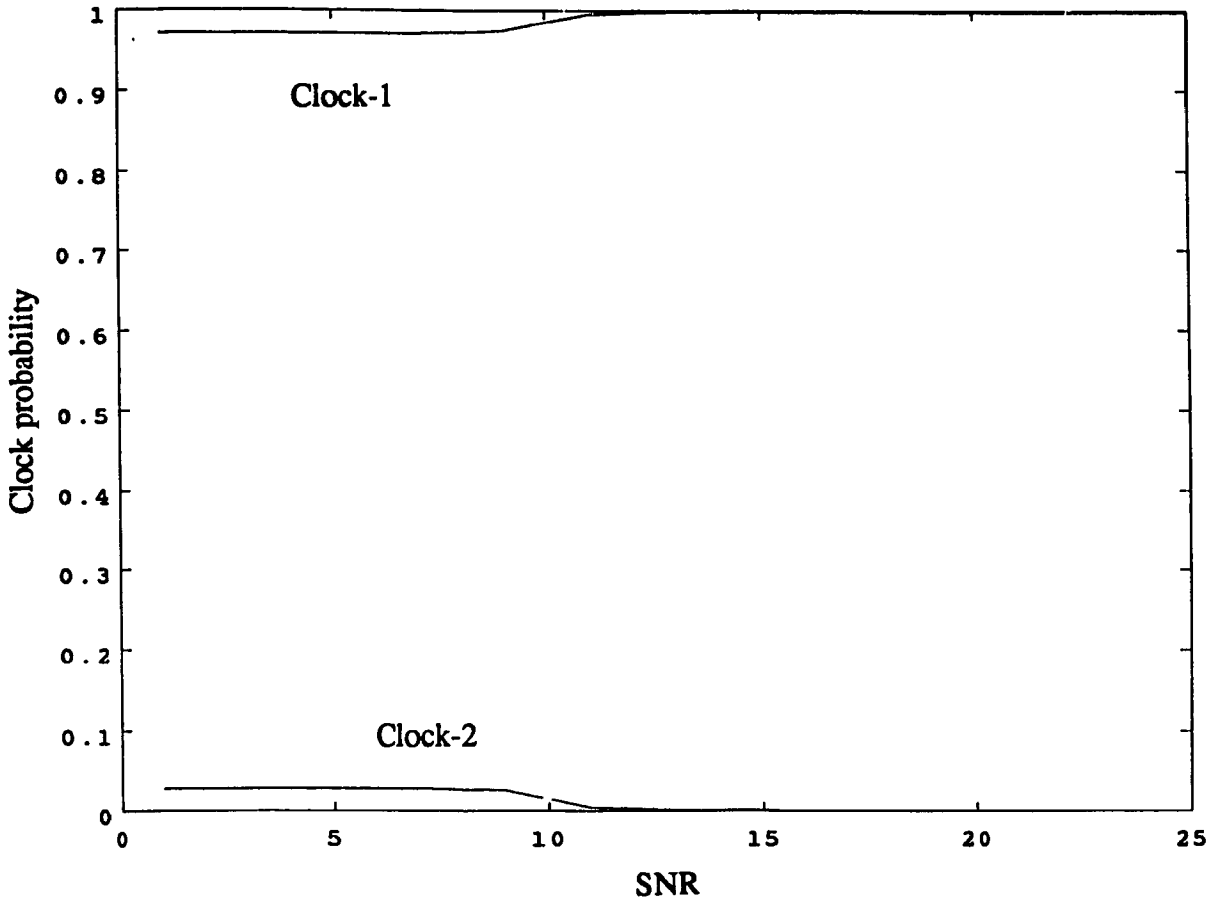

Fig. 6.17 Clock probability versus signal to noise ratio (SNR) for multi tone jamming case, parameters are; spread spectum bandwidth = 7.68 Mhz., bit rate = 2Kbps., $M-ary$ system of M = 4, Reed Solomon code (64, 32), number of subcodes L = 4, threshold setting C_1= 3

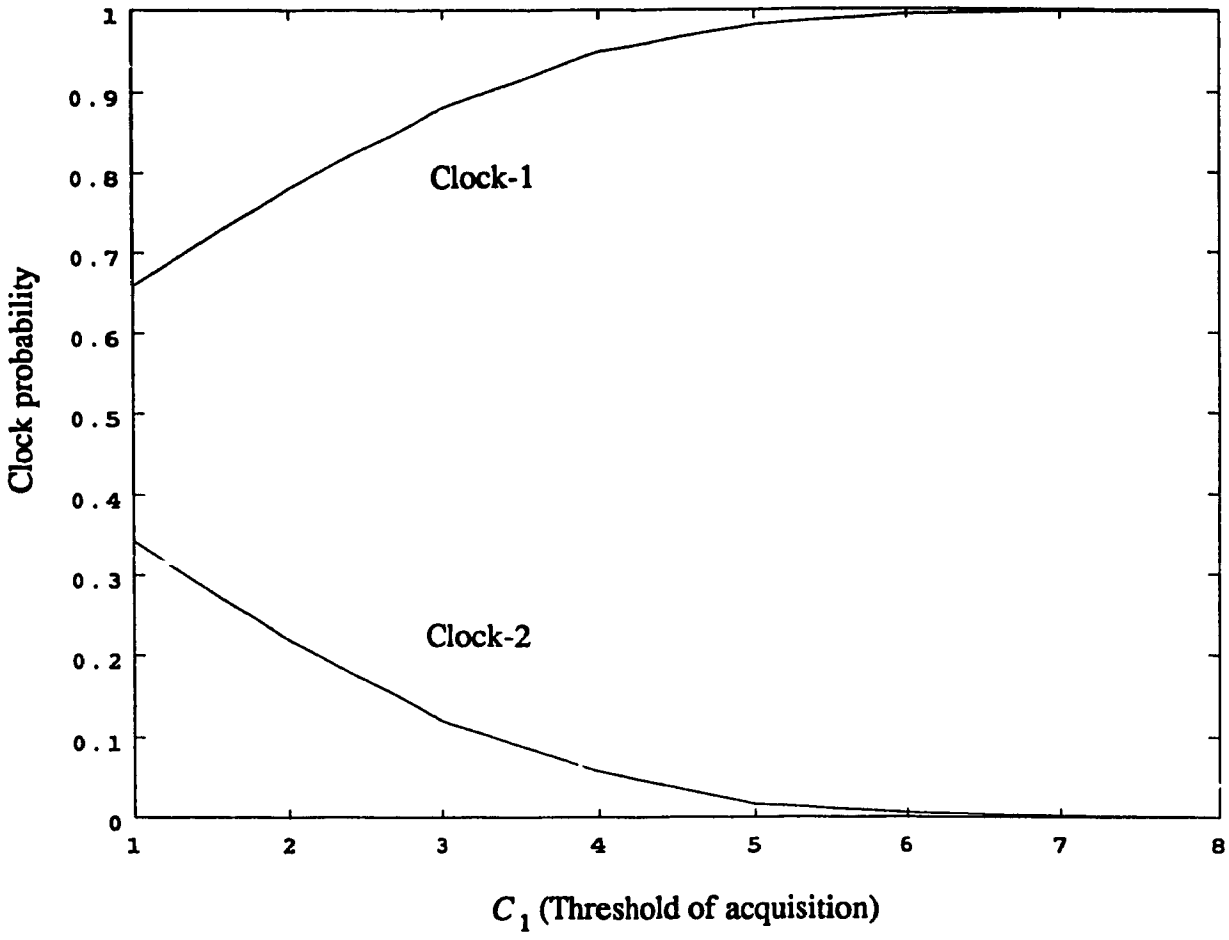

Fig. 6.18 Clock probability versus acquisition threshold setting C_1 for single user case, parameters are; spread spectum bandwidth = 7.68 Mhz., bit rate = 2Kbps., M*−ary* system of M = 4, Reed Solomon code (64, 32), number of subcodes L = 8, signal to noise ratio (SNR) =.10

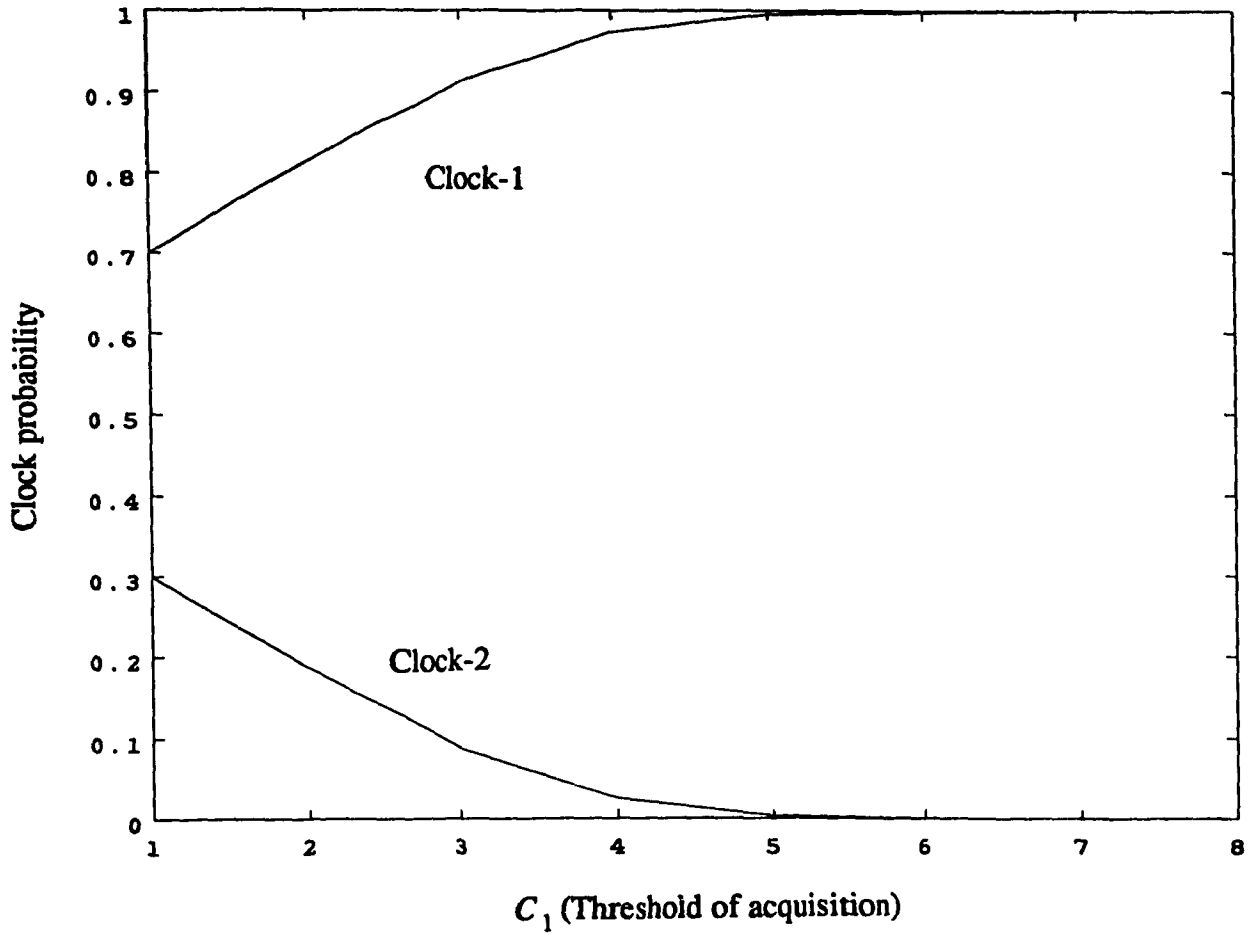

Fig. 6.19 Clock probability versus acquisition threshold setting C_1 for single user case, parameters are; spread spectum bandwidth = 7.68 Mhz., bit rate = 2Kbps., *M –ary* system of $M = 4$, Reed Solomon code (64, 32), number of subcodes $L = 8$, signal to noise ratio (SNR) =10.0

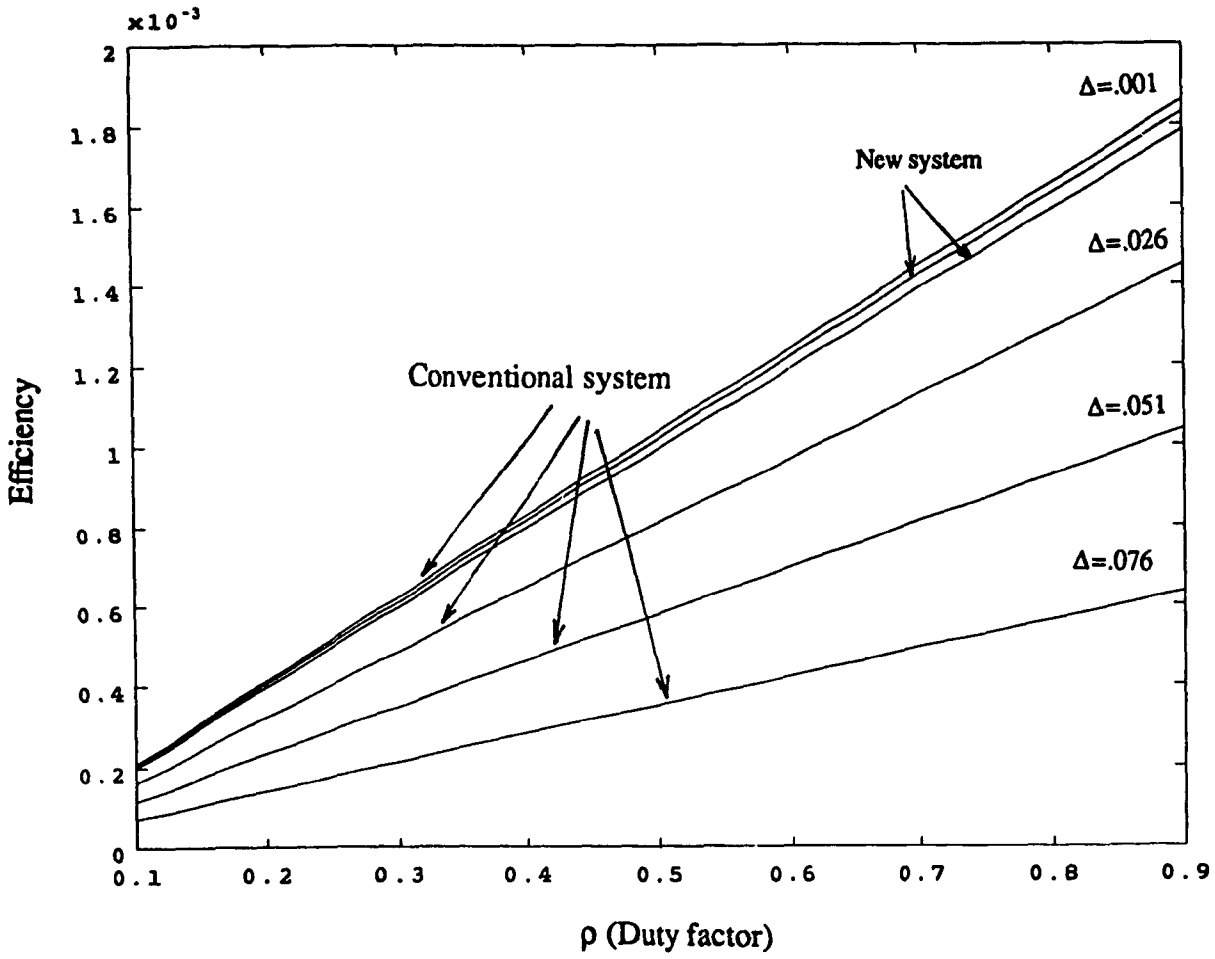

Fig. 6.20 Efficiency versus duty factor (ρ) for new spread spectrum system and conventional spread spectrum system for multi access case, the parameters are; spread spectum bandwidth = 7.68 Mhz., bit rate = 2Kbps., $M-ary$ system of M = 4, Reed Solomon code (64, 32), number of subcode L=4, threshold setting C_1 = 2, SNR = .1 and for the conventional system Δ (the ratio of average acquisition time to data transmission time) as a parameter.

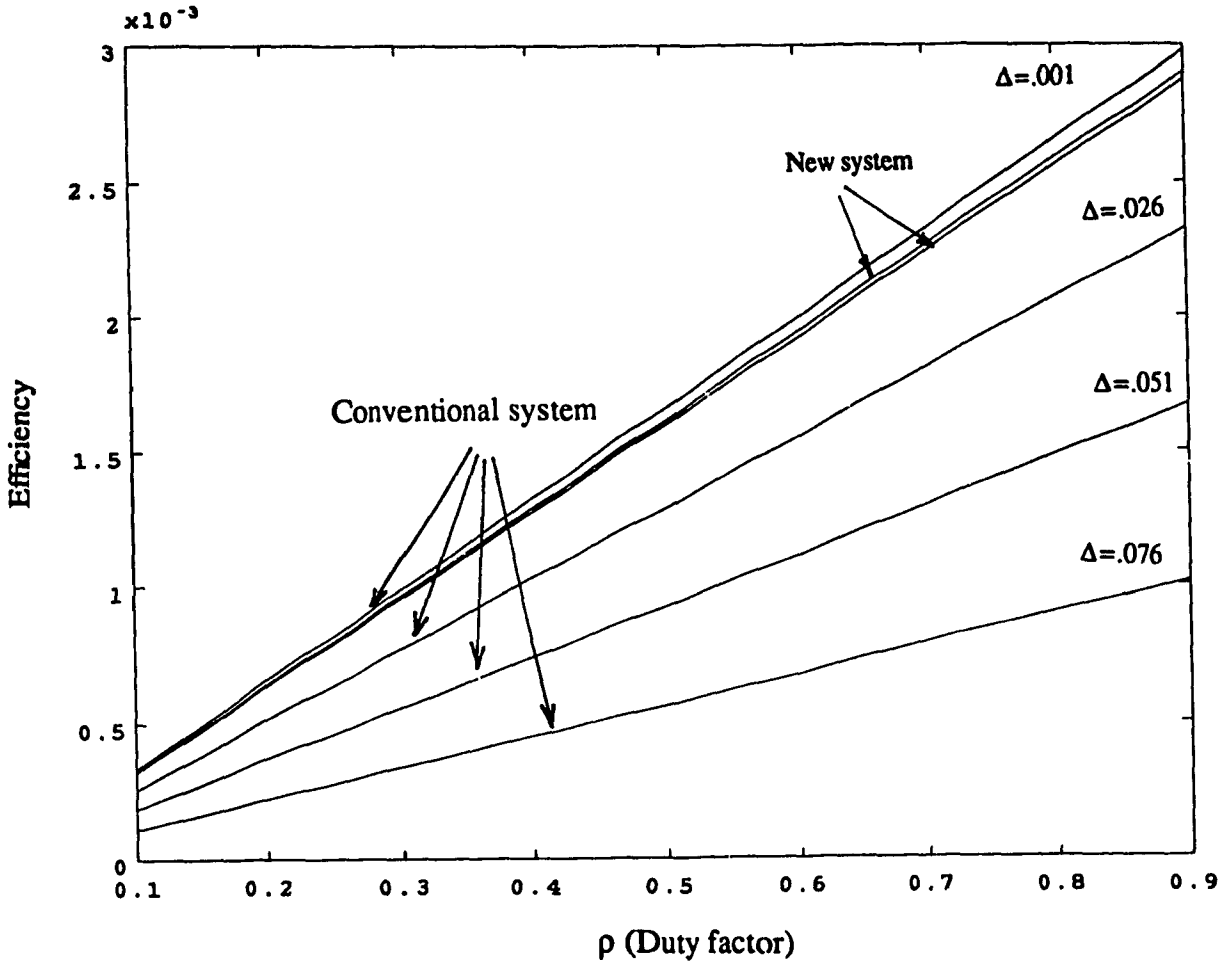

Fig. 6.21 Efficiency versus duty factor (ρ) for new spread spectrum system and conventional spread spectrum system for multi access case, the parameters are; spread spectum bandwidth = 7.68 Mhz., bit rate = 2Kbps., *M−ary* system of M = 4, Reed Solomon code (64, 32), number of subcode L=4, threshold setting C_1 = 2, SNR = 10.0 and for the conventional system Δ (the ratio of average acquisition time to data transmission time) as a parameter.

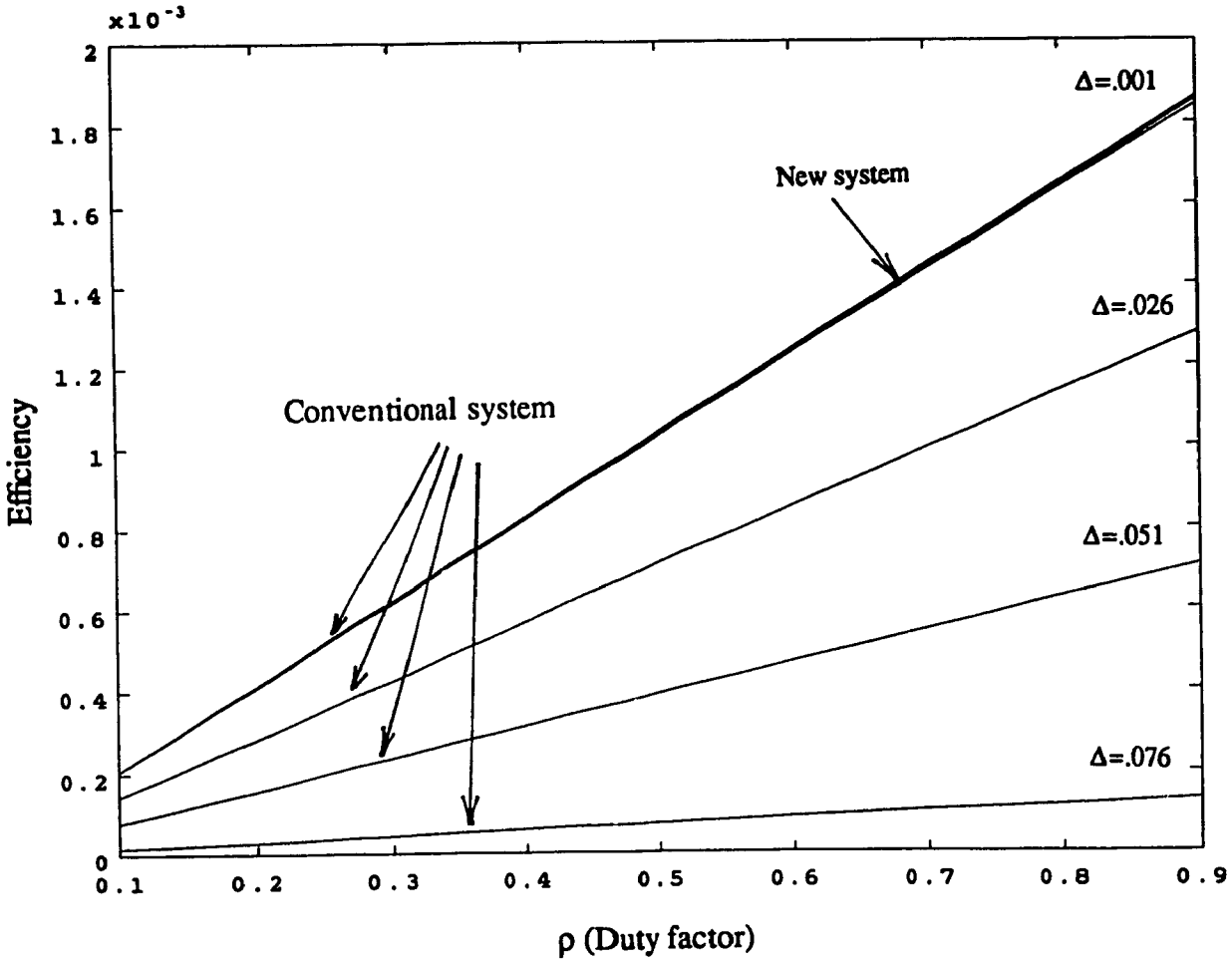

Fig. 6.22 Efficiency versus duty factor (ρ) for new spread spectrum system and conventional spread spectrum system for multi access case, the parameters are; spread spectum bandwidth = 7.68 Mhz., bit rate = 2Kbps., $M-ary$ system of M = 4, Reed Solomon code (64, 32), number of subcode L=8, threshold setting C_1 = 4, SNR = .1 and for the conventional system Δ (the ratio of average acquisition time to data transmission time) as a parameter.

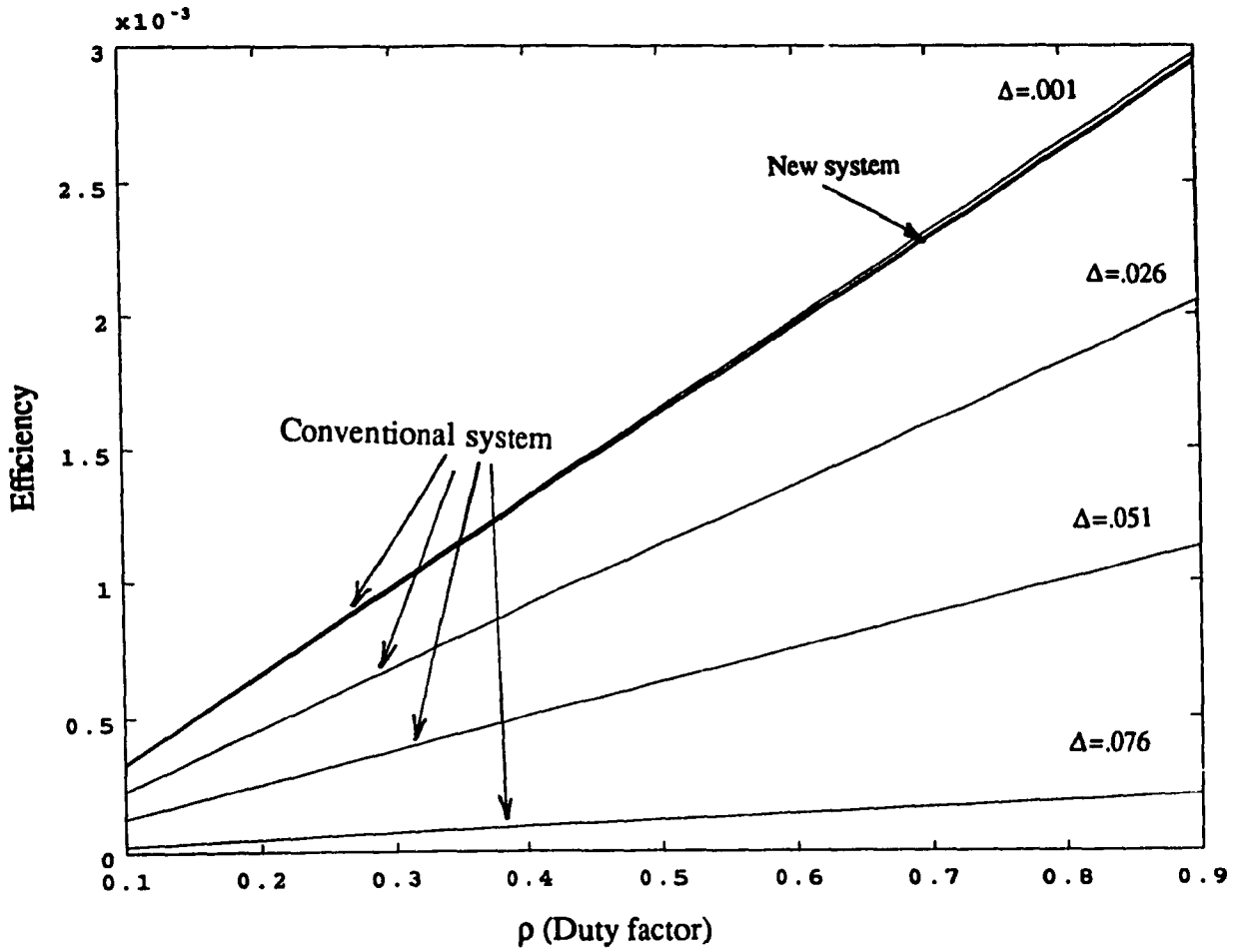

Fig. 6.23 Efficiency versus duty factor (ρ) for new spread spectrum system and conventionalclassic spread spectrum system for multi access case, the parameters are; spread spectum bandwidth = 7.68 Mhz., bit rate = 2Kbps., *M−ary* system of M = 4, Reed Solomon code (64, 32), number of sub-code L=8, threshold setting C_1 = 4, *SNR* = 10. and for the convetional system Δ (the ratio of average acquisition time to data transmission time) as a parameter.

Appendix 6 A

The probability of acquisition for the single dwell serial search system

Finding the probability of acquisition of a single dwell PN acquisition in k or fewer dwells requires first obtaining an expression for the probability density function of the number of dwells to obtain successful synchronization [6.1], [6.4].

The generating function flow graph for acquisition time can be written as the triple sum [6.1]

$$U(z) = \frac{P_D\, z}{q} \sum_{i=0}^{\infty} \sum_{l=0}^{q-1} \sum_{h=0}^{i(q-1)+l} \binom{i(q-1)+l}{h} P_{FA}{}^{h} (1-P_{FA})^{i(q-1)+l-h} \ast (1-P_D)^{i} z^{iq+l+hK} \quad \text{(6A-1)}$$

where P_D is the probability of detection, P_{FA} is the probability of false alarm, q indicates the total number of cells tob searched.

We define

$$N_{ACQ} \equiv N_u' + m + nK \quad \text{(6A-2)}$$

where N_u' represents the number of cells searched without success of detection prior to the $k-th$ search during which the correct cell will be detected, m is location of the correct cell, n denotes the actual number of false alarms and for each of these false alarms a penalty $K\tau_d$ is assessed.

N_{ACQ} is the integer valued random variable which represents the total number of cells that have been examined when successful synchronization (acquisition) occurs. If p_j denote the probability that the system acquires on the $j-th$ cell tested or in terms of N_{ACQ}.

$$p_j = Pr(N_{ACQ} = j) \; ; \quad j = 1, 2, 3, \ldots\ldots \quad \text{(6A-3)}$$

then z has the moment generating function

$$U(z) = \sum_{j=0}^{\infty} z^j p_j \tag{6A-4}$$

We make the assumption that the system acquires within a single search of q cells, i.e., $N_{ACQ} < q$. This is equivalent to considering only the $i=0$ term in the summation over i since the index i represents the number of times that the entire group of cells has been previously examined. Making this simplification (A-1) reduces to

$$U(z)\,|_{\,i=0} = \frac{P_D}{q} \sum_{l=0}^{q-1} \sum_{h=0}^{l} \binom{l}{h} P_{FA}^h (1-P_{FA})^{l-h} z^{l+hK+1} \tag{6A-5}$$

Now, making the equivalence between the coefficients of z^j in (6A-4) and (6A-5) provides

$$P_{ACQ}(j) = Pr(N_{ACQ} \leq j) = \sum_{i=0}^{j} p_i \tag{6A-6}$$

Where N_{ACQ} is the integer valued random variable which represents the total number of cells that have been examined when successful synchronization (acquisition) occurs. p_j denote the probability that the system acquires on the $j-th$ cell tested. p_j is given by

$$p_j = \frac{P_D}{q} \sum_{h=0}^{h+1} \binom{j-1-hK}{h} P_{FA}^h (1-P_{FA})^{j-1-h(K+1)} \tag{6A-7}$$

$$\left\lfloor \frac{J}{K} \right\rfloor K+1 \leq j < \min \left\{ \left(\left\lfloor \frac{j}{K} \right\rfloor + 1 \right) K, q \right\} \tag{6A-8}$$

$$h \equiv \left\lfloor \frac{\left\lfloor \frac{j}{K} \right\rfloor K}{K+1} \right\rfloor \tag{6A-9}$$

and the notation $\lfloor a \rfloor$ represents the largest integer less than or equal to a. Furthermore, the term corresponding to $h = \hat{h} + 1$ clearly has meaning only if $j - 1 - (\hat{h} + 1)K \geq 0$; otherwise its contribution is assumed equal to zero.

Appendix 6 B

Error probabilities of the FH multi access cases

For finding the throughput and clock probabilities of the system we need to find the probability of bit error in both cases, i.e., for conventional SS system and the new 'SUGARW' system under different situations, i.e., only AWGN or AWGN and tone jamming and multi access jamming.

Now, to find the probability of one Reed-Solomon symbol error on the channel. We assume that (N, K) RS codes over GF(2^{km}) are employed; thus there are $m-M-ary$ symbols in each RS symbol and each $M-ary$ symbol contain k bits. We upper bound the probability RS symbol error by

$$P_{RS} \leq 1-(1-P_h)^{U-1}\,[(1-\rho_j)(1-P_0)^m+\rho_j(1-P_{j,0})^m] \qquad (6B\text{-}1)$$

Where M, U, P_h, ρ_j and m are the $M-ary$ size, the number of users, the probability of hit, the jammer band ratio, and number of $M-ary$ symbols per RS inner code symbol, respectively. Now

$$P_h = (1+\frac{(m/\beta_s)}{L_b})\frac{N}{K} \qquad (6B\text{-}2)$$

Where, L_b is the number of frequency hop bands, β_s is the number of symbols per hop and the multiplication by N/K takes care of the fact that data bandwidth expands by the use of codes thus decreasing the processing gain (PG) and increasing the probability of frequency hit.

P_o, $P_{j,0}$ are the symbol error probability on the channel affected only by AWGN or (AWGN and partial band jamming), respectively. The probabilities P_0, $P_{j,0}$ in eq. (6B-1) will now be given [6.10],

$$p(\eta)=\sum_{i=1}^{M-1}\frac{(-1)^{i+1}}{1+i+i\beta(\eta)}\exp(-\frac{i\Lambda(\eta)}{i+1+i\beta(\eta)}) \qquad (6B\text{-}3)$$

Where,

$$\beta(\eta) = \Lambda/(1+\gamma^{-2}) \tag{6B-4}$$

$$\delta(\eta) = \Lambda/(1+\gamma^{2}) \tag{6B-5}$$

$$\Lambda(\eta) = \textit{coded symbol SNR} = (E_b \log_2 M/\eta)\frac{K}{N} \tag{6B-6}$$

E_b is the uncoded bit SNR,

$\eta/2$ is the double sided noise density,

γ^2 is the scatter/fading power ratio,

If $\gamma^2=0$ this implies $\beta(\eta)=0$, $\delta(\eta)=\Lambda(\eta)$ which is the pure AWGN reception case

If $\gamma^2=\infty$, this implies $\beta(\eta)=\Lambda(\eta)$ and $\delta(\eta)=0$ which is the Rayleigh fading reception case.

$P_{0,j}$ is simply obtained by replacing η by $(\eta+N_j)$ where N_j is given by

$$N_j = \frac{J}{W\rho_j} \tag{6B-7}$$

Where W is the spread spectrum bandwidth, J is the jammer power and ρ_j is the jammer band ratio or the duty factor.

To find the error improvement obtained by RS coding we follow the sequence of events taking place following the $M-ary$ noncoherent symbol detection and the associated RS symbol error given by P_{RS} of eqn (6B-1). The decoder combines N (RS symbols) each consisting of m MFSK symbols to give (K, N) MFSK symbols. The probability of one RS symbol being in error following the inner decoder is given by,

$$P_{sc} = \sum_{j=t+1}^{N} \frac{j+t}{N} \binom{N}{j} (P_{RS})^j (1-P_{RS})^{(N-j)} \tag{6B-8}$$

where t is the error correction capability of the decoder.

Now, a decoding error in one RS symbol does not necessarily mean every one of the m (MFSK) symbols are in error, also, if orthogonal MFSK is used we obtain for the final decoded bit error

$$P_b = \frac{M}{2(M-1)} \frac{P_{sc}\,(eq.\ (6B-7)\ with\ \ m_i=1)}{P_{sc}\,(from\ \ eq.\ (6B-7))} P_{sc}^{in} \qquad \text{(6B-9)}$$

The middle term represents the conditional probability of one MFSK symbol error given one RS symbol error.

For the case of finding the decoded bit probability under bad clock (i.e., no code alignment) we assume the detected probability of bit error as equal to .5 (i.e., because the detected bit may be right or wrong with 50% probability due to code misalignment). In this case the probability of symbol error becomes

$$P_0 = (1-(1-P_b)^{\log_2 M}) \qquad \text{(6B-10)}$$

when there is no partial band jamming present then the RS symbol error can be found from eq.(6B-1) with ρ_j equals to zero ($\rho_j = 0$)

$$P_{RS} \leq (1-(1-P_h)^{U-1}[(1-P_o)^m]) \qquad \text{(6B-11)}$$

The probability of one RS symbol being in error following the inner decoder is still given by eq. (6B-8) with P_{RS} replaced by P_{RS} (eq. (6B-11)). The final bit error probability is still given by eq. (6B-9) with P_{sc}'s found for this case.

Now, for the case of single user multitone or equivalent partial band jamming eq.(6B-1) reduces to

$$P_{RS} \leq 1-[(1-\rho_j)(1-P_0)^m + \rho_j(1-P_{j,o})^m] \qquad \text{(6B-12)}$$

and P_0 and $P_{j,0}$ for the signal present case are still given by eq. (6B-3) and for the case of no code alignment P_0 is given by eq. (6B-10).

REFERENCES

[6.1] M.K. Simon, J.K. Omura, R.A. Scholtz, B.K. Levitt, 'Spread Spectrum Communications', Computer Science Press.

[6.2] A.K. Elhakeem, G.S. Takhar, S.C. Gupta, 'New Code Acquisition Techniques in Spread Spectrum Communications', IEEE, Trans. on Comm., Vol. COM-28, pp. 246-259, February 1980.

[6.3] W.K. Alem, 'Spread Spectrum Acquisition and Tracking Performance for Shuttle Communication Links', IEEE, Trans. on Comm., November 1978.

[6.4] L. Zeimer, R.L. Peterson, 'Digital Communications and Spread Spectrum Signals', McMillan Publishers, 1985.

[6.5] A.K. Elhakeem, Anisur Rahman, 'SUGARW, A New Purely Random Spread Spectrum System for Multi Access', Fourteenth Biennial Symposium for Communications, Queens's University, Canada, May-June 1988

[6.6] D.V. Sarwate and M.B. Pursley, 'Correlation Properties of Pseudo-Random Sequences', Proceedings of the IEEE, Vol. 68, No. 5, pp. 593-619, May 1980

[6.7] L.B. Milstein and P.K. Das, 'Spread Spectrum Receiver Using Surface Acoustic Wave Technology', IEEE, Trans. on Communications., Vol. Com. 25, No. 8, pp. 841-847, August 1977

[6.8] D.M. Dicarlo, and C.L. Weber, 'Statistical Performance of Single Dwell serial Synchronization System', IEEE, Trans. on Communications, Com.-28, No-8, pp 1382-88, Aug 1980.

[6.9] G. Cooper, R. W. Nettleton, 'A Spread Spectrum System for High Capacity Mobile Communications', IEEE, Trans. on Vehicular Technology, Vol. VT-27, No.-4, November 1978.

[6.10] E. Geraniotis, J. W. Gluck, 'Coded FH/SS Communications in the Prescence of Combined Partial Band Noise Jamming, Rician Non-selective Fading, Multi User Interference', IEEE, Journal on Selected Areas in Communications, Vol. SAC-5, No.-2, February 1987.

[6.11] M.A. Rahman, A.K. Elhakeem, 'Throughput Analysis of the 'SUGARW; Acquisitionless Spread Spectrum System in Multi Access and Tone Jamming Environments', Proceedings of the IEEE, GLOBECOM '90, Sandiego, California, USA., Dec. 1990.

[6.12] M.A. Rahman, A.K. Elhakeem, 'Throughput Analysis of the 'SUGARW; Acquisitionless Spread Spectrum System in Multi Access and Tone Jamming Environments', Fifteenth Biennial Symposium on Communications, Queens University, Kingston, Ontario, Canada, June 1990.

CHAPTER VII

CONCLUSIONS

7.1 Conclusions

Acquisition is one of the most important component in a spread spectrum system. Acquisition operating characteristics are affected by like user interference and tone jamming. We have analyzed and evaluated the spread spectrum (SS) acquisition operating characteristics under multiple access jamming and tone jamming conditions.

Error correction coding is essential for Frequency Hopping spread spectrum system, both acquisition and acquisitionless systems. The use of concatenated codes can provide the desired error performance.

The ensemble average error bound of convolutional codes has been used for determining the error probability of concatenated convolutional codes at different stages of concatenation and to determine the relationship between the exponential bound parameter $E_c(R)$ and the rate R at different stages of concatenation.

Three stages of concatenation (of convolutional codes) were found to achieve an acceptable error rate and going to four levels did not produce much effect, thus motivating us to accept a two level RS/RS or RS/Trellis concatenated code as a good candidate for our new 'SUGARW' system.

Spread spectrum systems require large bandwidth compared to the conventional systems and the bandwidth is limited by allocations. Trellis codes for

bandlimited channels result from combining convolutional coding with modulation. Concatenated trellis code application to Frequency Hopping noncoherent MFSK spread spectrum systems under multiple access and partial-band jamming effects have been tried and comparisons were made with concatenated RS codes. It was found that for 4–*ary* MFSK systems the concatenated trellis code outperforms the RS concatenated code and can withstand six times the number of users than the RS case for moderate bit error probability.

A new spread spectrum system that does not require acquisition has been presented. The notion of purely random code has been defined and the multi access capabilities has been investigated. The new system code is readily acquired through a parallel bank of matched filters and the notion of initial acquisition is taken out completely. The new system, however, needs an acknowledgement channel and ARQ. The use of which combined with a trellis code should aid the rejection of false code matched filter peaks which should finally lead to better error performance, less retransmission and improved multi access capabilities.

It is possible to have a SS system that does not need acquisition. In this thesis we have introduced such a system and proved that in many cases, the throughput of the 'SUGARW' system is higher than a conventional system. It was found that in the 'SUGARW' SS system the clocks probabilities deteriorates if the acquisition threshold is decreased keeping the number of subcode and SNR fixed. Moreover, increasing the number of subcode keeping everything fixed have resulted in deteriorating the receiver performance. In formulating the demodulation decision at the receiver, coding has been found

to be more critical than the acquisition at high SNR; at low SNR there is no relative importance of the thresholds δ and θ but still increasing δ makes more sense. The performance of the new 'SUGARW' SS system has been found to be better than the conventional SS system that requires acquisition for its operation, if Δ the ratio of the average acquisition time to the data transmission time is greater than .001.

The advantage of the system is that it avoids need for acquisition and starts right away. In this system by dynamically changing the code very long code can be obtained. Acquisition and verification hard ware is eliminated. The system is most suitable for the application where the transmission is intermittent with large periods of silence particularly for secure mobile communications. For military applications special chips have to be used, added with few delays, etc., to hide the identities of the 4 short codes used.

The drawback of the system is that the receiver is more complex than the conventional spread spectrum system and for a continuously operating link this system is not suitable.

7.2 Further Research Work

1. The performance analysis of the concatenated combined modulation and coding of Frequency Hopping multi access systems in the channels with erasures and side information, comparisons with other code types.

2 The performance evaluation of the combined modulation and coding for the Frequency Hopping multi access system with asymmetric signal

constellation and comparing with the performance of the symmetric signal constellations.

3. Investigation of the performance of the new acquisitionless system with four or more receiver banks in fading environments.

4. Computer simulation of the acquisition less system in real time.

5. Hardware implementation of the suggested system can be done.

6. Investigation of the programmability of the 4 short subcode in real time and application to indoor communications.